COMBINATION EFFECT OF PHOTODYNAMIC THERAPY (PDT) AND CHEMOTHERAPY ON ORAL CANCER CELL LINES

TEOH JIA JIE

MASTER OF SCIENCE

FACULTYOF ENGINEERING & SCIENCE
UNIVERSITI TUNKU ABDUL RAHMAN
JAN 2012

COMBINATION EFFECT OF PHOTODYNAMIC THERAPY (PDT) AND CHEMOTHERAPY ON ORAL CANCER CELL LINES

By

TEOH JIA JIE

A dissertation submitted to the Department of Bioscience & Chemistry,
Faculty of Engineering & Science,
Universiti Tunku Abdul Rahman,
in partial fulfillment of the requirements for the degree of
Master of Science in Cell Biology
Jan 2012

ABSTRACT

High concentration chemotherapy is often accompanied by undesirable side effect. Therefore, strategies to boost chemotherapy efficacy while reducing its working dosage are needed. Photodynamic therapy (PDT) is an alternative modality that kills cells effectively with relatively lower toxicity compared to chemotherapy. In this study, the combinatory effect of Hypericin-mediated PDT and cisplatin/doxorubicin/vinblastine-based chemotherapy was studied in HSC-2, HSC-3 and HSC-4 oral cancer cell lines. The concentration-response effects of independent drug treatments and combination drug treatments were evaluated using 3-(4,5-dimethylthiazol)-2,5-diphenyltetrazolium bromide (MTT) assay. Synergistic, additive or less than additive drugs interactions were determined from isobolographic analysis. Modes of cell death for chosen synergistic or additive drug combinations were analysed using flow-cytometric method. Eventually, cell death mediators (caspase-7, -8, -9, Bcl-2 and Bax) was studied using Western Blot. Combination treatment of Hypericin-mediated PDT and Cisplatin (HYP-PDT+CIS) exhibited less than additive effect in HSC-2 but produced additive effect in HSC-3 and synergistic effect in HSC-4. Hypericin-mediated PDT and Doxorubicin (HYP-PDT+DOX) exhibited synergistic effect in all three cell lines. Combination of Hypericin-mediated PDT and Vinblastine (HYP-PDT+VIN) exhibited synergistic effect in HSC-2 and HSC-4 but additive effect in HSC-3. In addition, "thresholds of synergism" was found in specific isobolograms. From flow-cytometric analysis, selected HYP-PDT+CIS combination did not produce significant cell death in HSC-3 but produced

earlier onset of apoptosis in HSC-4. Selected HYP-PDT+DOX or HYP-PDT+VIN combination produced earlier onset of apoptosis and necrosis in all three cell lines. All selected combinations resulted in high Bax:Bcl-2 ratio. Caspase-8 was activated in cell lines treated with HYP-PDT+CIS and HYP-PDT+VIN. Caspase-9 was activated in cell lines treated with HYP-PDT+DOX. Caspase-7 was activated downstream in apoptosis cascade. In conclusion, this study demonstrated the possibility to produce better cell killing with lower working concentrations of chemotherapeutic agents with the complement of HYP-PDT.

ACKNOWLEDGEMENTS

First and foremost I offer my sincerest gratitude to my supervisor, Dr Anthony Ho Siong Hock and my co-supervisor, Dr. Lee Hong Boon who have supported me thoughout my dissertation with their patience and knowledge whilst allowing me the freedom to work in my own way.

In daily laboratory works I have been aided by several people. Dr. Lim Yang Mooi who will always listen to and discuss with me when I met problems in the research works. The laboratory officers from the university, Mr. Su Kok Khiong, Mr. Tan Kim Chong and Ms. Sung Suet Phun always keep me stocked with general supplies. Mr. Lim Siang Hui from Cancer Research Initiatives gave me useful guidance in using flow cytometer, as well as some insightful ideas regarding cell death. Mr. Wong Swee Kiat, my old classmate who is currently a sale representative from Research Biolabs, who helped me in looking for suitable antibodies for use in western-blot assay.

Of course, I have been blessed with a friendly and cheerful group of fellow friends. Wong Chin Piow, Tiong Yee Lian, Teng Ooiean, Tee Shin Leong, Yap Wei Hsum, Wong Teck Yew (Clifford), Tan Hor Yue, Yeoh Sze Mun, Yip Shiau Chooi, Kua Rou Zhing, Tan Su Yin, and Tan Sok Yee are all of those who always entertain me with funny laugh. Apart from that, Seng Hoi Ling, Tan Yong Hui, Yap Pui Woon, Ong Siew Ling, Siow Then Soong and many other fellow friends from the other laboratories are all people who make

me happy. We have great dinner time together and we have discussion about the problems in project together.

APPROVAL SHEET

This dissertation entitled "*COMBINATION EFFECT OF PHOTODYNAMIC THERAPY (PDT) AND CHEMOTHERAPY ON ORAL CANCER CELL LINES*" was prepared by TEOH JIA JIE and submitted as partial fulfillment of the requirements for the degree of Master of Science in Cell Biology at Universiti Tunku Abdul Rahman.

Approved by:

_____
(Dr. Anthony Ho Siong Hock)
Date: _____
Supervisor
Department of Bioscience & Chemistry
Faculty of Engineering & Science
Universiti Tunku Abdul Rahman

_____
(Dr. Lee Hong Boon)
Date: _____
Co-supervisor
Cancer Research Initiatives Foundation (CARIF)

Date: 22 DEC 2011

PERMISSION SHEET

It is hereby certified that **TEOH JIA JIE** (ID No: **06UEM07952**) has completed this dissertation entitled "***COMBINATION EFFECT OF PHOTODYNAMIC THERAPY (PDT) AND CHEMOTHERAPY ON ORAL CANCER CELL LINES***" under the supervision of DR. Anthony Ho Siong Hock (Supervisor) from the Department of Bioscience & Chemistry, Faculty of Engineering & Science, and Dr. Lee Hong Boon (Co-Supervisor) from the Cancer Research Initiatives Foundation (CARIF).

I hereby give permission to

(i)   my supervisors to write and prepare a manuscript of these research findings for publishing in any form, if I did not prepare it within six (6) months time from this date, provided, that my name is included as one of the authors for this article. Arrangement of names will depend on my supervisors;

(ii)   the University to upload softcopy of my thesis in pdf format into UTAR Institutional Repository, which will be made accessible to UTAR community and public.

DECLARATION

I hereby declare that the dissertation is based on my original work except for quotations and citations which have been duly acknowledged. I also declare that it has not been previously or concurrently submitted for any other degree at UTAR or other institutions.

_____
(TEOH JIA JIE)
5 JAN 2012

TABLE OF CONTENTS

LIST OF TABLES

LIST OF FIGURES

LIST OF ABBREVIATIONS

Å	Angstrom
AIF	apoptosis-inducing factor
ALA	aminolevulinic acid
ANT	adenine nucleotide translocator
APAF-1	Apoptotic protease activating factor 1
APS	Ammonium persulfate
BCA	bicinchoninic acid
BCG	Bacillus Calmette-Guérin
Bcl-2	B-cell Lymphoma-2
BH	Bcl-2 homology
BSA	Bovine serum albumin
Ca^{2+}	Calcium ion
CGM	Complete growth medium
CIS	Cisplatin
COX-2	Cyclooxygenase-2
CTCL	cutaneous T-cell lymphoma
CypD	Cyclophilin D
DD	Death domain
DHFR	dihydrofolate reductase
DISC	death-inducing signaling complex
DMSO	Dimethyl sulfoxide
DNA	Deoxyribonucleic acid
DOX	Doxorubicin

EDTA	ethylenediaminetetraacetic acid
ERCC1	excision repair cross complementation group-1
EU	European Union
FBS	Fetal bovine serum
FITC	Fluorescein isothiocyanate
HCl	Hydrocloride
H-MESO-1	Human maglinant mesothelioma
HPD	hematoporphyrin derivatives
HRP	Horse radish protein
HSC	Human squamous carcinoma
HYP	Hypericin
IAP	Inhibitor of apoptosis
IC_{30}	30% inhibitory concentration
IC_{50}	50% inhibitory concentration
IC_{70}	70% inhibitory concentration
IC_{90}	90% inhibitory concentration
IgG	Immunoglobulin G
$J\ cm^{-2}$	Fluence
mA	Miliampere
MCF-7/Adr	Adriamycin resistance breast cancer cell line
MDR	Multidrug-resistance
MEMw	Minimum Essential Medium without phenol red
mg	Miligram
ml	Mililiter
mm	Milimeter

MOPP	Drug regimen of nitrogen mustard, vincristine, procarbazine and prednisone
MTT	3-(4,5-dimethylthiazol)-2,5-diphenyltetrazolium bromide
MVAC	Drug regimen of methotrexate, vinblastine, amethopterin and cisplatin
mW	Miliwatt
nm	Nanometer
OMM	Outer membrane of mitochondria
PARP	Poly (ADP-ribose) polymerase
PBS	Phosphate bufferred saline
PDT	Photodynamic therapy
PGP	P-glycoprotein
PI	Propidium Iodine
PKC	Protein kinase C
POMP	Drug regimen of methotrexate, vincristine, 6-mecarptourine and prednisone
PS	phosphatidylserine
PTP	Permeability Transition Pore
PVDF	Polyvinylidene Fluoride
RIP1	receptor interacting protein-*1*
ROS	Reactive oxygen species
rpm	Round per minute
S0	ground state
S1	single state
SD	Standard deviation

SDS	sodium dodecyl sulfate
T1	triplet state
tBid	truncated Bid
TEMED	Tetramethylethylenediamine
TM	Treatment Medium
TNF- α	Tumor necrosis factor- alpha
TRAIL	Tumor necrosis factor-related apoptosis-inducing ligand
V	Volt
VDAC	voltage-dependant anion channel
VEGF	Vascular Endothelial Growth Factor
VIN	Vinblastine
$W\ cm^{-2}$	Fluence rate
λ_{max}	Maximum absorption wavelength
μg	Microgram
μl	Microliter
φ_{Δ}	Quantum yield of reactive oxygen species

CHAPTER 1

INTRODUCTION

The search for better cancer treatments is a world-wide concern. The current trend of drug discovery focuses on finding single-agent anticancer drugs and involves firstly, primary screening of compounds, identification of leads, lead optimization and lastly lead development. Then, a prospective drug candidate needs to undergo clinical trials. The whole discovery process may take up to 10 years before the drugs can be applied clinically. Pharmaceutical companies have to spend approximately $1042 million to develope a new single agent anticancer drug and the failure rate is frequently more than 75% (Venkitaraman, 2010). Futhermore, cancer often involves multiple genes and biochemical pathways (Kinzler & Vogelstein, 2002). Multiple-agent therapy may be better than single-agent therapy in combating cancer (Zimmermann, Lehar, & Keith, 2007). To develop combination regimens, the benefits of using clinically approved anticancer drugs rather than novel compounds include saving time and resources from developing new drugs and to shorten clinical trials. The aim of utilizing drug combinations are to take advantage of synergistic biological effects or reduce the dosage of individual drugs which reduces toxicity, without compromising overall clinical efficacy.

Chemotherapy is a systemic treatment suitable for virtually all stage of tumors due to its systemic distribution throughout the body. It is usually performed with high dose administration of anti-cancer drugs (Adelstein, Tan

1

& Lavertu, 1996). Among the clinically approved anticancer drugs, cisplatin is a platinum-based compound. The drug inhibits DNA replication by crosslinking intra-strand guanine bases in DNA (Chevalier & Soria, 2004). Doxorubicin is an anthracycline antibiotic capable of inhibiting topoisomerase II and producing reactive oxygen species (ROS) (Streckyte *et al*., 1999; Torkarska-Schlattner, Zaugg, Zuppinger, Wallimann, & Schlattner, 2006). Vinblastine is a microtubule inhibitor. The drug can bind to tubulin and destabilize microtubule structure (Duan, Sterba, Kolomeichuk, Kim, Brown & Chambers, 2007). On the other hand, photodynamic therapy (PDT) is a treatment utilizing photosensitizer, light and oxygen. The photosensitizer can be activated when exposed to light to produces ROS which kills cancer cells. Hypericin is a photosensitizer for PDT. It is a polycyclic quinone capable of generating ROS upon light activation (Agostinis, Vantieghem, Merlevede & de Witte, 2002).

An important consideration for using PDT is the accessibility of the tumour to light irradiation. Therefore, deep or very large tumours are not amenable to PDT (Agostinis *et al*., 2002) Oral cancers are excellent candidates for PDT because the oral cavity can be very easily accessed by light irradiation tools when photodynamic therapy (PDT) is to be carried out, either for *in vitro* or *in vivo* investigation (Allison, Cuenca, Downie, Camnitz, Brodish & Sibata, 2005). Furthermore, oral cancer ranked among the top six leading caused of cancer death in South-east Asia alone. In Malaysia, oral cancer ranked 12th most frequent cancer in males and 13th most frequent cancer in females (Lim & Yahaya, 2004).

Therefore, the objectives of this project were to evaluate the combination efficacy of existing clinically approved anticancer drugs, cisplatin, doxorubicin, and vinblastine with hypericin mediated PDT (Hyp-PDT). Three oral cancer cell lines with different genetic backgrounds namely HSC-2, HSC-3 and HSC-4, were tested in various drugs combination using a matrix approach and cell killing assessed by the MTT cell proliferation assay. Drug interactions were categorized as being synergistic, additive or less than additive based on isobolographic analyses. Meaningful synergistic or additive drug combinations were subjected to flow cytometry to quantify apoptosis and cell cycle arrest activity. Investigation of the mediators of apoptosis specifically caspases and Bcl-2 proteins, was carried out using Western blotting to shed light on the killing action of drug combinations.

CHAPTER 2

LITERATURE REVIEW

2.1   Cancer

The term, cancer, is equivalent to malignant tumour neoplasm. It is used to describe the biological behavior of the disease where of abnormal cells grow beyond their usual boundaries and invade adjoining parts of the body and spread to other organs (World Health Organization (WHO), 2009a). Cancer encompasses a group of more than 100 diseases that may affect any part of human body, causing degradation of life quality and eventually death (WHO, 2009b).

Cancer is a complex disease, often involving several mutations of genes and multiple biochemical pathways, in which environmental and non-genetic factors clearly take part in different stages of tumour development as well (Kinzler & Vogelstein, 2002). The heterogeneity basis of cancer explains the difficulty of designing a universal treatment and suggests that the use of single agents, in conventional western medical treatments, may not combat the disease effectively. Instead, multi-targeted approaches, such as combinatorial treatment that attack complex disease system from different facets are gaining attention (Zimmermann *et al*., 2007).

2.2 Epidemiology of Oral Cancer

Oral cancer is the sixth most common cancer reported worldwide in 1990, with highest mortality in south-central Asia, probably due to popular habit of chewing tobacco (Pisani, Parkin,Bray & Ferlay,1999). In western countries, the survival rate of oral cancer is approximately 50% (Kinzler & Vogelstein,2002). In United States, approximately 29,000 people were estimated to be diagnosed to have oral cavity cancer each years (National Cancer Institute (NCI), 2004).

In South-East Asia, oral cancer is ranked among the top six leading causes of cancer deaths in 2005. In Malaysia, oral cancer, including mouth, gum and tongue ranked 12th most frequent cancer in males and 13th most frequent cancer in females (Lim & Yahaya, 2004). The incidence of oral cancer is different by races (Lim, 2002). In 2003, the incidence of oral cancer was 0.5 per 100,000 in Malays, 1.2 per 100,000 in Chinese and 4.4 per 100,000 in Indians. Tongue cancer has the similar distribution trend (Lim & Yahaya, 2004).

2.3 Contemporary Treatments against Oral Cancer

2.3.1 Surgery, Radiotherapy and Chemotherapy

Surgery is no doubt still the choice of primary treatment for oral cancer due to the ease of accessibility of oral cavity. In most clinical cases, early phase cancer, such as Stage I or Stage II, are the best candidate for surgical

salvage, while later stage of cancer might required more radical dissection (Maria, Sader, Preston & Fisher, 2007; Yao *et al*., 2007). Dissection of tumour tissue, if done properly, can reduce the chances of one year post-surgery recurrence rate down to 23% (Ord, Kolokythas & Reynolds, 2006). However, the success of surgery is highly dependent on the surgeon alone, due to the surgical margin effect. It was reported that microscopic tumour located close to or at the inked resection margin, which is under full control of a surgeon, will increase recurrence rate at least by a factor of two (Binahmed, Nason & Abdoh, 2007). Furthermore, surgery often results in loss of function in certain organs, such as tongue for speech and swallowing (Tei, Maekawa, Kitada, Ohiro, Yamazaki & Totsuka, 2007), or serious complication such as infection of wound (McGurk, Fan, MacBean & Putcha, 2007; Belusic-Gobic, Car, Juretic,Cerovic, Gobic, Golubovic, 2007). A new approach called laser microsurgery emerged in early 2000's, designed to reduce morbidity and preserve function of organs, yet, the cure rate does not improve significantly compared to conventional surgery (Gottschlich & Ambrosch,2004; Yao *et al*., 2007).

Since Emil Grubbé first used the X-ray to treat a breast cancer patient in 1896, radiotherapy had been a standard treatment in modern clinical use (Bernier, Hall & Giaccia, 2004). It is not only offered as primary treatment but also as adjuvant treatment for unresectable tumour, such as locoregional reccurrence (Dinshaw, Agarwal, Ghosh-Laskar, Gupta & Shrivastava, 2006). Current ideology of radiotherapy on cancer is based on hyperfractionation, where the tumour is irradiated multiple times with smaller. This helps to

increase the total concentration applied, but minimizes the morbidity associated with a single large concentration (Bernier *et al*., 2004). Complications of radiotherapy such as mucositis or dermatitis are prevalent among patients, leading towards longer hospitalization or longer recovery time (Dinshaw *et al*., 2006).

Chemotherapy is rarely used alone in oral cancer treatment but more as palliation or neoadjuvant treatment, to reduce the size of tumour before operation, or adjuvant treatment after a dissection of tumour (Forshaw, *et al*.,2006; Gebski, Burmeister, Smithers, Foo, Zalcberg & Simes, 2007). The drug regimen includes methotrexate, cisplatin, 5FU bleomycin and vinblastine (Barr, Cowan & Nicolson, 1997). Conventional chemotherapeutic agents are commonly applied in high concentration to kill rapidly dividing tumour cells. Even though most of normal cells are not dividing, such characteristic is capable to induce serious side effect on rapidly dividing normal cells of epidermis, as well as causing systemic toxicity (Symonds & Foweraker, 2006; Lind, 2007). Newer chemotherapeutic agents focus on molecular target, inhibiting specific protein in tumourigenesis pathway or inducing protein in cell death pathway. The major drawback for such drugs is the delivery method to its legitimate target (Wu, Lee, Lu & Lee, 2007).

Nevertheless, combination therapy is now the trend in cancer treatment. Instead of standing alone, three of these major approaches often compliment each other in clinical setting (Yao *et al*., 2007).

2.4   Chemotherapy : A Conventional Way

2.4.1   Brief History of Chemotherapy

The age of chemotherapy started when Goodman and Gilman first use nitrogen mustard to treat a non-Hodgkin's lymphoma in 1942. Even though the remission of tumour is short-termed, the principle of chemotherapy was established. Systemic injection of drugs to induce tumour regression broke the monopoly of surgery and radiotherapy in cancer treatment since then (Chabner & Roberts, 2005). Shortly after World War II, Sydney Farber discovered the relationship of folic acid with the proliferation of acute lymphoblastic leukemia (ALL). This effort brought the discovery of first anticancer drug, amethopterin (methotrexate), which was able to induce remission in children with ALL, in 1948. The first human solid tumour was reported to be cured with methotrexate in 1958 **(**Villela, Stanford & Shah, 2006**).** Several attempts were carried out to decipher the mechanism of action for methotrexate. It was understood only in late 1950's, methotrexate specifically inhibits dihydrofolate reductase (DHFR). However, these mechanistic studies provided a fundamental understanding of pharmacological principles on cancer chemotherapy (Chabner & Roberts, 2005).

The age of modern chemotherapy began from 1960's when more and more new drugs came to clinical trials. National Cancer Institute of United States played a central role in searching for new drug candidates (Chabner & Roberts, 2005). In 1963, Johnson and colleagues discovered vinca alkaloid, which is able to block microtubule polymerization and cell division (Johnson,

Armstrong, Goman & Burnett, 1963). In 1965, Rosenberg and colleagues found cisplatin through an experiment to inhibit *Escherichia coli* cell division (Rosenberg,Van Camp & Krigas, 1965). Combination chemotherapy for cancer came into application with the formation of earliest regimens such as, POMP (methotrexate, vincristine, 6-mecarptourine and prednisone) and MOPP (nitrogen mustard, vincristine, procarbazine and prednisone) (Frei *et al.*, 1965; Moxley, De Vita, Brace & Frei, 1967), with mixture of drugs that has minimal overlapping toxicity (Thomas, Sharma & Steward, 2006). Simultaneously, the principle of high concentration chemotherapy, proposed by Schabel and Skipper in 1960's, had its stand until today (Chabner & Roberts, 2005).

Modern chemotherapy slowly transformed into targeted chemotherapy with the increasing understanding of tumour metabolism and discovery of growth factor, signaling molecule, cell cycle proteins, modulator of apoptosis and angiogenesis promoter (Hanahan & Weinberg, 2000). For example, the discovery of Judah Folkman and colleagues on the role of angiogenesis in cancer proliferation and metastasis led to the discovery of VEGF (Vascular Endothelial Growth Factor)-inhibitors (Lucchi *et al.*, 1997).

2.4.2   Categories of Chemotherapeutic Agents

Majority of current chemotherapeutic agents can be divided into several major categories including, antimetabolites, mitotic inhibitors,

topoisomerase inhibitors, alkylating agents and platinum compounds.

Methotrexate was one of the first anticancer drugs developed in 1940's. It is a folate antagonist, which specifically targets dihydrofolate reductase (DHFR) (Volpato, Fossati & Pelletier, 2007). Methotrexate depends on active transport by reduced-folate transporter 1 to condense inside the cell. It will be converted into methotrexate-polyglutamate complex within the cell and then bind to DHFR, leading to inhibition of thymidylate and purines (Chabner & Roberts, 2005). Other examples of antimetabolites currently in use are cytosine arabinoside (arabinosides), 6-mercaptopurine (antipurines) and 5-Fluorouracil (antipyrimidines) (Thomas *et al*., 2006).

Vinblastine, a microtubule inhibitor, comes from periwinkle plant *Catharanthus roseus* and has been used in cancer treatment for the past 30 years. It binds to tubulin, destabilizing microtubules, leading to M-phase cell cycle arrest and apoptosis in the end. Therefore, it is commonly viewed as a cytostatic agent rather than cytotoxic agent in cancer treatment (Kavallaris, Verrills & Hill, 2001; Duan, Sterba, Kolomeichuk, Kim, Brown & Chambers, 2007). Other than vinca alkaloid, paclitaxel and docetaxel are other mitotic inhibitors in clinical use (Thomas *et al*., 2006).

Doxorubicin, another powerful chemotherapeutic agent that had been in clinical use since late 1960s, is an anthracycline antibiotic capable of inhibiting topoisomerase II and intercalating DNA, causing apoptosis in many types of cancer (Torkarska-Schlattner *et al*., 2006). Etoposide is another type

of topoisomerase II inhibitor, whereas camptothecin is topoisomerase I inhibitor (Thomas *et al*., 2006).

Cisplatin or cis-diammine-dichloroplatinum(II), a platinum-based compound commonly used in treatment against several type of cancers for more than 30 years (Rabik & Dolan,2007). It is a DNA alkylating agent that crosslinks intra-strand guanine bases, thus, inhibiting DNA replication (Chevalier & Soria, 2004). Carboplatin and oxaliplatin are improved version of platinum alkalyting agents (Thomas *et al*., 2006).

2.4.3   Pros & Cons of Chemotherapy

Chemotherapy is a systemic treatment suitable for virtually all stage of tumours due to its nature of circulation throughout the body. Palliative chemotherapy is the standard treatment available to metastasized cancer when surgery and radiotherapy are no longer a reasonable option (Adelstein, Tan & Lavertu, 1996). Application of chemotherapy does not require expensive machine. It can be applied intravenously or orally to the patients. Other than being use as single modality, chemotherapy is compliment to conventional treatments, such as the use of neoadjuvant chemotherapy to reduce the volume of solid tumour prior to surgery or radiotherapy and the use of adjuvant chemotherapy after surgery or radiotherapy to reduce the risk of recurrence (Thomas *et al*., 2006).

However, non-specific cell killing to other proliferating tissue and relatively long treatment cycle increase the overall morbidity of treatment (Boyer & Tannock, 2005). Other than that, the clinical efficacy of high-concentration chemotherapy is limited by its toxicities or side effects to patient and multidrug-resistance (MDR) phenotype by tumour cells (Katabami *et al*. 1992; Rabik & Dolan,2007, Nielsen, Maare & Skovsgaard, 1996).

Cisplatin-based chemotherapy is accompanied with ototoxicity , nephrotoxicity and peripheral neurotoxicity in patients (Rabik & Dolan,2007). The inevitable drawback of doxorubicin is related to its concentration-dependent cardiotoxicity, limiting its cumulative concentration in clinical application (Christiansen & Autschbach, 2006) while vinblastine is related to myelosuppression and neurotoxicities in clinical use (Hait, Rubin, Alli & Goodin,2007).

On the other hand, cisplatin-resistance occurred through inactivation by antioxidants or adapted reduced accumulation in cells (Rabik & Dolan, 2007) and more prominently, by the increased rate of nucleotide excision repair (NER) controlled by a key gene called excision repair cross complementation group-1 (*ERCC1*) (Ferry, Hamilton & Johnson, 2000; Gossage & Madhusudan, 2007). Doxorubicin and vinblastine resistance was suggested to be the result on the overexpression of MDR proteins such as P-glycoprotein (PGP) (Nielsen, Maare & Skovsgaard, 1996) or c-Jun (Duan *et al*., 2007).

2.5   Photodynamic Therapy (PDT)

2.5.1   Brief History of Photodynamic Therapy

The use of visible light as therapeutic agent could be dated back to thousands years ago. Ancient Egyptian, Indian and Chinese civilizations used light to treat vitiligo, rickets, psoriasis and skin cancer (Dolmans, Fukumura & Jain, 2003). Greeks in ancient times exposed their entire body to sun in the occurrence of disease. The Greek physician, Herodotus, who was regarded as the father of heliotherapy, proposed sun exposure as an essential way for restoration of health. However, the use of light only gained clinical attention toward the end of the 19th century (Ackroyd, Kelty, Brown & Reed, 2001).

Early use of light in clinical setting was termed phototherapy, which was developed by a Danish physician, Niel Finsen, who described the use of red light to treat smallpox. This finding brought Finsen a Nobel Prize in 1903 and marked the beginning of modern light therapy (Spikes, 1997; Bonnett, 2000).

The earliest record showing that chemicals irradiated with light could induce cell death was a serendipitous discovery by Oscar Raab, a German medical student in 1900. Raab observed death of paramecium with presence of acridine red when he performed the experiment in a thunderstorm that changed the ambient light condition (Ackroyd, Kelty, Brown & Reed, 2001; Kessel, 2004). In the same year, the first case of photosensitizer application on human was reported by Prime, a French neurologist, who used oral eosin to

treat epilepsy. Prime found patients developed dermatitis in sun-exposed areas of the body (Ackroyd, Kelty, Brown & Reed, 2001). These discoveries led von Tappeiner, in 1903, working together with Jasionek, a dermatologist, to study topical application of eosin with presence of white light to treat skin cancer. In 1907, together with Jodbauer, von Tappeiner showed the involvement of oxygen in photosensitization reaction and they regarded this phenomenon as "Photodynamic Action" (Dolmans, Fukumura & Jain, 2003).

The most studied photosensitizer is porphyrins. Scherer was the first to produce hematoporphyrin in 1841 when he was exploring the nature of blood. Hausmann of Vienna then reported the effect of light and hematoporphyrin application on paramecium and mice in 1911 (Spikes, 1997; Ackroyd, Kelty, Brown & Reed, 2001). Freidrich Meyer-Betz was the first to investigate the consequence of human exposure to hematoporphyrins. He injected 200mg of hematoporphyrins into himself and observed swelling and pain in light-exposed areas (Bonnett, 2000). The ability of photosensitizer to localize in malignant tumour was then reported in 1924 and 1942 (Ackroyd, Kelty, Brown & Reed, 2001).

In 1972, Diamond and colleagues from San Francisco first proposed the use of phototoxic and tumour-localizing properties of hematoporphyrin derivatives (HPD) in treatment of cancer and coined the term "Photodynamic Therapy (PDT)". Later in 1975, Dougherty and co-workers demonstrated the use of HPD and red light to eradicate breast cancer in mice. In the same year, Kelly and co-workers reported similar result in bladder cancer and in 1976 he

initiated the first human trial with HPD. Since 1980s, PDT was studied in many human tumours such as tumour of eosophagus, lung, stomach, head and neck, breast and brain (Ackroyd, Kelty, Brown & Reed, 2001; Kessel, 2004).

PDT was first approved by Canada in 1993 in which Photofrin® (HPD) was allowed in treatment of bladder cancer. Subsequent approval of Photofrin® was granted in several other countries including France, Germany, Japan, Netherlands, United States and European Union(EU)(Allison, Mota & Sibata, 2004; Mitton & Ackroyd, 2005). By 2003, two more photosensitizers, Metrix® (5-aminolevulinic acid) and Foscan® (metatetrahydroxyphenylchlorin), passed the clinical trials and was approved by European Union (Dolmans, Fukumura & Jain, 2003).

2.5.1.1 Non-oncologic Application of Photodynamic Therapy

Apart from oncologic application of photodymanic therapy, interesting to mention, photodynamic therapy is even more extensively used in treatment of age-related macular degeneration (AMD), which is a leading cause of irreversible blindness in developed countries including United States. Starting from April 2000, Verteporfin-mediated PDT (Visudyne®) is approved for clinical application due to its superiority in reducing vision loss after treatment compared to previous modalities such as thermal laser therapy and surgery (Ambati, Ambati, Yoo, Ianchulev & Adamis, 2003; Gohel, Mandava, Olson & Durairaj, 2008).

Photodynamic therapy is viewed as a modality with lower toxicity effect on patient. Although another modality with higher efficiency called antiangiogenic therapy that involves down-regulation of Vascular endothelial growth factor (VEGF) was introduced later in 2005 with the introduction of anti-VEGF drugs such as Bevacizumab or Ranibizumab, photodynamic therapy remains as a beneficial combination option in AMD treatment (Gohel, Mandava, Olson & Durairaj, 2008;).

For example, a study on more than 1000 patients in United States concluded that combination of Verteporfin-PDT and Bevacizumab leads to vision benefit in AMD for most patients, especially for those who never received any form of treatment (Kaiser, 2009). Another drugs combinatorial study on AMD treatment in Unites States using Verteporfin-PDT and Ranibizumab also reported better effectiveness and lower rate of adverse effects (Antoszyk, Tuomi, Chung. & Singh,2008).

2.5.2 Mechanism of PDT action

Upon irradiation by light, a photosensitizer is excited from ground state (S0) to first excited single state (S1) and then to first excited triplet state (T1) with longer lifetime via intersystem crossing. Many believe the excited triplet state of photosensitizer can react in two ways, namely Type I and Type

II mechanism, as shown in Figure 2.1 (Ochsner, 1997; Schmidt-Erfurth,U. & Hasan, 2000).

In Type I mechanism (Electron Transfer Mechanism), electron transfer occurs among the excited triplets with a substrate. The substrate can be another photosensitizer triplet or biological substance. Such reactions give free radicals and radical ions. These free radical species react with molecular oxygen, generating reactive oxygen species (ROS) such as superoxide anions or hydroxyl radicals (Sharman, Allen & Lier, 1999; Guedes & Eriksson, 2005). These ROS are responsible for oxidative damage in target cells. After reaction with molecular oxygen, the photosensitizer radicals revert to its ground state, in which the whole process can be repeatedly performed with light excitation (Sharman, Allen & Lier, 1999; Chen *et al.*, 2010).

In contrast, Type II mechanism (Energy Transfer mechanism) involves a straightforward energy transfer of triplet state photosensitizer to ground state molecular oxygen, generating zwitterionic singlet oxygen, which in turn, causing oxidative damage in target cells (Fernandez, Bilgin & Grossweiner, 1997). Triplet state photosensitizer losing its energy will then return to its ground state, ready for another excitation (Bonnett, 2000).

Apart from Type I and Type II mechanism, an additional Type III mechanism (Photobinding Mechanism) has been suggested. In Type III mechanism, the first excited first excited single state (S1) of photosensitizer directly donates its excitation energy to DNA, forming cycloadducts,

producing intercalation effect or causing cross-linking of DNA (Llano, Raber & Eriksson ,2003).

Among these mechanisms, however, it is generally accepted that Type II mechanism or singlet oxygen production predominates during PDT (Sharman, Allen & Lier, 1999).
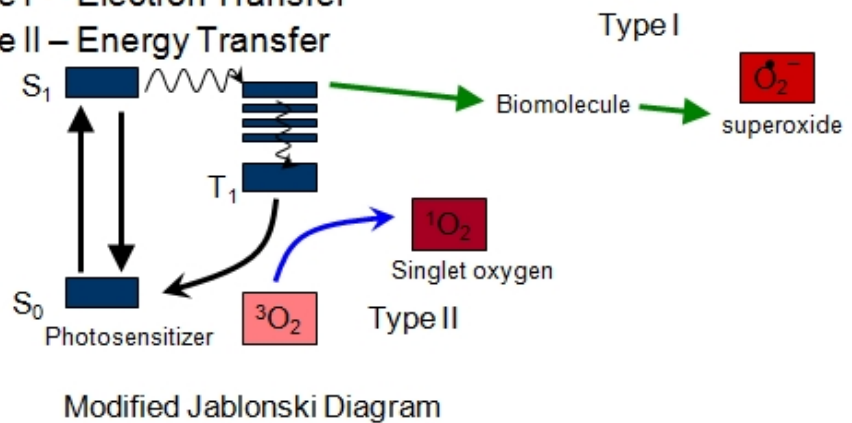
Figure 2.1   Singlet O2 act on unsaturated lipids, cholesterol,α-amino acids, purine bases. Lifetime of singlet O2 is less than 0.04μs and the diffusion pathlength is less than 0.02 μm (Moan & Berg, 1991).

2.5.3   Light Sources & Delivery Approaches

PDT requires precise light dosimetry in application (Shmidt-Erfurth & Hasan, 2000). Light concentration, in photomedicine, refers to the amount of light arriving at the surface of target cells layer, which can be measured with commercial light meter. In PDT, the quantity of light is usually recorded as

fluence and fluence rate. Fluence is the total light energy arriving at a unit surface area of a target (unit: J cm^{-2}). On the other hand, fluence rate is the rate of energy or power density (unit: W cm^{-2}) (Bonnett, 2000).

In PDT, although many light sources can be used, the laser is most recommended as a standard light source. In the context of precise light dosimetry, laser is intense, adjustable, coherent, monochromatic and can be focused and transmitted using various light delivery system such as optic fiber, which can help in light delivery. Among the ranges of laser, diode lasers are the best choice. They are light, portable, reliable and relatively inexpensive compared to other types of laser (Shmidt-Erfurth & Hasan, 2000).

Lasers, however, are still relatively expensive to maintain. Therefore, alternative light sources, for examples, incandescent lamps and arc lamps, are used by many (Whitehurst, Byrne & Moore, 1993; Szeimies, Hein, Baumler, Heine & Landthaler, 1994). In general, the light wavelengths of PDT fall in between 600nm and 900nm. At wavelengths lower than 600nm, light scattering increases in target tissue while at wavelength higher than 900nm, water absorption predominates (Shmidt-Erfurth & Hasan, 2000). In order for incandescent lamps or arc lamps to function, proper light wavelength filters and power rheostat are needed (Stable & Ash, 1995).

2.5.4 Photodynamic Therapy: Advantages and Limitations

In oncology, the mainstay treatments for cancers are still surgery, radiotherapy and chemotherapy. Yet, these treatments often bring relatively higher rate of complications (Nyst, Tan, Stewart & Balm, 2009). Therefore, PDT is another choice of treatment with minimal complication considerations. The advantages of PDT include low toxicity and high specificity. It can be repeated multiple times without inducing cumulative toxicity or resistance and can be combined to primary modality as neoadjuvant, adjuvant or intraoperative treatments (Radu *et al.*, 2005). It can be applied as neoadjuvant treatment before the mainstay treatments or adjuvant treatment after the mainstay treatments (Hopper, 2000; Brown, Brown & Walker, 2004). The non-invasive characteristic of PDT gives excellent functional and cosmetic outcomes with lower morbidity. These characteristic made PDT an excellent treatment for small localized superficial tumour on skin. Furthermore, PDT also works in pleural and peritoneum areas where the underlying tissues are unable to tolerate curative radiation concentrations. In large tumours, light can be directed straight into the tumour with interstitial light delivery method, down-sizing the affected tissue area in surgical resection (Hopper, 2000). Unlike chemotherapy or radiotherapy, which can generally be employed once, PDT can be applied several times without compromising future treatment options for recurrent and residual tumour. These properties contribute to improvement in quality of life after patients' treatment cycles (Hopper, 2000; Nyst, Tan, Stewart & Balm, 2009).

In contrast, PDT has limitation in treating disseminated tumours because light irradiation to whole body with effective dosage is not available (Brown, Brown & Walker, 2004). In systemic treatment using PDT, exposure to sunlight often produces normal skin sensitization, causing serious dermal side effects such as large-scale erythema, oedema, urticarial lesions and pruritus (Ochsner, 1997). Due to hypoxic condition within the large tumour, PDT is less effective against large tumours (Delaey, Vandenbogaerde, Merlevede & de Witte, 2000). At the same time, current clinically approved photosensitizers have absorption peak below 700nm. At light wavelength below 700nm, light only penetrates few millimeter through tissue, limiting PDT application to smaller tumours found closer to the surface (Chatterjee, Fong & Zhang, 2008).

2.5.5   Photosensitizer

Photosensitizers are classified into three generations (DeRosa & Crutchley, 2002). First generation represents Haematoporphyrin derivative (HPD) and its analogues. Photofrin® is one of the clinically approved first generation photosensitizer (Bonnett, 2000). The chemical structure of Photofrin® is shown in Figure 2.2 below.
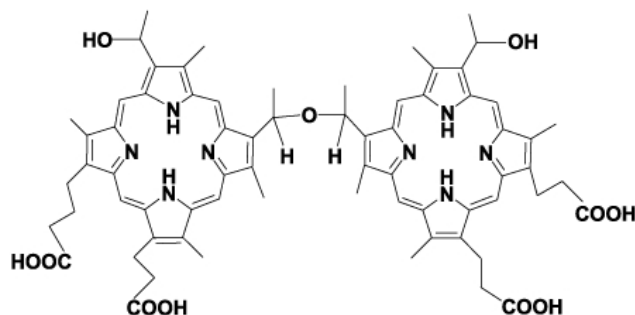
Figure 2.2   Structure of Photofrin ®, a first generation photosensitizer.

Unlike first generation photosensitizers, second generation photosensitizers are structurally distinctive from HPD and they are not a mixture of compounds (DeRosa & Crutchley, 2002). They have greater selectivity for tumour tissue and shorter retention time in body. Furthermore, second generation photosensitizers absorb light at long-wavelength (675nm - 800nm), which allow light penetration of 2-3cm through tissue (Bonnett, 2000). Two examples of second generation photosensitizer are Foscan® and Visudyne®. Both of their chemical structures are shown in Figure 2.3.
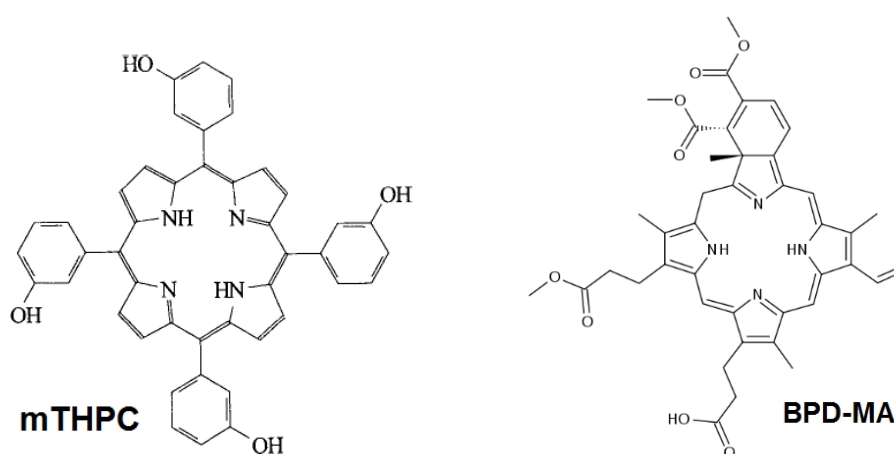
Figure 2.3   Structure of mTHPC (Foscan ®) and BPD-MA (Visudyne®).

In contrast, third generation photosensitizers are second generation photosensizers bound to carriers for selective accumulation in tumour tissue (DeRosa & Crutchley, 2002). One example is Luzitins® in Figure 2.4 below.
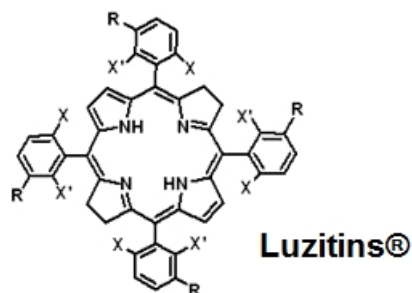
Figure 2.4   Structure of Luzitins®, a third-generation photosensitizer in development.

2.5.6   Hypericin

Hypericin, a natural polycyclic quinone (naphthodianthrone) derived from plants of *Hypericum* species, is a second generation photosensitizer (Figure 2.5). The most well-known within the genus is *Hypericum perforatum* or St. John's wort, a perennial herb with golden yellow flowers, growing to a height of 30–90 cm (Sharman, Allen & van Lier, 1999; Agostinis *et al*., 2002; Guedes & Eriksson, 2005).
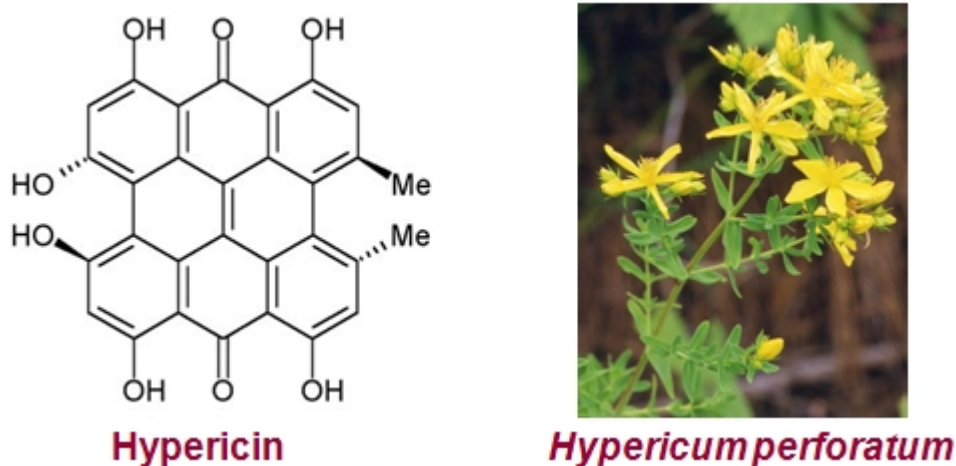
Figure 2.5   The chemical structure of Hypericin. Hypericin originated from flowering plant called *Hypericum perforatum*.

Hypericin is a potent photosensitizer with high singlet oxygen quantum yield and minimal dark toxicity (DeRosa & Crutchley, 2002). It has λ_{max} at 590nm and φ_Δ of 0.36 in ethanol (Bonnett, 2000). Although hypericin exhibits photocytotoxicity by impairing bioenergetic pathway of mitochondria, it was suggested that hypericin does not accumulate in mitochondria. Subcellular localization of hypericin was reported in the membranes of endoplasmic reticulum and Golgi complex. In other studies, hypericin was also found to localize in plasma membrane and nuclear membrane (Agostinis *et al*., 2002).

Hypericin-mediated PDT is oxygen dependant. It may cause apoptosis and necrosis. A shift toward necrosis appears when hypericin concentration or light concentration is increased. On the other hand, it was suggested that photosensitizers localizing to mitochondria promote apoptosis while photosensitizers targeting plasma membrane or lysosomes are favorable to necrosis (Agostinis *et al*., 2002).

The uptake of hypericin by cells was suggested to involve membrane-associated intracellular translocation processes. Hypericin appears as monobasic salt in physiological condition. In contact with cell membrane, it will be taken up by cellular lipid membrane and form lipophilic ion pairs. Hydrophobic characteristic allows hypericin to accumulate inside cell in a time dependant manner (2-4 hours) (Agostinis *et al.*, 2002).

Hypericin entered Phase III clinical trial for topical phototherapy of cutaneous T-cell lymphoma (CTCL) in 2008.

2.6   Combination Treatment

Oncogenesis is multigenic and most cancers accumulate four to seven mutations. Even cancers that arise from single molecular abnormality can develop resistance to agents targeting that locus. Therefore, treatment targeting only one pathway may not be effective in cancer therapy. In contrast, combination drugs targeting multiple targets simultaneously are better in controlling complex disease systems (Jackman, Kaye & Workman, 2004; Zimmermann *et al.*, 2007; Sarkar & Li, 2009). Compared to single drug treatment, it is relatively more difficult for biological system to compensate the action of two or more drugs at the same time, thus, reducing probability to develop adaptive resistance. (Zimmermann *et al.*, 2007). For example, Cao and colleagues showed TNF- α and doxorubicin together alleviates resistance of MCF-7/Adr cells in combination treatment. (Cao, Ma, Tang, Shi & Lu,

2006). Furthermore, Khdair and co-workers (2009) group of researchers recently showed combination of chemotherapy and PDT overcome tumour drug resistance *in vivo* (Khdair *et al*., 2009).

Combination tests using clinically approved drugs with known targets may reveal unexpected interaction between disease pathways and potential synergy between the drugs. Thus, these findings can rapidly move into clinical setting (Zimmermann *et al*., 2007). Several *in vivo* experiments showed synergy of combination treatment. Combination of doxorubicin with PDT was shown to give synergistic effect at killing lung cancer in mouse (Streckyte *et al*., 1999). Inhibition of epidermal growth factor receptor in conjunction with PDT also exhibited synergism on ovarian cancer in *vivo* (del Carmen *et al*., 2005).

High concentration chemotherapy is still the mainstay in cancer treatment. However, the side effect accompanied such treatment is often intense (Symonds & Foweraker, 2006; Lind, 2007). Combination treatment may have potential in lowering dosage in treatment while still providing similar or greater cell killing effect with lesser side effects (Jackman, Kaye & Workman, 2004). For instance, Nonaka and colleagues demonstrated Photofrin ® -PDT and cisplatin in combination enchanced cytotoxicity on lyphoma cell using lower effective dosage (Nonaka, Ikeda & Inokuchi, 2002).

Drugs for combination can be selected from clinically approved agents where the properties had already been extensively studied, indirectly saving

the cost for new drugs discovery. *In vitro* test of various drugs combinations continues to be an easiest way to explore molecular mechanism that combine to produce synergistic effects (Zimmermann *et al*., 2007).

2.6.1 Drugs Interaction: Synergy, Antagonism & Additivity

Synergy and antagonism refer to cell response rate (for eg. cytotoxicity or growth inhibition), when treated with a combination of drugs, that is greater or lesser than expected from independent drug action, respectively. Additivity occurs when the drug components in a combination work independently and contribute equally to the action. Apart from synergy, additivity response may help to reduce drugs toxicity by allowing concentration reduction while still maintaining same effectiveness (Jackman, Kaye & Workman, 2004).

2.6.2 Evaluating Drugs Interaction in Combination Therapy

Generally, any two anticancer drugs can yield a pair for combination test. In the search for feasible drug combinations, ability to compare efficiently the activity of a drug combination with its component independently is emphasized. Synergistic drugs interaction can occur over a range of concentrations, which means that a systematic search of synergistic combinations involves testing of both independent drugs in several different ratios. In such circumstance, a concentration-response matrix design with cell-

based assays, taking in all possible pairing of serially diluted independent drugs, provides an easy way to investigate the interaction of molecular target in biological networks (Zimmermann *et al.*, 2007).

Concentration-response matrix, however, generates huge amount of data which requires further method of drugs interaction analysis. A graphical method called isobolographic analysis is classical method for such analysis. Isobolographic analysis involves construction of a plot called isobologram. It was first introduced by Fraser early in 1870's. This method was extended by Loewe and Muischnek (1926), Loewe (1953) and Berenbaum (1981) and reviewed by Gressner (1974), Wessinger(1976) and Berenbaum (1989) (Meadows, Gennings, Carter Jr. & Bae, 2002, 2nd degree reference).

In an isobologram (Figure 2.6), equieffective pairs of drug X and drug Y concentrations are represented using rectangular coordinates (x,y). Concentration of drug X alone (x) and Y alone(y), both with a fixed response rate, for example, IC_{50}, are represented as axial point (x,0) and (0,y) respectively. The straight line connecting both of these points is named "line of additivity". By plotting different concentration of combination that yield IC_{50} in the isobologram, analysis can be done by checking whether the coordinate of IC_{50} combination falls on (additive), below (synergistic) or above (less than additive) the line of additivity (Tallarida & Raffa, 1996). Several coordinates of combinations in different ratios can be plotted in one isobologram to generate an isoeffective-curve to reveal a range of ratios that give synergistic response (Gressner, 1995).

Due to its nature of graphical presentation, isobologram is limited in the analysis of two to three drugs combination (Meadows, Gennings, Carter Jr. & Bae, 2002). Furthermore, isobolographic method can only illustrate a fix response level at a time (Martinez-Irujo, Villahermosa, Alverdi & Santiago, 1996). However, isobolographic analysis is still the simplest way to characterize the interaction between two drugs compare to non-graphical methods such as interaction index and statistical models (Meadows, Gennings, Carter Jr. & Bae, 2002).

Example of IC_{50} isobologram (Elvira *et al.*, 2004)
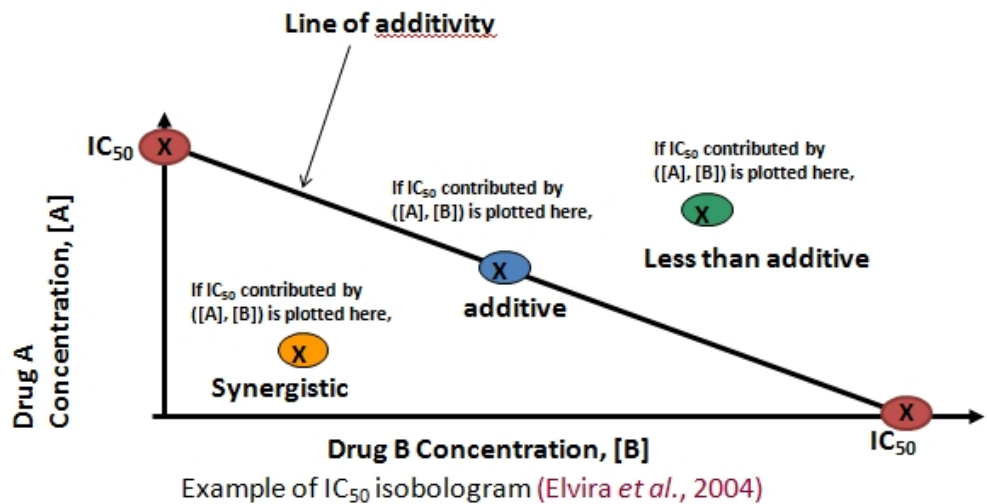
Outcome	Definition
Synergistic	[A] + [B] > sum of independent A and B (desirable)
Less than additive	[A] + [B] < sum of independent A and B (undesirable)
Additive	[A] + [B] = sum of independent A and B (desirable)

Figure 2.6   Example of IC_{50} isobologram. A line of additivity is constructed by linking IC_{50} concentration of independent drug A and independent drug B. The concentration of drug A ([A]) and concentration of drug B ([B]) that combined to give IC_{50} concentration was plotted in graph. Therefore, all points plotted in isobologram are comparable IC_{50} concentration. If the plotted point falls below the line of additivity, the combination is

synergistic. The combination is less than additive if the data point stays above the line of additivity (Elvira *et al.*, 2004).

2.7 Multiple Combination Approaches in Oral Cancer Clinical Treatment

2.7.1 Combination of Conventional Therapies

Combination of surgery and radiotherapy had been a core treatment for squamous cell carcinoma of head and neck. Radiotherapy, in particular, is often used as post-operative adjuvant treatment (Yao *et al.*, 2007). In a clinical study of more than 5000 cancer patients, researchers found that application of radiotherapy after a primary surgery significantly improved the overall survival rate of patient (Kao, Lavaf, Teng, Huang & Genden, 2008).

Combination approach by multi-agents chemotherapy aims to achieve optimal tumour killing rate, yet maintaining the toxicity induced by single agents alone, with concurrent use of efficient drugs that lack overlapping toxicity (Peters, Wilt, Moorsel, Kroep, Bergman & Ackland, 2000). For instance, the combination of cisplatin/sodium thiosulfate and vinblastine/peplomycin resulted in more than 50% complete response in oral cancer patients. However, these combinations exhibited bone marrow toxicity (Wada *et al.*, 1995; Bamias *et al.*, 2004). Another report also demonstrated that combination of cisplatin-carboplatin infusion before surgery or radiotherapy showed up to 50% complete response rate (Imal *et al.*, 1995).

Another noteworthy regimen is cisplatin-based MVAC, consisting of methotrexate, vinblastine, doxorubicin (amethopterin) and cisplatin. Each of the components in this regimen has different mechanism of actions and targets. In clinical setting, it is reported to be superior to chemotherapy with cisplatin alone, although the toxicity is higher (Soloway, Ishikawa, Taylor & Ezell, 2006). MVAC regimen is still regarded as the golden standard in treating in metastatic advanced bladder cancer (Pectasides, Pectasides, Economopoulos, 2006; Kuczyk *et al*., 2004) and cervical cancer (Long *et al*.,2006; Dowdy, Boardman, Wilson, Podratz, Hartmann & Long, 2002). It was shown to exhibit at least 75% response rates on bladder, lung, subcutaneous tissue and lymph nodes metastasis (Otani *et al.*, 1991).

There was even being reported a combination of chemotherapy and radiotherapy was able to achieve two-year survival rates from 28 to 72% in squamous cell carcinoma. The survival rates are comparable to the survival rates of surgical resection alone which is more invasive (Geh, 2002). Chemoradiotherapy is better at preservation of function by avoiding tissue resection. This provides an alternative for patients with unresectable tumour (Yao *et al*., 2007). The combination of three modalities may improve survival rate. For instance, chemoradiotherapy can be applied before a primary surgery. Anyway, all of these come with a cost. The risk of acute treatment-related toxicity increase in relative to the frequency and concentration of treatment (Geh, 2002).

2.8 Combination of Photodynamic Therapy with Conventional Therapy

2.8.1 Combination of PDT and Surgery

Combining photodynamic therapy (PDT) with conventional treatment modalities such as surgery, radiation and chemotherapy had been reported in various types of tumours (Luksiene, Kalvelyte & Supino, 1999; Ris, 2005; Zhang, Zhu, Pan, Ma & Shao, 2007).

PDT, in most cases, is combined with surgery as neoadjuvant or adjuvant treatment. Neoadjuvant PDT treatment is performed earlier than surgery with the aim of reducing tumour size prior to surgery (Berr *et al.*, 2000). Tumour with unresectable size can be down-staged with neoadjuvant chemotherapy before a surgery is performed. Clinical report by Forshaw and colleagues showed benefits of neoadjuvant chemotherapy in locally advance oesophagus carcinoma (Forshaw *et al.*, 2006). In basal cell carcinoma model, topical application of PDT prior to surgery could reduce tumour size and therefore, reducing excision defect on patients (Oakford & Keohane, 2005). Similar report was demonstrated in other types of cancer in different countries (Sugiyama, Nishida, Hasuo, Fujiyoshi & Yakushiji, 1998; Termrungruanglert, Tresukosol, Vasuratna, Sittisomwong, Lertkhachonsuk & Sirisabya, 2005).

In contrast, adjuvant PDT treatment is normally applied straight after tumour resection to suppress recurrence rate (Ris, 2005). However, the benefits are varied according to the population of patients studied and the type

of photosensitizer being used (Dilkes, DeJode, Rowntree-Taylor, McGilligan, Kenyon & McKelvie, 1996; Biel,2002).

Other than that, the fluorescent nature and the ability of photosensitizers to accumulate in tumour also permit them to be used as surgical-aid in fluorescence-guided resection of tumour. For example, Foscan®, was successfully used to determine tumour margins and detect residual tumour in clinical operation (Kostron, Fiegele & Akatuna, 2006). In oral cancer, topical application of photosensitizer, via mouth-rinsing, demonstrated selective fluorescence in tumour tissue. This approach may supplement conventional histopathology biopsy one day (Leunig *et al.*, 2001).

2.8.2   Combination of PDT and Radiotherapy

Stewart and colleagues (1998) suggested that PDT may compliment radiotherapy in treating large tumours. In several reports, photosensitizers were suggested to be used as radiosensitizers in radiotherapy (Luksiene, Kalvelyte, Supino, 1999; Kulka *et al.*, 2003). Luksiene and colleagues demonstrated in murine breast cancer model, where combination of photosensitizer with gamma irradiation produced an additive effect *in vivo*. The additive effects were not dependent on the administration sequence of each treatment (Luksiene, Kalvelyte, Supino, 1999). However, the ability of photosensitizer to act as radiosensitizer greatly depended on cell type studied. Out of three *in vitro* models tested (colon cancer, bladder cancer,

glioblastoma), colon cancer model did not response well to the combination of Photofrin-PDT and radiotherapy (Kulka *et al.*, 2003).

Nonetheless, radiotherapy can also act as adjuvant therapy to PDT. Corti and colleagues reported a 45% increase in complete response rate when radiotherapy was given subsequently to PDT in inoperable early esophageal cancer patients (Corti *et al.*, 2000).

2.8.3   Combination of PDT and Chemotherapy

Chemotherapy is associated with significant side effects while PDT is a low morbidity, repeatable treatment in cancer. Despite of high-concentration related side effect, chemotherapy time-proven efficacy makes it inevitable in some cancer treatments. Therefore, combination with PDT may solve this problem (Brown, Brown & Walker, 2004). Throughout the years, many had reported efficacy of combination PDT-Chemotherapy *in vitro* and *in vivo*. These studies demonstrated feasibility of PDT to be used in combination with chemotherapy in oral cancer treatment (Streckyte *et al.*,1999; Chen, Chiang, Kuo, 2005; Akita *et al.*,2006; Kleban *et al.*,2006; Uehara, Inokuchi & Ikeda, 2006).

In *in vitro* models, combinations of 5-Aminolaevulinic acid (ALA)-based PDT with calcipotriol (analogue of vitamin D3) or Cyclooxygenase-2 (COX-2) inhibitor were shown to induced synergistic cell killing effects against human squamous carcinoma cells (Akita *et al.*,2004; Akita *et*

al.,,2006). Chen & colleagues showed a similar result when they used commercial available COX-2 selective inhibitor, Celebrex, together with ALA-based PDT in different types of oral squamous carcinoma cell lines (Chen, Chiang, Kuo, 2005). These results supported earlier observation by Kelley and colleagues that combination of iron and ascorbate with photofrin in oral cancer cell model required lower concentration of photofrin to achieve similar result when compared with just photofrin alone (Kelley, Domann, Buettner, Oberley & Burns, 1997).

In vivo studies incorporating chemotherapy, especially cisplatin and doxorubicin, with PDT were reported by several groups on different cancer models (Casas, Fukuda, Riley & Batlle, 1997; Canti, Nicolin, Cubeddu, Taroni, Bandieramonte & Valentini, 1998; Streckyte *et al.*, 1999; Uehara, Inokuchi & Ikeda, 2006). These studies concluded that – PDT was able to reduce the working concentration of cisplatin used, yet still achieve comparable treatment results. This could result in lower morbidity of overall treatment (Canti, Nicolin, Cubeddu, Taroni, Bandieramonte & Valentini, 1998; Uehara, Inokuchi & Ikeda,2006). Casas and colleagues also reported enhancement of PDT with prior application of doxorubicin. They speculated that this might in part due to the weakening of cellular defense by free radical generated from doxorubicin before aminolevulinic acid (ALA)-based PDT (Casas, Fukuda, Riley & Batlle, 1997). In similar study, Streckyte and colleagues pointed out that the combination sequence of doxorubicin and ALA-based PDT greatly influenced the outcome (Streckyte *et al.*, 1999).

Clinical combination of PDT and chemotherapy is not yet in the mainstream. The hindrances of such advancement included difficulty in establishing optimum variables of components in PDT and high capital cost for laser source (Brown, Brown & Walker, 2004). Nonetheless, there were a few attempts in recent years to combine PDT with chemotherapy in a clinical setting. Szyhula and colleagues reported that PDT in conjunction with conventional BCG-therapy gave improved response rate for recurrent bladder cancer in a two years follow-up study (Szygula *et al*., 2004). Another study reported that combination of PDT with 5-fluorouracil improved therapeutic effect of treatment in esophagocardiac cancer (Zhang, Zhu, Pan, Ma, Shao, 2007).

Therefore, combination of PDT with chemotherapy for the aim of clinical use is still an attractive option to be explored.

2.9   Modes of Cell Death

2.9.1   Autophagy

Among three types of cell death, autophagy plays a recycler role. It is evolutionarily conserved to be initiated by cellular stress associated with nutrient deprivation. In times of famine, double membrane vesicle (autophagosomes) forms in the cytosol that encapsulates all organelles and cytoplasm. Autophagosomes will fuse with lysosome to form autolysosomes (Festjens, Berghe & Vandenabeele, 2006). Eventually, the whole cell is

degraded and recycled into nutrients. However, based on evidence from yeast, slime molds, nematodes and plants, autophagy is believed to be a survival strategy rather than a mechanism of cell death (Edinger & Thompson, 2004).

2.9.2   Necrosis : Passive Cell Death or Programmed Necrosis?

Necrosis is characterized morphologically by swelling of cell, vacuolation of cytoplasm and eventually, rupture of plasma membrane (Figure 2.7). The cellular content leaking into extracellular environment will induce increment in proinflammatory cytokine secretion from independently activated macrophages, leading to local inflammatory response (Festjens, Berghe & Vandenabeele, 2006). Under severe conditions, cells die through rapid unregulated breakdown of membranes, accompanied by rapid disruption of cytoplasmic structure and nucleaus. These observations once led to the assumption that necrosis cell death is passive and unregulated. However, studies showing the involvement of regulated necrosis in physiological and pathological conditions, for example, renewal of small intestine and the activation-induced death of primary T lymphocytes suggest that some aspects of necrosis may also be programmed (Proskuryakov, Konoplyannikov & Gabai, 2003).
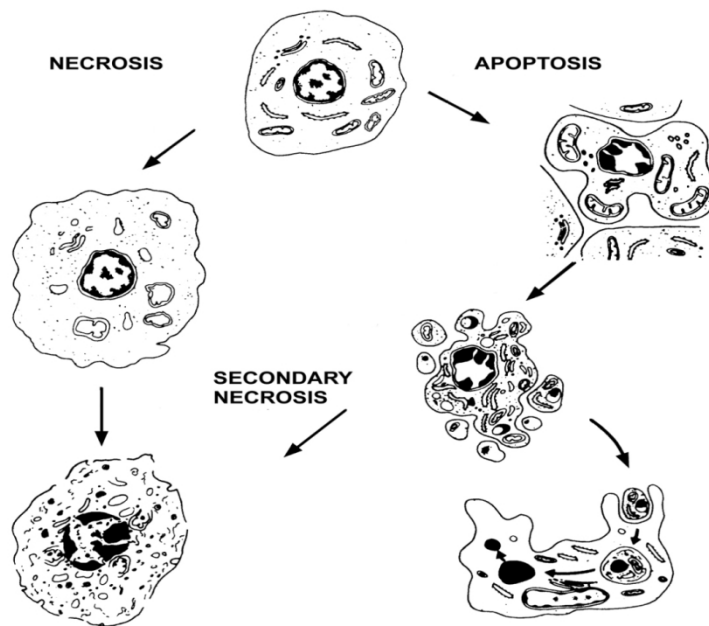
Figure 2.7   Differences of apoptosis and necrosis.

Necrosis is the result of extensive crosstalk between several biochemical and molecular events at different cellular level. It is characterized by three consecutive phases: initiation, propagation and execution (Festjens, Berghe & Vandenabeele, 2006). RIP1, PARP, CypD, calpains and cathepsins are several key components involved in the initiation, whereas, RIP1 plays the key role as central initiator. Calcium and reactive oxygen species (ROS) will then take part in propagation and execution phases, causing damages to protein, lipid and DNA, leading to disruption of cell integrity (Festjens, Berghe & Vandenabeele, 2006; Golstein & Kroemer, 2006).

2.9.3 Apoptosis : Programmed Cell Death

Apoptosis, in Greek, means "falling of petals or leaves from trees", is a term used to describe programmed cell death in distinctive phenotype different from traumatic cell death such as necrosis. It was first described by John Kerr, Andrew Wyllie and Alastair Currie in 1972. Instead of increased mitosis, it was proposed that the impairment of genetically regulated cell-suicide program, leading to decreased cell death breaks the balance between proliferation and death and might be responsible for the formation of neoplasia. (Kerr, Wyllie and Currie, 1972; Wyllie, Kerr & Currie, 1980; Rudin & Thompson, 2002).

Apoptosis is widely recognized for its physiological importance in natural homeostasis, turnover of tissues, development of embryo or tissue and lymphocytes interaction (McConkey, Zhivotovsky & Orrenius, 1996). Defective in apoptosis regulation was found to link with the pathogenesis of several diseases such as cancer (Holdenrieder & Stieber, 2004; Makin & Dive, 2001), viral infection (Wang *et al.*, 2006; Yoshizaki *et al.*,2007), autoimmune diseases (Gougeon & Montagnier, 1993; Mountz, Wu, Cheng & Zhou,1994) and neuropsychiatric disorders (Margolis, Chuang & Post,1994).

Apoptosis can be characterized into 3 phases: initiation, effector phase and degradation, each involves different protein in caspase family. Initiation phase involves oxidative stress, DNA damages and cytokine activation that act as stimulus for apoptosis. In effector phase, proteases and nucleases activation

occur and they participate in degradation phase (Hail Jr., Carter, Konopleva & Andreeff, 2006). The morphological changes of apoptosis stage are shown in figure 2.7.

2.9.4   Caspases Family: The Killer Protein

Caspases or cysteine aspartyl-specific proteases are the major players in apoptosis. Caspases constitute a family of 11 intracellular cystein proteases and can be found in most mammalian cells. Caspases reside in cytosol as single chain proenzymes (Reed, 2003). Although some of the caspases participating in homeostasic cellular function are not associated with apoptosis, about two-third of them work in collaboration in proteolytic cascades where the caspases activate themselves and each other to cause apoptosis. These apoptotic-associated caspases are divided into two types called initiator caspases (*e.g.*, caspases-8 and -9), and their downstream effector caspases (*e.g.*, caspases-2, -3, and -7) (Hail Jr., Carter, Konopleva & Andreeff, 2006). Two pathways involving these caspases are characterized extensively. They are intrinsic pathway (mitochondria dependent pathway) and extrinsic pathway (death receptor dependant pathway)(Kim, 2005).

2.9.5 Apoptosis Pathways

The intrinsic pathway depends on the release of cytochrome c from mitochondria intermembrane space into cytosol. In cytosol, APAF-1 oligomerizes upon binding with cytochrome c, and then binds procaspase-9 to form apoptosome, a multiprotein caspase-activating complex. The apoptosome will activate effector caspase-3 and caspase-7 (Kim, 2005; Hail Jr., Carter, Konopleva & Andreeff, 2006). The intrinsic pathway and the pathways to be reviewed later are shown in schematic diagram in Figure 2.8.
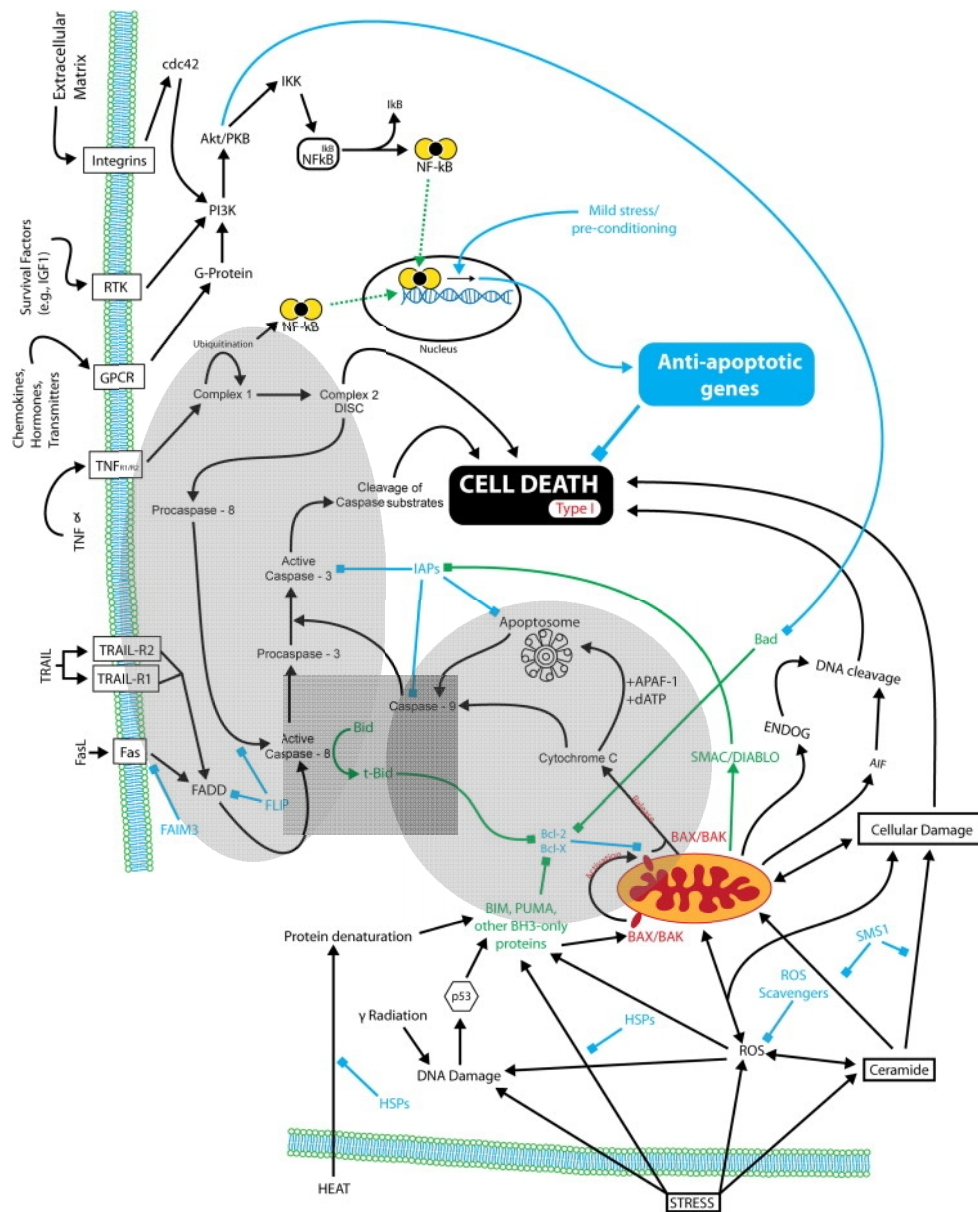
Figure 2.8   Pathways of apoptosis. The round shading refers to intrinsic pathway and the oval shading refers to extrinsic pathway. The square shading refers to the cross-talk link between these two pathways. (Park, Stefanis & Greene, 1997)

The release of cytochrome c from mitochondria can be induced by several stimuli, such as growth factor deprivation, oxidants, Ca^{2+} overload, oncogene activation, DNA-damaging agents and microtubule-attacking drugs (Reed, 2005). Another protein family, namely Bcl-2 protein family is the central regulator in intrinsic pathways (Reed, 2005). During apoptosis stress, induction of proapoptotic Bcl-2 members (e.g., Bax, Bad and Bak) destabilized antiapoptotic Bcl-2 members (e.g. Bcl-2 and Bcl-X_L) which reside in the outer mitochondria membrane. When the ratio of proapoptotic Bcl-2 family proteins to antiapoptotic Bcl-2 family proteins becomes greater, mitochondria permeability transition becomes greater, allowing release of cytochrome c (Hail Jr., Carter, Konopleva & Andreeff, 2006). Overexpression of antiapoptotic Bcl-2 or Bcl-X_L is present in more than half of all cancers (Reed, 2005).

The extrinsic pathway is activated by tumour necrosis factor (TNF) family ligands (eg. Fas and TRAIL receptors) containing death domain (DD) in their cytosolic tail (Kim, 2005). Binding of these domains to cell surface receptors promote recruitment of several intracellular protein, including procaspase-8, forming death-inducing signaling complex (DISC) that activates caspase-8. Caspase-8 directly activates effector caspase-3 leading to apoptotic death (Reed, 2003; Kim, 2005). Some studies also showed crosslinking of extrinsic pathway with downstream action of intrinsic pathway in certain cell types. In such cases, caspase-8 cleaves Bid in cytosol to give truncated Bid (tBid) that translocates to outer mitochondria membrane. Oligomers of tBid change mitochondria membrane permeability and cause cytochrome c-

mediated caspase activation (Kim, 2005; Hail Jr., Carter, Konopleva & Andreeff, 2006). In other study, tBid is shown to change the conformation of Bax, allowing Bax to interact with voltage-dependant anion channel in outer mitochondria membrane, which eventually, triggers the loss of mitochondria membrane potential (Hail Jr., Carter, Konopleva & Andreeff, 2006).

Other than two pathways mentioned before, apoptosis can also occur in a caspase-independent manner. For example, apoptosis-inducing factor (AIF) localized within mitochondria translocates through cytosol to nucleus and binds to DNA, inducing nuclear chromatin condensation and large-scale DNA fragmentation through caspase-independent pathway. Mitochondrial Omi/HtrA2, on the other hand, antagonizes inhibitors of apoptosis (IAPs), enabling increased caspase activity. IAP cleavage by Omi/HtrA2 is independent of caspase activity (Kim, 2005). Similar to AIF, granzyme B and endoG, in response to apoptotic stimuli, could also induce DNA fragmentation without caspase activity (Donovan & Cotter, 2004).

2.10 Bcl-2 Proteins Family

Bcl-2(B-cell Lymphoma-2) is a 25kDa protein localized primarily on the outer membranes of mitochondria, endoplasmic reticulum and nucleus. It is the first protein of Bcl-2 Family discovered in non-Hodgkin's lymphoma as an oncogene. While apoptosis is the key switch to cell death, Bcl-2 is the regulator of the key (Verma, *et al*., 2006). Currently, more than 30 Bcl-2

homologues are known and they are group as Bcl-2 protein family (Skommer,Wlodkowic & Deptala, 2007). The members can be divided into two group – anti-apoptotic and pro-apoptotic. Anti-apoptotic members (death antagonists) include Bcl-2, Bcl-XL, Bcl-W, A1, Mcl-1 and all known viral homologues protein. Pro-apoptotic members (death agonists) include Bax, Bid, Bak, Bid, Harakiri, Bim, Bik, Bad and Bcl-Xs (Sharpe, Arnoult & Youle, 2004; Verma, *et al.*, 2006).

Each of these members possess up to four conserved Bcl-2 homology (BH) domains. Therefore, in molecular level, they can also be differentiated into 3 categories. The first category is the BH3-only pro-apoptotic members such as Bid, Bik, Bad, Bim, Noxa and PUMA. Second category carries multi-domain pro-apoptotic members such as Bax, Bok and Bak which comprised of BH1, BH2 and BH3 domains. Third category is the anti-apoptotic members such as Bcl-2, Bcl-xL and Bcl-w, all of which consist all four BH domains (BH1, BH2, BH3, BH4) (Donovan & Cotter, 2004).

2.10.1 Bcl-2 Regulation in Intrinsic Pathway of Apoptosis

Bcl-2 and its mammalian homologues in anti-apoptotic group inhibit Apaf-1-mediated activation of caspase-9 (Coultas & Strasser, 2003). There are currently two proposed mechanisms of regulation. Pro-apoptotic members may form channels in outer membrane of mitochondria or they could regulate pre-existing channels such as Permeability Transition Pore (PTP) (Donovan &

Cotter, 2004). These channel forming mechanism are based on the finding that Bcl-2 family members resemble diphtheria toxin, a membrane-located pore-forming molecule (Kirkin, Joos & Zőrnig, 2004)**.**

In healthy cell, Bax exists as monomer in cytosol or loosely attached to outer membrane of mitochondria (OMM). In response to apoptotic stimuli and the release of mitochondria intermembrane space proteins, Bax translocate to OMM and oligomerizes (Sharpe, Arnoult & Youle, 2004). Four Bax molecules oligomerized, forming pore with an estimated size of 22Å, leading to leakage of cytochrome *c* (Donovan & Cotter, 2004). PTP is a large conductance pore complex made up of voltage-dependant anion channel (VDAC) in the outer membrane, adenine nucleotide translocator (ANT) in the inner membrane and cyclophilin D in the matrix. In response to death stimuli, PTP opens, causing swelling of mitochondria (Donovan & Cotter, 2004; Verma, *et al*., 2006). Pro-apoptotic members (Bax and bak) cause opening of PTP while anti-apoptotic members (Bcl-2 and Bcl-xL) induce closure of PTP (Donovan & Cotter, 2004).

Anti-apoptotic members and pro-apoptotic members in Bcl-2 family hold themselves in check. For examples, anti-apoptotic members such as Bcl-2 and Bcl-xL will form heterodimer with pro-apoptotic members, Bax and Bak, thereby, inactivating pro-apoptotic oligomers (Kirkin, Joos & Zőrnig, 2004; Verma, *et al*., 2006). Besides, some cellular factors outside Bcl-2 family could also interact with Bcl-2 proteins and modulate their actions. For instance, several proteins such as 14-3-3ε, BNIP3, Ku70 or p53 can either inhibit

oligomerization of pro-apoptotic Bax or block the function of anti-apoptotic Bcl-2, acting as an activator and de-repressor (Donovan & Cotter, 2004; Skommer, Wlodkowic & Deptala, 2007).

2.10.2 Bcl-2 Regulation in Extrinsic Pathway of Apoptosis

Despite most of the evidence showed Bcl-2 proteins involvement in mitochondria-mediated apoptosis, recent findings suggested that Bcl-2 proteins are also involved in mitochondria-independent apoptosis pathways (Kirkin, Joos & Zőrnig, 2004).

In death receptor-mediated (extrinsic) pathway, Fas/Fas-L or TNF stimulation recruits initiator caspase-8. Activated caspase-8 can cleave BH-3 only Bcl-2 protein, Bid, producing truncated Bid (t-Bid) (Sharpe, Arnoult & Youle, 2004). t-Bid may interact directly with Bax, inducing Bax to bind, intercalate and permeabilize mitochondria membrane (Skommer,Wlodkowic & Deptala, 2007). Although Bax alone could induce release of cytochrome *c*, joining of t-bid provide synergistic effect to induce mitochondria permeability (Sharpe, Arnoult & Youle, 2004).

2.10.3 Bcl-2 Regulation in Caspase-independent Apoptosis

Cell death factors such as AIF, Granzyme B, Omi and endonucleus G participate in caspase-independent apoptosis. Bcl-2 overexpression achieves its function to suppress cell death by inhibiting release of AIF from mitochondria. In contrast, Bax or t-Bid overexpression increases efflux of AIF from mitochrondria. Similar to AIF, subcellular localization of Granzyme B, Omi and endoG also relies on the regulation of Bcl-2 proteins. Bax and t-Bid promote their release from mitochondria while Bcl-2 prevents these events (Donovan & Cotter, 2004).

CHAPTER 3

METHODS & MATERIALS

3.1 Standard Preparations and Procedures

3.1.1 Culture Medium, Drugs & Reagents

The photosensitizer hypericin (HYP) and cytotoxic drugs vinblastine (VIN), doxorubicin (DOX), cisplatin (CIS) were purchased from Merck Bioscience. Minimum Essential Medium without phenol red (MEMw) and fetal bovine serum (FBS) were purchased from Hyclone. The 0.25% Trypsin was from Gibco. Phosphate buffered saline (PBS) was purchased from Amresco (USA), All tissue culture flasks and 96-well microtiter plates were purchased from Orange (Belgium).

3.1.2 Medium Preparation

First, 9.5g of MEMw was dissolved in 1L distilled water and 2.2g of sodium bicarbonate was added and dissolved. Solution was sterile-filtered using membrane with 0.22μm pore size. FBS was added to 10% (v/v) concentration after filtration. This medium is hereby mentioned as Complete Growth Medium (CGM). Treatment Medium (TM) contained only 5% of FBS to reduce binding to HYP-PDT. The media were kept in 4°C until use. CGM and TM was never kept more than two weeks.

3.1.3 PBS (1X) Preparation

PBS premix was dissolved in 1L distilled water to prepare 1X PBS. The solution was sterile-filtered using membrane with 0.22μm pore size. The solution was kept in room temperature in cold and dark place. PBS (1X) was never kept more than two weeks.

3.1.4 Cell lines and culture conditions

Human squamous carcinoma cell lines (HSC-2, HSC-3 and HSC-4) were obtained from Health Science Research Resource Bank (HSRRB), Japan. All three cell lines were established in the Department of Oral and Maxillofacial Surgery, Tokyo. They were all established from tumor specimens of metastatic lymph nodes. The primary site of HSC-2 is floor of mouth. It is well differentiated. The primary site of HSC-3 and HSC-4 was tongue. HSC-3 is poorly differentiated and HSC-4 is well differentiated (Michi, Morita, Amagasa & Murota, 2000). The cells were maintained in complete growth medium (CGM). Cells were cultured in humidified CO_2 incubator at 37°C. When the cell monolayer reached 70% - 80% confluency, trypsinisation was performed to harvest cells for treatment test. To perform trypsinisation, the depleted medium was removed and cells layer was rinsed with PBS. Adequate 0.25% trypsin was added to cover confluent cell monolayer. Cells detached from vessel surface after approximately 5 minutes of incubation at 37°C. The cells-trypsin mixture was collected for centrifugation. Trypsin was

removed after centrifugation and cells were resuspended in fresh medium. For sub-culturing, resuspended cells was added to fresh complete growth medium (CGM) in 1:5 ratio into a new cell culture vessel. For experimental treatment purpose, the harvested cells were subjected to trypan blue exclusion counting assay to determine the cell concentration and also to make sure the cell viability was more than 95%. These cells were then being incubated with treatment medium (TM) over the experimental period.

3.1.5   Chemotherapeutic Agents & Photosensitizer Preparation

Doxorubicin and vinblastine were diluted in DMSO, while cisplatin were diluted in sterile distilled water, to a concentration of 1mg/ml aseptically and kept at -20°C. They were directly dissolved in media to desired working concentration in experiments and serial dilutions were performed as necessary. The final concentration of solvent in experimental condition was always kept below 0.1% (v/v), which will not affect the proliferation of cells (Kuriu *et al*.,1991; Kaneski, Constantopoulos & Brady,1991). Preparation of hypericin stock solution (1mg/ml) was the same as mentioned above except every step was done in subdued light condition.

3.1.6   Light Irradiation

Irradiation was carried out using custom-made light box, equipped with broad spectrum Philips Halotone 300W incandescent halogen lamp and a transparent glass tank fully filled with distilled water to filter infrared wavelength that may produce heat to cells during irradiation period (Figure 3.1a and Figure 3.2). The light wavelength was filtered with 500nm long-pass filter (Edmund Optics, USA). Fluence rate was fixed at $7.07mW/cm^2$ prior to irradiation using Ophir Handheld Light Meter with 3A-P-SH-V1 ROHS Head with built-in 800nm low-pass filter (Ophir Laser Measurement Group, Israel).

Figure 3.1b showed that diameter of sensor aperture is 12mm. Therefore, the total area for sensor is $\pi(0.6cm)^2 = 1.131cm^2$. During the light irradiation step in experiment, light power measured by light meter was 8mW. Hence, light power measured (8mW) divided by total area of sensor $(1.131cm^2)$ gives the final fluence rate $(7.07mW/cm^2)$.

Hypericin has maximum absorption wavelength (λ_{max}) at 590nm and another absorption wavelength at 545nm. Since the light source is tungsten halogen bulb (shown in figure 3.1a) which may emit a whole spectrum of visible light, by using a 500nm long-pass filter, combined with a built-in 800nm low-pass filter in light meter sensor, the light with wavelength <500nm and >800nm can be eliminated from sensor final reading, giving a better accuracy in final measurement of actual fluence rate.

As shown in figure 3.1a, during cell irradiation step, light was directed toward the bottom of microtiter plate or culture dish through a reflection mirror for 10 minutes. Treatment medium (TM) with drugs was not removed and remained with the cells throughout the irradiation period. Fluence received by each sample was $4.242J/cm^2$. This is calculated based on Fluence rate ($7.07mW/cm^2$) and irradiation time (10 minutes).

Fluence received by each sample is,

$$\underline{0.00707W} \times 600s \quad = \underline{0.00707J} \times \quad 600s \quad = \quad 4.242J/cm^2$$
$$cm^2 \qquad\qquad\qquad s \cdot cm^2$$
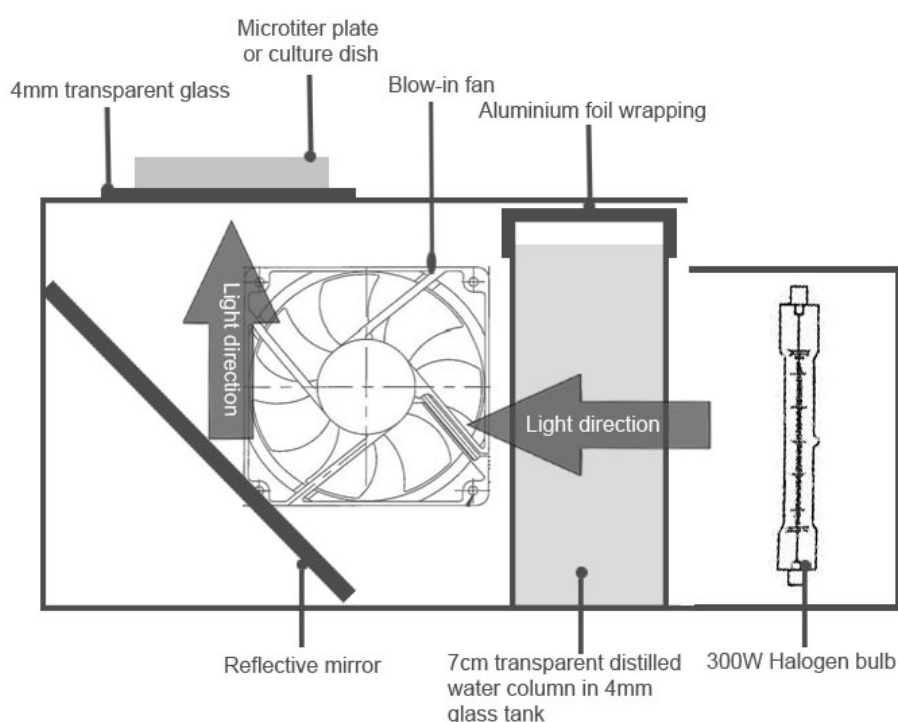
Figure 3.1a   Schematic set-up of light box. The whole setup was installed in a custom-made black steel box.
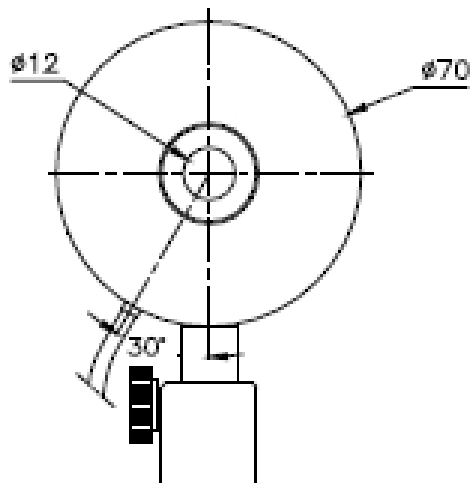
Figure 3.1b   Diameter of sensor aperture is 12mm. Therefore, the total area for sensor is $\pi(0.6cm)^2 = 1.131cm^2$. In this study, light power measured by light meter was 8mW. Hence, 8mW divided by $1.131cm^2$ gives the final fluence rate $7.07mW/cm^2$.

Figure 3.2   Actual image of light box. A rheostat was fixed with the power source for power adjustment during calibration.

3.2   Evaluating Drug Interaction

3.2.1   Preparation of MTT assay solution

3-(4,5-dimethylthiazol)-2,5-diphenyltetrazolium bromide (MTT) was purchased from Amresco, US. Dimethysulfoside (DMSO) was from Fisher Scientific (USA). MTT powder (0.5g) was dissolved in 100ml PBS(1X) to give a 5mg/ml concentration. The solution was kept in 4°C. The solution was never kept more than one month. It was discarded if dark crystal was found forming spontaneously in the solution.

3.2.2   MTT Assay (Cytotoxicity Assay)

MTT (3-[4,5-dimethythiazol-2-yl]-2,5-diphenyltetrazolium bromide) assay is a rapid colorimetric microtiter plate assay to evaluate cytotoxicity of drugs. It was developed by Mosmann in 1983 and was recognized by National Cancer Institute (NCI, USA) as standard tool for the purpose of drugs screening. The assay depends on the mitochondrial succinate dehydrogenase to convert soluble yellow MTT salt into insoluble purple formazan crystal. Mitochondrial succinate dehydrogenase activity can only be found in viable cells and therefore, the amount of formazan formation is proportional to the number of living cell in culture. The formazan can be dissolved in DMSO and be quantified under microplate spectrophotometer with setting at 550nm.

Briefly, at the end of drug treatment incubation, 20μl of MTT solution (5mg/ml in PBS) was added to each well. The microtiter plate was incubated for another 3 hours at normal culture condition. Then, approximately 70% of the supernatant was removed and 100μl of DMSO was added to each well. The microtiter plate was kept in dark for 15 minutes and then agitated gently by hand to dissolve the formazan completely. Absorbance of each well at 550nm was obtain through microplate spectrophotometer. The percentage of viable cells was calculated relatively to the control wells of untreated cells.

3.2.3 Drug Treatment Independently

Cells were seeded into 96-well mircotiter plate in a density of 2×10^4 cells per well. The cells were incubated overnight. At the following day, all the medium was discarded and replaced with 100μl treatment medium (TM) containing either hypericin, cisplatin, doxorubicin or vinblastine, prepared as a series of ten concentrations by serial dilution. Each concentration was tested in triplicate. The microtiter plate was incubated in dark for four hours prior to light irradiation. Plates were irradiated with fluence of $4.242J/cm^2$ as described in section 3.1.7. Dark control of all single agents without light irradiation was performed as well. All works were carried out in subdued light condition.

Modified MTT assay (Mosmann, 1983) was carried out after 72 hours incubation in dark. Data was collected using monochromatic microplate reader at 550nm and cell viability was calculated as described in section 3.2.2. The

percentage of cell viability was calculated as mean absorbance of drug well / (mean absorbance of positive control well – mean control of negative control well) x 100%. Each test was repeated at least three times.

3.2.4   Drug Treatment in Combination

Cells were seeded as described previously. The cells were incubated overnight. Six fixed concentrations (0.02μg/ml, 0.06μg/ml, 0.10μg/ml, 0.12μg/ml, 0.14μg/ml, 0.16μg/ml) of HYP-PDT and five different concentrations of chemotherapeutic agents (cisplatin, doxorubicin or vinblastine) were selected with respect to single drug concentration-response curve of each cell line. They were both added in a checker-box fashion (Figure 3.3) into the test wells in microtiter plate, in triplicates.

Every concentration was dissolved in 100μl of Treatment Medium (TM). All works were carried out in subdued light condition and TM was used in the whole process. The plates were incubated in dark for four hours and irradiated with light giving fluence of 4.242J/cm^2 as described in section 3.1.7 thereafter. Dark controls of all combination tests were performed in parallel. Modified MTT assay (Mosmann, 1983) was carried out after 72 hours incubation in dark. Data was collected as previously described. Each test was repeated at least three times.

								-ve	blank
Five selected chemo-drug concentrations in 4 replicates downward				←Five selected chemo-drug concentrations in 4 replicates downward→				-ve	blank
This area consist of all 0.02µg/ml HYP-PDT				This area consist of all 0.06µg/ml HYP-PDT				-ve	blank
								-ve	blank
								-ve	blank
←Five selected chemo-drug→ concentrations in 4 replicates downward				←Five selected chemo-drug→ concentrations in 4 replicates downward				-ve	blank
This area consist of all 0.10µg/ml HYP-PDT				This area consist of all 0.12µg/ml HYP-PDT				-ve	blank
								-ve	blank

								-ve	blank
←Five selected chemo-drug→ concentrations in 4 replicates downward				←Five selected chemo-drug→ concentrations in 4 replicates downward				-ve	blank
This area consist of all 0.14µg/ml HYP-PDT				This area consist of all 0.16µg/ml HYP-PDT				-ve	blank
								-ve	blank
Empty area				Empty area				-ve	blank
								-ve	blank
								-ve	blank

Figure 3.3   Layout of combination drugs added in checker-box fashion in two 96-well plates. The abbreviation "-ve" in diagram means "negative control", which is cells with medium without drugs.

3.2.5 Isobolographic Analysis of Drugs Interaction

Fixed concentration-response IC_{90} isobolograms were constructed using data obtained from single drug concentration-response curve (Gressner, 1995). Briefly, the concentration of CIS, DOX, VIN or HYP that killed 90% (IC_{90}) of each cell line after 72 hours of light irradiation was determined. IC_{90} of HYP-PDT was plotted on Y-asix and IC_{90} of CIS, DOX or VIN was plotted on the X-axis. The theoretical line of additivity was attained by joining both IC_{90} data points. Positive and negative standard deviations of each independent drug were connected with a straight line to build a region of additivity.

The results of combination drugs treatment obtained from section 3.2.4 was being arranged into a concentration-response curve (fixed HYP concentration; Percentage of Viability versus CIS, DOX or VIN concentrations). IC_{90} concentrations contributed by both drugs could then be extracted from these concentration-response curves as shown in Figure 3.4.
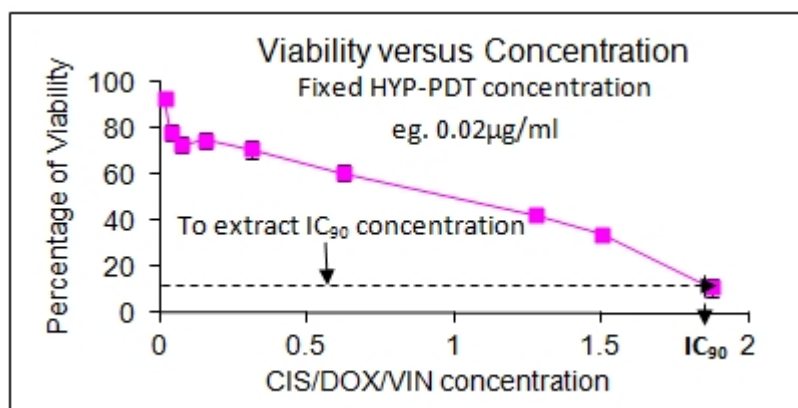
Figure 3.4   Extraction of IC_{90} concentration of CIS, DOX or VIN concentration from combination with fixed HYP-PDT concentration. The results were then arranged into coordinates in form of (Y, X) where Y equals to HYP-PDT concentration (Y- axis) and X equals to CIS/DOX/VIN concentration (X-axis).

The coordinated was then plotted into isobologram constructed previously. As per described in Figure 2.1c in section 2.6.2, if the coordinate of both drugs fell within the boundaries of additivity line and confidence limit, it was recognized as additive combination pair. Synergistic effect occurred if an IC_{90} data point of combination pair fell below the boundaries and antagonistic effect was recorded if the point is above the boundaries. The isobologram of IC_{50} or IC_{40} was constructed with same procedures.

3.2.7 Statistical Test

Paired Student's *t*-test was used in this study to evaluate significant difference among means. It was calculated by using GraphPad QuickCalc software which can be accessed through internet (http://www.graphpad.com/quickcalcs/ttest1.cfm). If $p>0.05$, difference is considered to be not statistically significant. If $p<0.05$, the difference is significant.

3.3   Determining Mode of Cell Death

3.3.1   Material

FITC Annexin V was purchased from BD Pharmingen (USA) as aqueous solution containing BSA and less than 0.09% sodium azide. Propidium Iodine (PI) was purchased from Merck (USA).

3.3.2   Time-course Treatment of Cells

Cells were seeded into 60mm culture dish in a density of 5×10^5 cells. The cells were incubated overnight. Prior to drug addition, old medium was discarded. Selected combination concentrations (combination drug pairs selection principle was further described in section 4.2.1.1) were dissolved in 3ml treatment medium (TM) and added to the cells. Five dishes for each

combination drug concentration was prepared corresponding to cell harvested at three hours, seven hours, fifteen hours, twenty four hours and a control dish. Each set was done in triplicates. The cells were incubated four hours in dark and then irradiated light giving fluence of $4.242J/cm^2$ as described in section 3.1.7 and then returned to the incubator.

Cells were harvested at 3, 7, 15 and 24 hours post-irradiation by gentle trypsinisation and subjected to FITC-Annexin V experiment as described in section 3.3.4. Controls consisted of cells treated with individual drugs at concentration used in the combination experiment which was either IC_{40}, IC_{50} or IC_{90} and untreated cells. Each experiment was repeated at least three times.

3.3.3   Preparation of PI Solution

Propidium Iodine (PI) powder (5mg) was dissolved in 5ml distilled water to give 1mg/ml PI solution. The solution was aliquoted and kept in -20°C while the solution to be used in assay was kept in 4°C. PI solution was never kept more than one month and the stock was never kept more than six months.

3.3.4   FITC Annexin V staining of membrane   Phosphatidylserine (PS)

One of the earliest features of apoptosis in a cell is the loss of plasma membrane asymmetry. In this event, a membrane phospholipid, phosphatidylserine (PS) would be exposed on the outer surface of plasma membrane. Annexin V has high binding affinity on PS and it can be conjugated with fluorescence dye FITC. FITC fluorescence can be detected with flow cytometer and thereby binding of Annexin V on PS or the population of apoptotic cell can be detected. PI is another dye that can distinguish viable cells and dead cells and it can be detected by flow cytometer. PI is permeable to dead or damaged cell while it will be excluded by viable cells with intact membrane. Double staining with PI and FITC-Annexin V helps to determine population undergoing apoptosis (FITC Annexin V positive, PI negative), population undergoing necrosis or secondary necrosis seen in late apoptosis (both FITC Annexin V and PI positive), and viable population without measureable apoptosis (both FITC Annexin V and PI negative).

The staining of FITC-Annexin V and PI was performed according to manufacturer suggested protocol. Briefly, freshly harvested cells was washed twice with ice-cold 1X PBS and was resuspended to a concentration of ~1 x 10^6 cells/ml in 1X Binding Buffer. Cells suspension (~1 x 10^5 cells/ml), 100μl, was transferred into a 5ml polystyrene culture tube. FITC-Annexin V (5μl) and PI (2μl from 1mg/ml aliquot) were added to the cell suspension. The mixture was vortexed gently and incubated for 15 minutes at room temperature in dark. 1X binding buffer (400μl) was then added to the mixture

and the sample was analysed on a FACSCAN flow cytometer within one hour. The fluorescence was collected on FL1 (FITC) and FL2 (PI) in log mode with laser excitation at 488nm. For each sample, 10000 gated events were collected using CELLQuest[TM] software. A dot plot was set up using at least 10000 gated events with FITC Fluorescence (green) at the X-axis and PI Fluorescence (red) at the Y-axis. As shown in Figure 3.5 below, a gated area (R1) containing at least 10000 recorded events of properly resuspended single cells was determined in a dotplot of Side Scatter Height (SSC-Height) versus Forward Scatter Height (FSC-Height). This was to eliminate multiple cells sticking together to be counted in. A density plot of FL2 (PI intensity) versus FL1 (FITC intensity) was drawn using these gated data and a quadrant was set to separate viable, apoptotic or necrotic population. Quadrants were determined using controls of unstained cells, cells stained with FITC-Annexin V only and cells stained with PI only. Basal apoptosis value was subtracted from treated cells value by using untreated cells as control. Percentage of cells undergoing apoptosis was later determined using WinMDI v2.9 software.
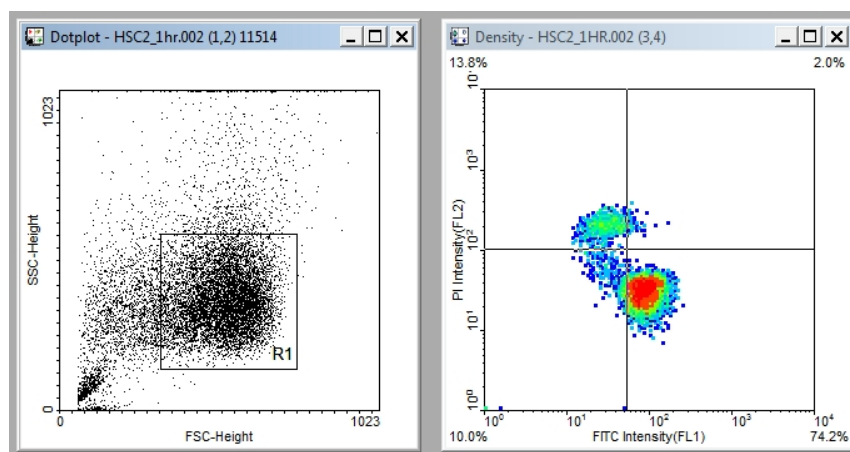
Figure 3.5   Example of gated Dotplot and density plot with quadrants. Dotplot on the left was gated (R1) and these data was used to construct density plot on the right.

3.4   Investigating Cell Death Mediators

3.4.1   Materials

Pierce® BCA protein Assay Kit, Halt^{TM} Protease Inhibitor Cocktail (EDTA free), M-PER® mammalian protein extraction reagent, Restore^{TM} Plus Western blot stripping buffer, StartingBlock blocking buffer, 3mm Western blot filter paper were purchase from Thermo Scientific (USA). Mouse monoclonal anti-Caspase-7 primary antibody, Goat anti-mouse secondary antibody and Immobilon^{TM} Western Chemiluminescent HRP Susbtrate were purchased from Millipore (USA). Mouse monoclonal primary antibodies (anti-Caspase-9, anti-Caspase-8, anti-Bax, anti-Bcl and anti-actin) were purchased from Chemicon International (USA). PageRuler^{TM} prestained protein ladder was purchased from Fermentas Life Sciences (USA). Red loading buffer pack (3X) was purchased from New England Biolabs (UK).

65

3.4.2 SDS-PAGE and Western Blot

3.4.2.1 Preparation of Cell Lysate

Following time-course treatment as described in section 3.3.2, approximately 5×10^6 cells were harvested for each time-point. The cell suspension was centrifuged at 3000rpm at 4°C for 10 minutes. Cells were washed with 1X ice-cold PBS and approximately 3 volumes of M-PER® mammalian protein extraction reagent and 1X , Halt^{TM} Protease Inhibitor Cocktail (EDTA free) were added. The mixture was vortexed and left on ice for 10 minutes. The lysate was then centrifuged at 10000rpm at 4°C for 10 minutes. The supernatant was collected into a new tube while the pellet was discarded. Pierce® BCA protein Assay Kit was used to determine protein concentration. All samples were kept at -20°C until use.

Prior to loading into polyacrylamide (PAGE) gel, Red loading buffer (3X) was added and mixed to the sample in 1:3 ratio. The mixture was boiled for five minutes and then allowed to cool to room temperature. Samples were subjected to quick centrifugation in order to bring down condensation. Protein loaded per lane is 30μg.

3.4.2.2 Gel Preparation

The glass plates were assembled according to manufacturer's instruction for the mini PROTEAN II (Biorad, USA). The composition of stacking gel and resolving gel was prepared according to Table 3.1.

Table 3.1   Composition of stacking gel and resolving gel

	4% Stacking gel	12% Resolving gel
Ultra pure water	2.42ml	3.4ml
1.5M Tris HCl pH8.8	-	2.5ml
0.5M Tris-HCl pH6.8	1ml	-
20% SDS	20µl	50µl
30% Bis-Acrylamide	0.53ml	4ml
10% Ammonium Persulfate	20µl	50µl
TEMED	2µl	5µl

Note: The total volume of above mixture is enough to prepare 4 mini gels.

All components were mixed and kept on ice except TEMED and APS which were added just prior to use. Resolving gel solution (12%) was pumped into the space between glass plates to a level of 1cm below the comb. Distilled water (1ml) was laid over the top. Once polymerized, ethanol was discarded. Casting set was leaved in room temperature for 5 minutes, allowing residual ethanol to be evaporated. After this, 4% stacking gel solution was added between the glass plates and the comb was inserted carefully without trapping air bubble. The comb was removed once the stacking gel polymerized. Glass

plates with gel were fixed into electrophoresis tank and immersed with running buffer. Each well was flushed prior to sample loading.

3.4.2.3 Sample Loading and Gel Electrophoresis

Protein sample of 30μg was loaded in each lane. The time-course samples were loaded in an ascending order. A lane was reserved for 3μl PageRuler™ prestained protein ladder on each gel. The gel was electrophoresed at 60mA (two gel per tank) until the dye front reach the bottom of the resolving gel.

3.4.2.4 Preparation of Membrane

PVDF membrane, 0.45μm (Millipore, USA) was cut according to the resolving gel size and was soaked in 100% methanol until becoming translucent. The membrane was then rinsed twice with distilled water and soaked in blotting buffer until use. At the same time, the sponges of blotting sandwich and two pieces of 3mm filter paper cut according to the size of membrane were soaked together in blotting buffer.

3.4.2.5 Transfer of Protein to Membrane

The gel was removed from the glass plates and the stacking gel was removed. The blotting sandwich was assembled and placed in the blotting tank in the following sequence,

Cathode (Negative Pole) – Sponge – filter paper – gel – membrane – filter paper – sponge – Anode (Positive Pole)

The whole blotting tank was immersed in iced water and placed on a magnetic stirrer. Proteins were transferred for 1 hour at 100V constant voltage. After the transfer, the membrane was removed from the sandwich and left to dry on a clean filter paper. The membrane was then kept at -20°C until use.

3.4.2.6 Blocking of Membrane

The membrane was placed in a small shallow tray. StartingBlock blocking buffer (Thermo Scientific, USA) was added to a level just enough to cover the membrane. The membrane was incubated in room temperature for one hour with gentle agitation. Blocking buffer was discarded after use.

3.4.2.7 Binding of Primary Antibody and Secondary Antibody

All primary antibodies were diluted to a 1:10000 concentration with StartingBlock blocking buffer. Immediately after blocking, a volume of primary antibody enough to cover the membrane was used to replace the blocking buffer. The membrane was incubated for two hours in room temperature with gentle agitation. After incubation, primary antibody solution was removed and the membrane was washed three times with 0.05% Tween-20 PBS in agitation, 10 minutes each time. The above procedures were repeated for all mouse primary antibodies (anti-Caspase-9, anti-Caspase-8, anti-Bax, anti-Bcl and anti-actin).

Secondary antibody, goat anti-mouse IgG conjugated with Horse Radish Peroxidase (HRP), was diluted to a 1:10000 concentration with StartingBlock blocking buffer. After washing, the membrane was incubated with secondary antibody solution for one hour in room temperature with gentle agitation. After that, secondary antibody solution was removed and the membrane was washed three times with 0.05% Tween-20 PBS (PBS-T) in agitation, 10 minutes each time.

3.4.2.8 Chemiluminensence Detection

Luminol reagent and Peroxide reagent in Immobilon^{TM} Western Chemiluminescent HRP Susbtrate was mixed in a ratio of 1:1 just prior to use.

The mixture (2ml) was added to a clean small shallow tray. A probed membrane was place inside and the tray was tilted few times to ensure Luminol-Peroxide mixture contact the whole membrane surface. The membrane was flipped and the tilting procedure was repeated.

Membrane was place in between two transparent plastic cards and excessive Luminol-Peroxide mixture was drained. Chemiluminencence signals on the membrane were detected using FluorChem®Xplor gel imaging system (Alpha Innotech, USA). Membrane images were saved directly from AlphaEase^{TM} FC StandAlone Ver.6.0.0.14 software.

3.4.2.9 Stripping Stained Membrane

After taking photograph in section 3.4.2.8, the membrane was stripped immediately. First, the blot was washed with PBS-T to remove chemiluminescent substrate. Then the blot was incubated for 10 minutes at room temperature in adequate amount of Restore Western Blot Stripping Buffer (Thermo Scientific, USA) to cover the whole membrane. The membrane was washed two times with PBS-T after incubation. The procedure of re-blocking of membrane was the same as described in section 3.2.4.6. The blocked membrane was reused once for the next immunoblot experiment.

CHAPTER 4

RESULTS

4.1   Drug Interaction Analysis

4.1.1   Cisplatin (CIS) Treatment Independently

Cytotoxic assay with Cisplatin (CIS) alone at concentration ranging from 0.02μg/ml to 15.00μg/ml on HSC-2, HSC-3 and HSC-4 cell lines produced concentration-dependant cell killing as shown in Figure 4.1. All cell lines were killed by CIS in a concentration-dependent manner. The values of IC_{20}, IC_{50}, IC_{70} and IC_{90} of each cell lines were recorded in Table 4.1. From Table 4.1, HSC-3 (IC_{90}=1.89μg/ml) was most responsive to CIS with light irradiation while HSC-2 (IC_{90}=7.60μg/ml) the least. The difference between both concentrations was significant ($P<0.05$). The concentration-dependent response of HSC-4 at IC_{20} (0.18μg/ml) and IC_{50} (1.05μg/ml) was similar to HSC-3 at IC_{20} (0. 04μg/ml) and IC_{50} (0.98μg/ml). However, HSC-4 (IC90=4.68μg/ml) was relatively less sensitive to CIS with light irradiation than HSC-3 (IC_{90}=1.89μg/ml) at higher killing rate. More CIS was needed to achieve 90% cell killing in HSC-4 than in HSC-3.

Dark control of CIS treatment show similar result as light irradiated CIS treatment. Paired student t-test (Table 4.1) showed no significant differences ($p>0.05$) between CIS treatments in dark (Figure 4.2) or light (Figure 4.1) in all cell lines. Therefore, several CIS concentrations were chosen for HSC-2 (0.44μg/ml, 0.88μg/ml, 1.75μg/ml, 3.50μg/ml, 7.00μg/ml),

HSC-3 (0.11μg/ml, 0.23μg/ml, 0.45μg/ml, 0.90μg/ml, 1.80μg/ml) and HSC-4 (0.25μg/ml, 0.50μg/ml, 1.00μg/ml, 2.00μg/ml, 4.00μg/ml) to be used in combination with HYP-PDT.
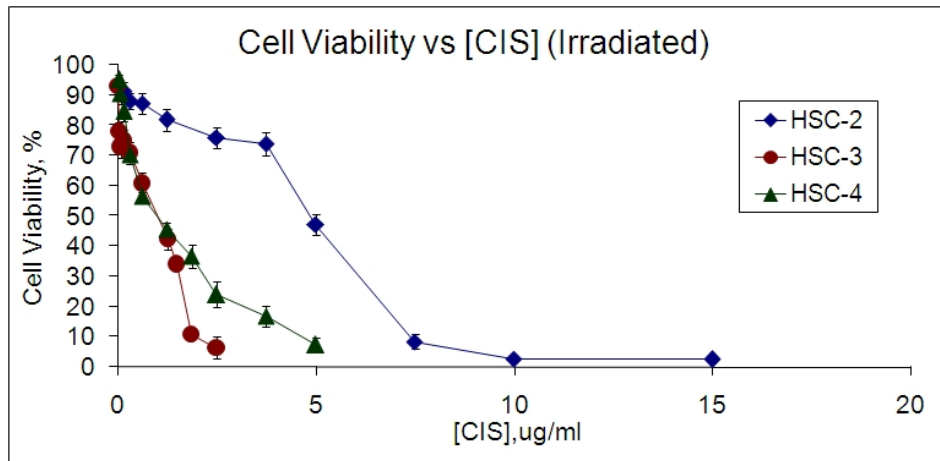
Figure 4.1   Cell viability versus CIS concentration (Irradiated). Cell survival rates of sample in percentage after 72 hours treatment with CIS independently (irradiated according to PDT treatment protocol) obtained using MTT assay. Each data point represented the mean ± standard deviation of three independent assays.
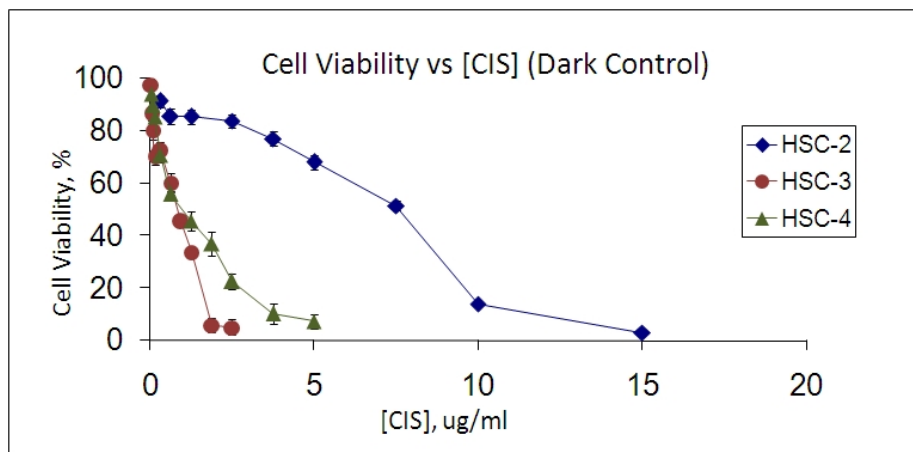
Figure 4.2   Cell viability versus CIS Concentration (Dark Control). Cell survival rates of dark controls in percentage after 72 hours treatment with CIS independently obtained using MTT assay. Each data point represented the mean ± standard deviation of three independent assays.

Table 4.1 Inhibitory concentrations of CIS. The CIS inhibitory concentrations and each standard deviation after 72 hours independent drug treatment (irradiated and dark controls) for HSC-2, HSC-3, HSC-4 cell lines.

	HSC-2 [CIS] (μg/ml) ± SD (μg/ml)		HSC-3 [CIS] (μg/ml) ± SD (μg/ml)		HSC-4 [CIS] (μg/ml) ± SD (μg/ml)	
	(Irradiated)	(Dark Control)	(Irradiated)	(Dark Control)	(Irradiated)	(Dark Control)
IC_{20}	1.90 ±0.14	1.92 ±0.63	0.04 ±0.01	0.08 ±0.02	0.18 ±0.03	0.20 ±0.01
IC_{50}	4.87 ±0.15	4.98 ±0.23	0.98 ±0.07	0.83 ±0.03	1.05 ±0.13	1.03 ±0.20
IC_{70}	6.10 ±0.10	6.42 ±0.14	1.57 ±0.05	1.35 ±0.02	2.17 ±0.10	2.15 ±0.09
IC_{90}	7.60 ±0.35	8.13 ±0.15	1.89 ±0.10	1.77 ±0.03	4.68 ±0.39	3.62 ±0.38
Two-tailed P value	0.1206		0.1333		0.3809	
	($p>0.05$) Difference is considered to be not statistically significant.		($p>0.05$) Difference is considered to be not statistically significant.		($p>0.05$) Difference is considered to be not statistically significant.	

Note: [Mean] (μg/ml) ± SD (μg/ml) represented data from three independent experiments.

4.1.2 Doxorubicin (DOX) Treatment Independently

Cytotoxic assay with Doxorubicin (DOX) alone at concentrations ranging from 0.01μg/ml to 2.00μg/ml with light irradiation on HSC-2, HSC-3 and HSC-4 cell lines produced concentration-dependant cell killing as shown in Figure 4.3. The values of IC_{20}, IC_{50}, IC_{70} and IC_{90} of each cell lines were recorded in Table 4.2. DOX concentration-response difference was not significant in all cell lines ($p>0.05$). HSC-3 required least DOX to achieve 90% cell killing rate ($IC_{90}=0.73$μg/ml) than HSC-2 ($IC_{90}=1.38$μg/ml) and HSC-4 ($IC_{90}=1.24$μg/ml) in the presence of light irradiation. However, the IC_{90} differences of HSC-3 with HSC-2 and HSC-4, respectively, were not significant ($p>0.05$) when assessed with paired student t-test. Paired student t-test (Table 4.2) showed no significant differences between CIS treatments in dark (Figure 4.3) or light (Figure 4.4) in all cell lines. Therefore, several DOX concentrations were chosen for HSC-2 (0.06μg/ml, 0.13μg/ml, 0.25μg/ml, 0.50μg/ml, 1.00μg/ml), HSC-3 (0.04μg/ml, 0.09μg/ml, 0.18μg/ml, 0.35μg/ml, 0.70μg/ml) and HSC-4 (0.01μg/ml, 0.03μg/ml, 0.10μg/ml, 0.30μg/ml, 0.90μg/ml, 1.20μg/ml) to be used in combination with HYP-PDT.
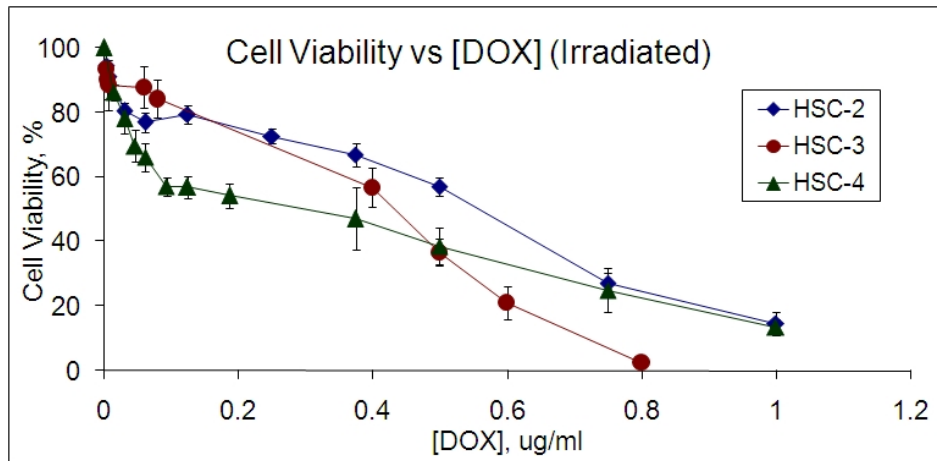
Figure 4.3   Cell viability versus DOX Concentration (Irradiated). Cell survival rates of irradiated samples in percentage after 72 hours treatment with DOX independently obtained using MTT assay. Each sample was irradiated according to PDT treatment protocol. Each data point represented the mean ± standard deviation of three independent assays.
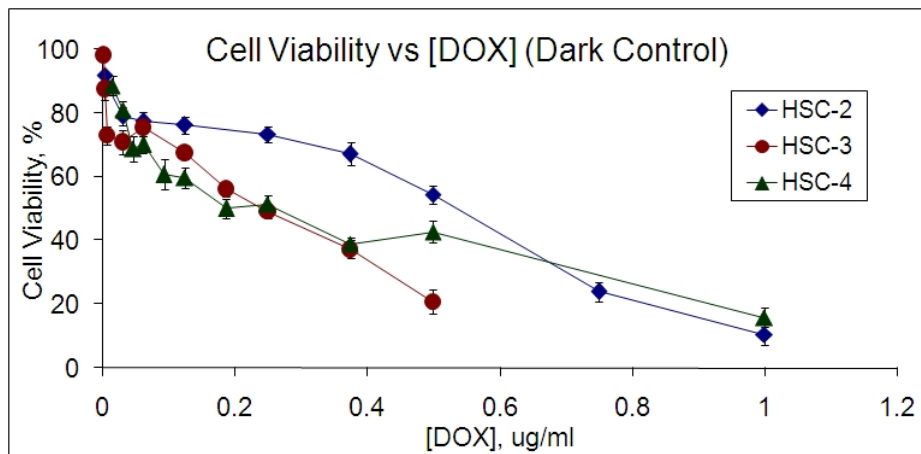
Figure 4.4   Cell viability versus DOX Concentration (Dark Control). Cell survival rates of dark controls in percentage after 72 hours treatment with DOX independently obtained using MTT assay. Each data point represented the mean ± standard deviation of three independent assays.

Table 4.2   Inhibitory concentrations of DOX. The DOX inhibitory concentrations and each standard deviation after 72 hours independent drug treatment (irradiated and dark controls) for HSC-2, HSC-3, HSC-4 cell lines.

	HSC-2		HSC-3		HSC-4	
	[DOX] (µg/ml) ± SD (µg/ml)		[DOX] (µg/ml) ± SD (µg/ml)		[DOX] (µg/ml) ± SD (µg/ml)	
	(Irradiated)	(Dark Control)	(Irradiated)	(Dark Control)	(Irradiated)	(Dark Control)
IC_{20}	0.04 ±0.02	0.02 ±0.01	0.13 ±0.07	0.01 ±0.01	0.03 ±0.01	0.03 ±0.01
IC_{50}	0.56 ±0.02	0.54 ±0.02	0.42 ±0.03	0.23 ±0.01	0.25 ±0.05	0.18 ±0.01
IC_{70}	0.74 ±0.02	0.69 ±0.03	0.55 ±0.02	0.42 ±0.02	0.65 ±0.10	0.70 ±0.04
IC_{90}	1.38 ±0.21	0.98 ±0.02	0.73 ±0.01	0.76 ±0.02	1.24 ±0.04	1.24 ±0.04
Two-tailed P value	0.2784		0.1267		0.8523	
	($p>0.05$) Difference is considered to be not statistically significant.		($p>0.05$) Difference is considered to be not statistically significant.		($p>0.05$) Difference is considered to be not statistically significant.	

Note: [Mean] (µg/ml) ± SD (µg/ml) represented data from three independent experiments.

4.1.3 Vinblastine (VIN) Treatment Independently

Cytotoxic assay with Vinblastine (VIN) alone at concentration ranging from 0.00016μg/ml to 0.50000μg/ml with light irradiation on HSC-2, HSC-3 and HSC-4 cell lines produced concentration-dependant cell killing as shown in Figure 4.5 (irradiated) and Figure 4.7 (dark control). The lowest VIN concentration is achieved by careful 2-fold serial dilutions from highest concentration tested (0.50000μg/ml). Paired student t-test (Table 4.3) showed no significant differences between VIN treatments in dark (Figure 4.7) or light (Figure 4.5) in all cell lines.

As shown in Figure 4.5, VIN inhibited viability of all cell lines in a concentration-dependent manner until a threshold near to 0.10000μg/ml. Any increment of drug concentration more than 0.10000μg/ml, gave constant growth inhibition rate in all cell lines respectively. This is confirmed by testing with 3 concentrations greater than 0.10000μg/ml, up to 0.50000μg/ml, in three cell lines respectively. This observation is constant with all previous publications that reported VIN as a cytostatic agent (Kavallaris, Verrills & Hill, 2001; Duan, Sterba, Kolomeichuk, Kim, Brown & Chambers, 2007).

Due to the fact that VIN is a cytostatic agent, cytotoxic test to obtain IC_{70} and IC_{90} concentration of VIN was not further conducted. Further increment of VIN concentration up to a tremendous level that is able to produce cytotoxicity of IC_{70} and IC_{90} is in contradiction to the actual clinical usage of the drugs. Therefore, only the inhibition rate obtained with the

concentration below 0.10000μg/ml (Figure 4.6) was taken into consideration for further combination study. In this case, only IC_{20} and IC_{50} data were recorded for HSC-2 and HSC-3. For HSC-4, since there is no IC_{50} data available for treatment with concentration below the cytostatic threshold (0.10000μg/ml) as per observed from Figure 4.6, IC_{20} and IC_{40} data were chosen and recorded. These inhibitory concentrations were stated in Table 4.3a and Table 4.3b.

Several VIN concentrations based on Figure 4.5 and Figure 4.6 were chosen for HSC-2 (0.0003μg/ml, 0.0006μg/ml, 0.0013μg/ml, 0.0050μg/ml, 0.0150μg/ml), HSC-3 (0.0003μg/ml, 0.0006μg/ml, 0.0013μg/ml, 0.0025μg/ml, 0.0050μg/ml) and HSC-4 (0.0003μg/ml, 0.0006μg/ml, 0.0013μg/ml, 0.0025μg/ml, 0.0050μg/ml) to be used in combination with HYP-PDT.
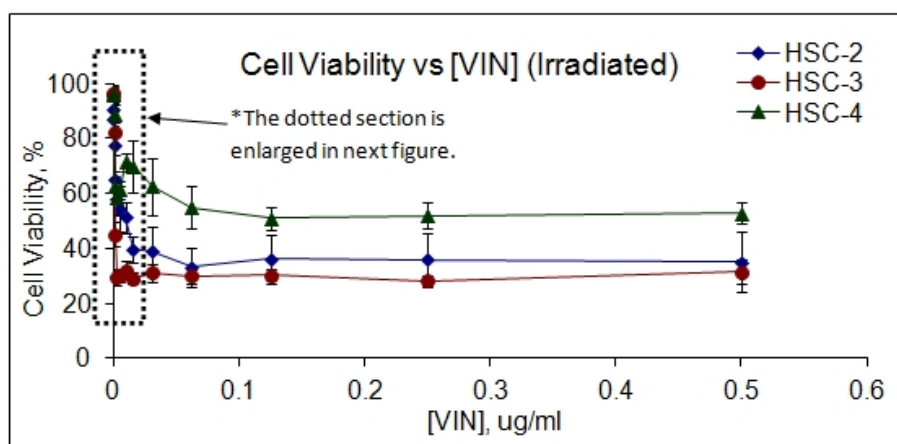
Figure 4.5   Cell viability versus VIN Concentration (Irradiated). Cell survival rates of irradiated samples in percentage after 72 hours treatment with VIN independently was obtained with MTT assay. Each sample was irradiated according to PDT treatment protocol. Each data point represented the mean ± standard deviation of at least three independent assays. The dotted section in this figure is enlarged in Figure 4.6.
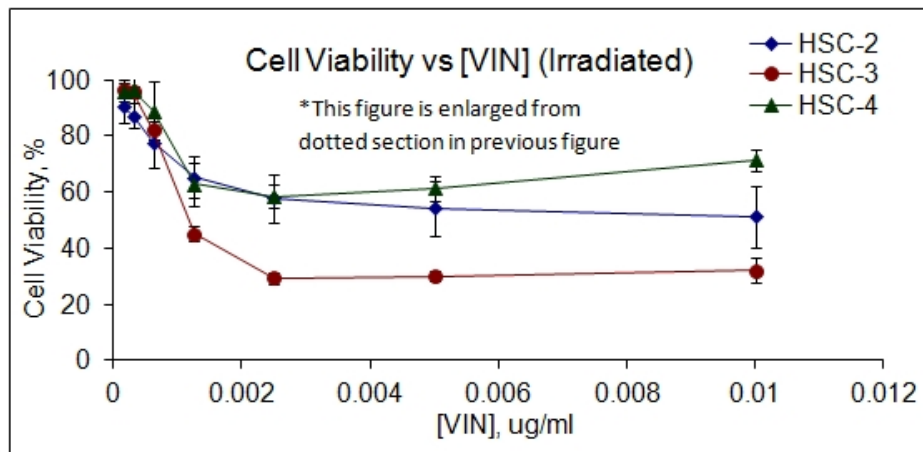
Figure 4.6   Graph enlarged from dotted section in Figure 4.5. This figure shows cell viability with VIN treatment from 0.10000μg/ml and below.
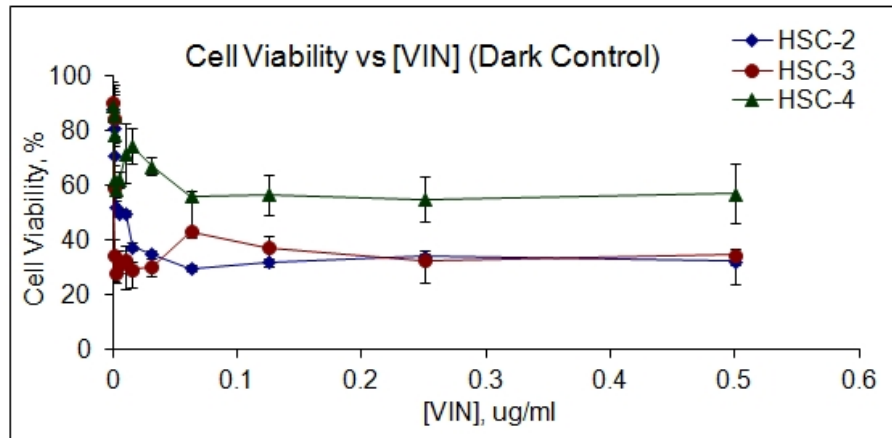
Figure 4.7   Cell viability versus VIN Concentration (Dark Control). Cell survival rates of dark controls in percentage after 72 hours treatment with VIN independently obtained using MTT assay. Each data point represented the mean ± standard deviation of three independent assays.

Table 4.3a   Inhibitory concentrations of VIN for HSC-2 and HSC-3. The VIN inhibitory concentrations and each standard deviation after 72 hours independent drug treatment (irradiated and dark controls) for HSC-2 and HSC-3 cell lines.

	HSC-2		HSC-3	
	[VIN] (µg/ml) ± SD (µg/ml)		[VIN] (µg/ml) ± SD (µg/ml)	
	(Irradiated)	(Dark Control)	(Irradiated)	(Dark Control)
IC_{20}	0.0005 ±0.0001	0.0007 ±0.0001	0.0007 ±0.0001	0.0006 ±0.0001
IC_{50}	0.0103 ±0.0015	0.0906 ±0.1264	0.0012 ±0.0001	0.0012 ±0.0001
Two-tailed P value	0.4991		0.4462	
	(p>0.05) Difference is considered to be not statistically significant.		(p>0.05) Difference is considered to be not statistically significant.	

Note: [Mean] (µg/ml) ± SD (µg/ml) represented data from three independent experiments.

Table 4.3b   Inhibitory concentrations of VIN for HSC-4. The VIN inhibitory concentrations and each standard deviation after 72 hours independent drug treatment (irradiated and dark controls) for HSC-4 cell lines.

HSC-4		
[VIN] (µg/ml) ± SD (µg/ml)		
	(Irradiated)	(Dark Control)
IC_{20}	0.00080±0.00012	0.00063 ±0.00034
IC_{40}	0.00125±0.00281	0.00130 ±0.03591
Two-tailed P value	0.4942	
	(p>0.05) Difference is considered to be not statistically significant.	

Note: [Mean] (µg/ml) ± SD (µg/ml) represented data from three independent experiments.

4.1.4 HYP-PDT Treatment Independently

Cytotoxic assay with HYP-PDT alone at concentration ranging from 0.02µg/ml to 0.20µg/ml on HSC-2, HSC-3 and HSC-4 cell lines produced concentration-dependant cell killing as shown in Figure 4.8. The values of IC_{20}, IC_{50}, IC_{70} and IC_{90} of each cell lines were recorded in Table 4.4. HSC-2, HSC-3 and HSC-4 treated with irradiated HYP-PDT (Figure 4.8) showed similar concentration-response curve, giving IC_{50} value of approximately 0.1µg/ml for all three cell lines. Hypericin in dark (figure 4.9) did not result in any cell killing as expected. Therefore, several HYP-PDT concentrations (0.02µg/ml, 0.06µg/ml, 0.10µg/ml, 0.12µg/ml, 0.14µg/ml, 0.16µg/ml) were chosen for HSC-2, HSC-3, HSC-4 to be used in combination with CIS, DOX or VIN.
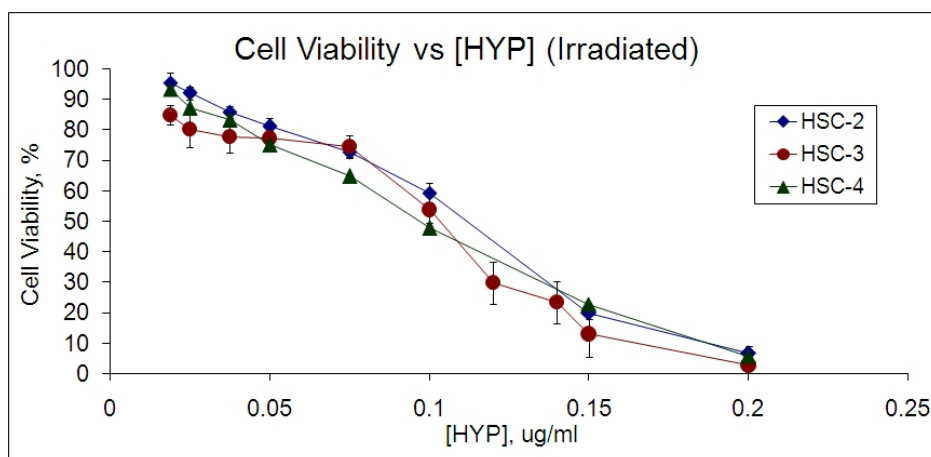
Figure 4.8   Cell viability versus HYP-PDT Concentration (Irradiated). Cell survival rates of irradiated samples in percentage after 72 hours treatment with HYP-PDT independently obtained using MTT assay. Each sample was irradiated according to PDT treatment protocol. Each data point represented the mean ± standard deviation of three independent assays at least.
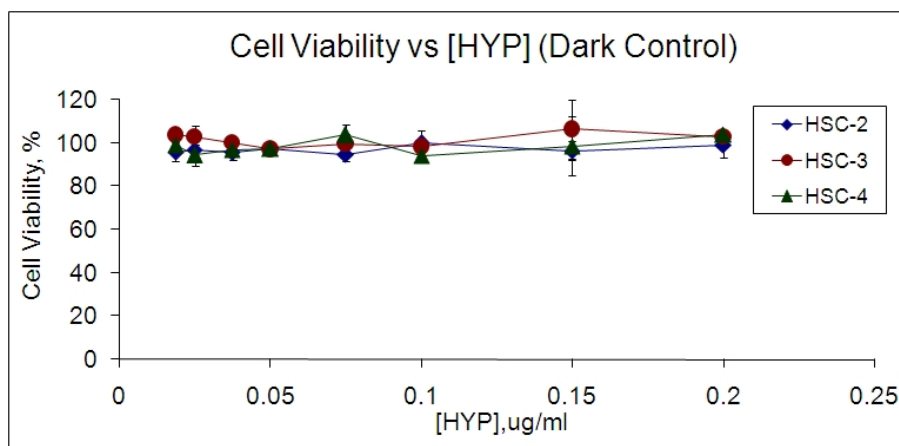
Figure 4.9   Cell viability versus HYP Concentration (Dark Control). Cell survival rates of dark controls in percentage after 72 hours treatment with HYP independently obtained using MTT assay. Each data point represented the mean ± standard deviation of three independent assays at least.

Table 4.4   Inhibitory concentrations of HYP-PDT. The HYP-PDT inhibitory concentrations and each standard deviation after 72 hours independent drug treatment (irradiated and dark controls) for HSC-2, HSC-3, HSC-4 cell lines.

| | HSC-2 | | HSC-3 | | HSC-4 | |
| | [HYP-PDT] (µg/ml) ± SD (µg/ml) | | [HYP-PDT] (µg/ml) ± SD (µg/ml) | | [HYP-PDT] (µg/ml) ± SD (µg/ml) | |
	(Irradiated)	(Dark Control)	(Irradiated)	(Dark Control)	(Irradiated)	(Dark Control)
IC_{20}	0.06 ±0.01	-	0.04 ±0.01	-	0.16 ±0.20	-
IC_{50}	0.11 ±0.01	-	0.10 ±0.01	-	0.09 ±0.0	-
IC_{70}	0.14 ±0.01	-	0.13 ±0.01	-	0.13 ±0.01	-
IC_{90}	0.19 ±0.01	-	0.16 ±0.02	-	0.19 ±0.01	-
Two-tailed P value	Unable to perform		Unable to perform		Unable to perform	

Note: [Mean] (µg/ml) ± SD (µg/ml) represented data from at least three independent experiments.

86

4.1.5 Drugs Interaction of HYP-PDT+CIS Combination Treatment

The concentration pairs of HYP-PDT+CIS that resulted in killing 50% (Table 4.5a) and 90% (Table 4.5b) of cells are as recorded. A range of HYP-PDT concentrations 0.02μg/ml, 0.06μg/ml, 0.10μg/ml, 0.12μg/ml, 0.14μg/ml and 0.16μg/ml were each used in combination with a series of CIS concentrations for each cell line as mentioned in section 4.1.1. The data in Table 4.5a and Table 4.5b, extracted from raw data recorded in Appendix I, were used to construct isobolograms to determined drugs interactions.

Table 4.5a   IC$_{50}$ isoeffect level HYP-PDT+CIS combinations. The CIS concentrations that killed 50% of HSC-2, HSC-3, HSC-4 cell lines when combined with six fixed concentrations of HYP-PDT.

	IC$_{50}$ isoeffect level HYP-PDT+CIS Combinations		
	HSC-2	HSC-3	HSC-4
	[CIS] (µg/ml) ± SD (µg/ml)	[CIS] (µg/ml) ± SD (µg/ml)	[CIS] (µg/ml) ± SD (µg/ml)
[HYP-PDT] (µg/ml)			
0.02	6.50 ±0.36	0.94 ±0.30	0.37 ±0.03
0.06	5.47 ±0.21	0.39 ±0.08	0.35 ±0.06
0.10	3.10 ±0.96	0.16 ±0.05	0.14 ±0.04

Note: [Mean] (µg/ml) ± SD (µg/ml) represented data from at least three independent experiments.

Table 4.5b   IC$_{90}$ isoeffect level HYP-PDT+CIS combinations. The CIS concentrations that killed 90% of HSC-2, HSC-3, HSC-4 cell lines when combined with six fixed concentrations of HYP-PDT.

| [HYP-PDT] (µg/ml) | IC$_{90}$ isoeffect level HYP+CIS Combinations | | |
| | HSC-2 | HSC-3 | HSC-4 |
	[CIS] (µg/ml) ± SD (µg/ml)	[CIS] (µg/ml) ± SD (µg/ml)	[CIS] (µg/ml) ± SD (µg/ml)
0.02	10.13 ±0.06	2.33 ±0.15	3.22 ±0.20
0.06	9.63 ±0.25	1.99 ±0.20	3.40 ±0.09
0.10	8.53 ±0.15	2.05 ±0.22	3.40 ±0.17
0.12	6.45 ±0.07	1.83 ±0.29	1.55 ±0.07
0.14	2.97 ±0.55	1.00 ±0.36	0.35 ±0.17
0.16	2.80 ±0.85	0.22 ±0.03	-

Note: [Mean] (µg/ml) ± SD (µg/ml) represented data from at least three independent experiments.

In HSC-2, less than additive effects were observed in all combination concentrations that would kill 50% and 90% of cells (Figure 4.10a and Figure 4.10d). Therefore, HYP-PDT+CIS combination treatment in HSC-2 was not further investigated.

For combination concentrations that would give 90% cell killing effect in HSC-3 (Figure 4.10e), additive interaction was observed only when low concentrations CIS (0.22μg/ml, approximately IC_{30}), was combined with high concentrations HYP-PDT (0.16μg/ml, approximately IC_{90}). For IC_{50} isoeffect level combination concentrations (Figure 4.10b), less than additive interaction was observed when high concentration HYP-PDT (0.10μg/ml, approximately IC_{50}) was combined with low concentration CIS (0.16μg/ml, approximately IC_{30}). The same effect occurred for combination of high concentration CIS (0.94μg/ml, $>IC_{90}$) and low concentration HYP-PDT(0.02μg/ml, $<IC_{20}$) as well. After IC_{50} isoeffect level concentrations, HYP-PDT+CIS only showed additive effect at relatively moderate concentration of HYP-PDT (0.06μg/ml, approximately IC_{30}) and CIS (0.39μg/ml, approximately IC_{30}) and this occurred within very specific concentration range within a narrow threshold (dotted circled region in Figure 4.10b). This additive drug concentration pair (HYP-PDT 0.06μg/ml and CIS 0.39μg/ml) can kill 50% of HSC-3 cells with only about 40% of CIS (IC_{50}=0.98μg/ml) or 60% HYP-PDT (IC_{50}=0.10μg/ml) needed to kill 50% of cells when used independently.

For IC_{90} isoeffect level combinations in HSC-4 cells (Figure 4.10f), synergistic interaction occurred when high concentration HYP-PDT was

combined with low concentration CIS (HYP-PDT 0.14μg/ml and CIS 0.35μg/ml). This synergistic effect can be achieved with less than 10% of CIS (IC_{90}=4.68μg/ml) or less than 75% HYP-PDT (IC_{90}=0.19μg/ml) needed to kill 90% of HSC-4 cells independently. Synergistic interaction shifted toward less than additive interaction (HYP-PDT 0.10μg/ml and CIS 3.4μg/ml) up to a threshold (dotted circled region) when HYP-PDT concentration decreased and CIS increased in combination. Beyond this threshold, with similar high CIS concentration (3.4μg/ml) (HYP-PDT 0.10μg/ml and CIS 3.4μg/ml), decrement of HYP-PDT concentration resulted in a shift towards a synergistic interaction (HYP-PDT 0.02μg/ml and CIS 3.21μg/ml). The the IC_{50} isoeffect level (Figure 4.10c), synergistic interaction was observed when low concentration HYP-PDT was combined with high concentration CIS (HYP-PDT 0.02μg/ml and CIS 0.37μg/ml). This synergistic effect can be achieved with approximately 35% of CIS (IC_{90}=1.05μg/ml) and less than 25% HYP-PDT (IC_{90}=0.09μg/ml) needed to kill 50% of cells when used independently. When HYP-PDT concentration increased beyond a threshold (dotted circled region), drug interaction shifted toward less than additive effect.
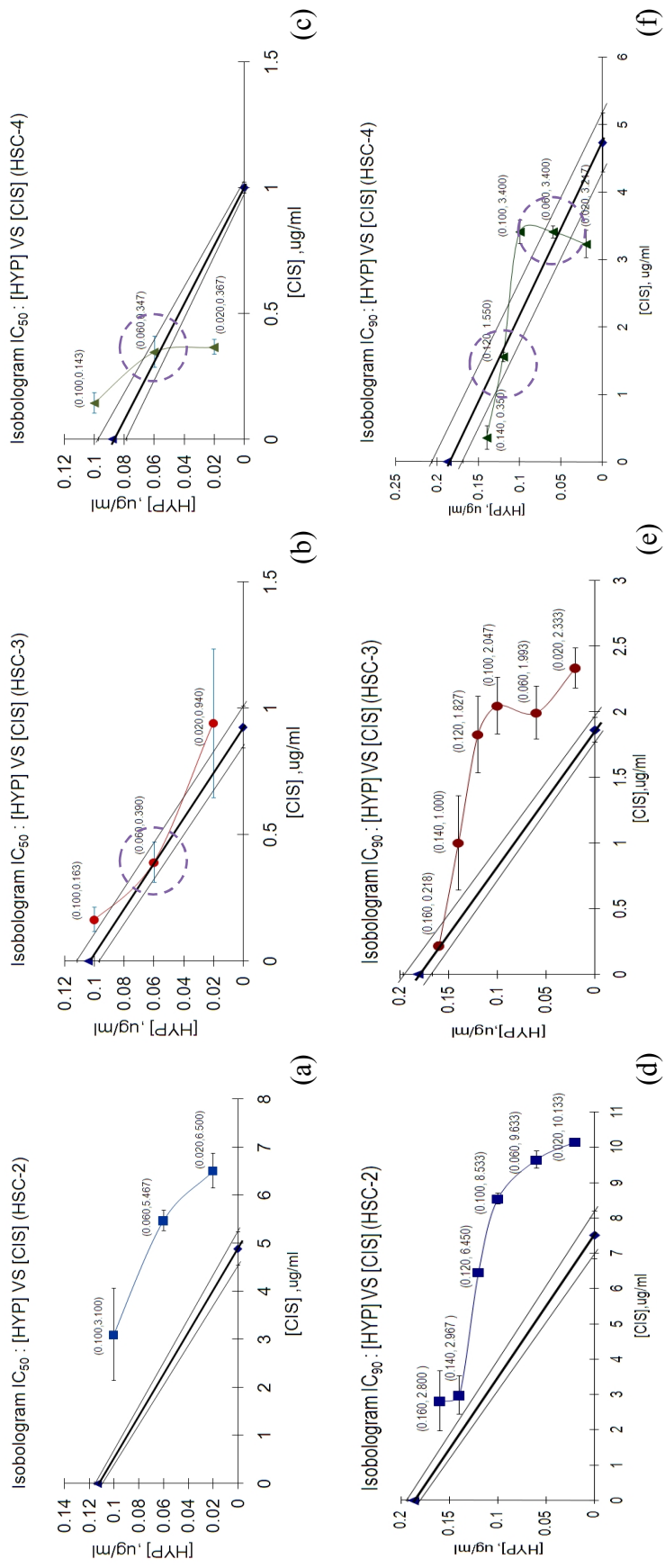
Figure 4.10(a-f)   Isobolograms of HYP-PDT+CIS combination. Isobologram of HYP-PDT and CIS concentrations in combination treatments that kill 50% of HSC-2(a), HSC-3(b), HSC-4(c) and 90% HSC-2(d), HSC-3(e), HSC-4(f) cell line. Thick solid line represents line of 'additivity' bounded by standard error. The numbers in parentheses (Y, X) above refers to (HYP-PDT concentration, CIS concentration) in µg/ml.

4.1.6 Drugs Interaction of HYP-PDT+DOX Combination Treatment

The concentration pairs of HYP-PDT+DOX that resulted in killing 50% (Table 4.6a) and 90% (Table 4.6b) of cells were recorded. Fixed HYP-PDT concentrations 0.02μg/ml, 0.06μg/ml, 0.10μg/ml, 0.12μg/ml, 0.14μg/ml and 0.16μg/ml were each used in combination with a series of DOX concentrations for all cell lines as described in section 4.1.2. The data in Table 4.5a and Table 4.5b were used to construct isobolograms to determined drugs interaction.

Table 4.6a   IC$_{50}$ isoeffect level HYP-PDT+DOX combinations. The DOX concentrations that killed 50% of HSC-2, HSC-3, HSC-4 cell lines when combined with six fixed concentrations of HYP-PDT-PDT.

	IC$_{50}$ isoeffect level HYP-PDT+DOX Combinations		
	HSC-2	HSC-3	HSC-4
	[DOX] (µg/ml) ± SD (µg/ml)	[DOX] (µg/ml) ± SD (µg/ml)	[DOX] (µg/ml) ± SD (µg/ml)
[HYP-PDT] (µg/ml)			
0.02	0.56 ±0.09	0.483 ±0.07	0.337 ±0.08
0.06	0.43 ±0.09	0.285 ±0.08	0.217 ±0.06
0.10	0.12 ±0.09	0.117 ±0.04	-
0.12	-	-	-
0.14	-	-	-
0.16	-	-	-

Note: [Mean] (µg/ml) ± SD (µg/ml) represented data from at least three independent experiments.

Table 4.6b   IC$_{90}$ isoeffect level HYP-PDT+DOX combinations. The DOX concentrations that killed 90% of HSC-2, HSC-3, HSC-4 cell lines when combined with six fixed concentrations of HYP-PDT.

	IC$_{90}$ isoeffect level HYP-PDT+DOX Combinations		
	HSC-2	HSC-3	HSC-4
	[DOX] (μg/ml) ± SD (μg/ml)	[DOX] (μg/ml) ± SD (μg/ml)	[DOX] (μg/ml) ± SD (μg/ml)
[HYP-PDT] (μg/ml)			
0.02	0.90 ±0.04	0.75 ±0.03	1.09 ±0.14
0.06	0.86 ±0.05	0.57 ±0.04	0.77 ±0.04
0.10	0.45 ±0.07	0.22 ±0.06	0.26 ±0.02
0.12	0.15 ±0.09	0.05 ±0.03	0.13 ±0.06
0.14	0.13 ±0.06	0.06 ±0.03	0.02 ±0.01
0.16	0.04 ±0.03	-	-

Note: [Mean] (μg/ml) ± SD (μg/ml) represented data from at least three independent experiments.

Figure 4.11a, Figure 4.11b and Figure 4.11c show isobolograms of HYP-PDT+DOX combination constructed using combination concentrations that were able to kill 50% of HSC-2, HSC-3 and HSC-4 cells, respectively. For all concentrations resulting in 50% cell killing, less than additive effect was observed regardless of HYP-PDT and DOX concentrations.

In all three cell lines analysed with IC_{90} isoeffect level isobologram, synergistic effects were observed with low concentrations of DOX and high concentrations of HYP-PDT up to a threshold point, represented by dotted-circled region in Figure 4.11d, Figure 4.11e and Figure 4.11f. Combination concentrations greater than the threshold gave mainly additive effects, except it showed less than additive effect in HSC-2 cells. HYP-PDT+DOX (IC_{90}=0.12μg/ml HYP-PDT and 0.15μg/ml DOX) kill 90% of HSC-2 cells with only about 15% of DOX (IC_{90}=1.38μg/ml) and 65% of HYP-PDT (IC_{90}=0.19μg/ml) needed to give same killing effect when used independently. In HSC-3 cells, synergistic pair of HYP-PDT+DOX (IC_{90}=0.10μg/ml HYP-PDT and 0.22μg/ml DOX) can kill 90% of HSC-3 cells with approximately 30% of DOX (IC_{90}=0.73μg/ml) and less than 65% HYP-PDT (IC_{90}=0.16μg/ml) needed to kill 90% of cells when used independently. In HSC-4 cells, all combination treatments showed at least additive effect. HYP-PDT+DOX (IC_{90}=0.10μg/ml HYP-PDT and 0.26μg/ml DOX) synergistic pair can kill 90% HSC-4 cells with approximately 20% of DOX (IC_{90}=1.24μg/ml) and less than 55% HYP-PDT (IC_{90}=0.19μg/ml) needed to kill 90% of cells when used independently.
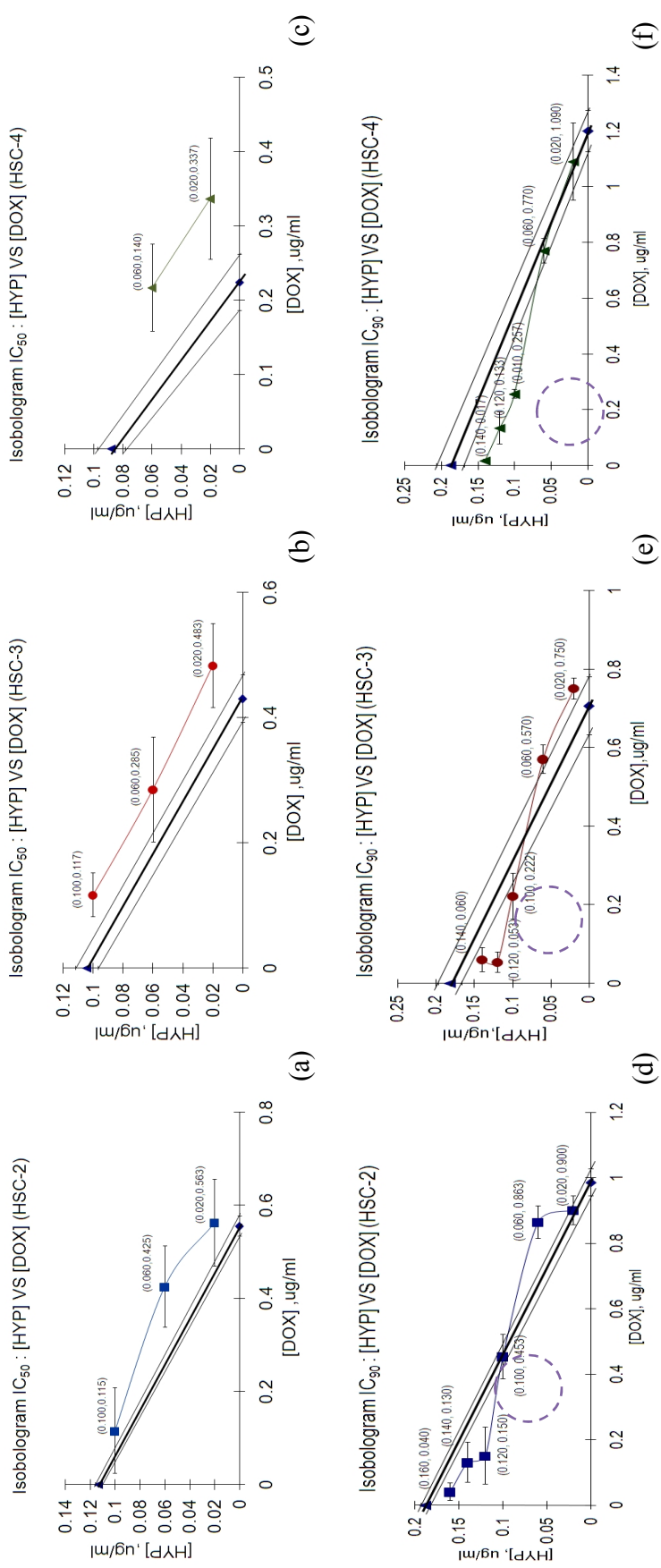
Figure 4.11(a-f)   Isobolograms of HYP-PDT and DOX concentrations in combination treatments that kill 50% of HSC-2(a), HSC-3(b), HSC-4(c) and 90% HSC-2(d), HSC-3(e), HSC-4(f) cell line. Thick solid line represents line of additivity' bounded by standard error. The numbers in parentheses (Y,X) above refers to the concentration of DOX (X) and HYP-PDT (Y) in µg/ml.

4.1.7 Drugs Interaction of HYP-PDT+VIN Combination Treatment

The concentration pairs of HYP-PDT+VIN that resulted in killing 50% of HSC-2 and HSC-3 cells and 40% of HSC-4 cells were recorded in Table 4.7.   fixed HYP-PDT concentrations 0.02μg/ml, 0.06μg/ml, 0.10μg/ml, 0.12μg/ml, 0.14μg/ml and 0.16μg/ml were each used in combination with a series of VIN concentrations as described in section 4.1.3. The data in Table 4.5a and Table 4.5b were used to construct isobolograms to determined drugs interactions. Due to cytostatic nature of VIN, only combination concentrations that would kill 50% of cell or less were evaluated.

Table 4.7   IC$_{50}$ isoeffect level HYP-PDT+VIN combinations in HSC-2, HSC-3 and IC$_{40}$ isoeffect level HYP-PDT+VIN combinations in HSC-4. The VIN concentrations that killed 50% of HSC-2, HSC-3 and 40% of HSC-4 cell lines when combined with six fixed concentrations of HYP-PDT.

[HYP-PDT] (µg/ml)	IC$_{50}$ isoeffect level HYP-PDT+VIN Combinations HSC-2 [Vinblastin] (µg/ml)± SD (µg/ml)	IC$_{50}$ isoeffect level HYP-PDT+VIN Combinations HSC-3 [Vinblastin] (µg/ml) ± SD (µg/ml)	IC$_{40}$ isoeffect level HYP-PDT+VIN Combinations HSC-4 [Vinblastin] (µg/ml)± SD (µg/ml)
0.02	0.0142 ±0.0008	0.0009 ±0.0001	0.0021 ±0.0007
0.06	0.0022 ±0.0018	0.0004 ±0.0003	0.0011 ±0.0002
0.10	0.0042 ±0.0008	-	-

Note: [Mean] (µg/ml) ± SD (µg/ml) represented data from at least three independent experiments.

In HSC-2 cells (Figure 4.12a), synergistic interaction (IC_{50} isoeffect level = 0.06μg/ml HYP-PDT and 0.002μg/ml VIN) was observed only in specific concentration range bounded in between 0.04μg/ml - 0.08 μg/ml HYP-PDT and 0.003μg/ml - 0.007μg/ml VIN. This synergistic effect can be achieved with approximately 20% of VIN (IC_{50} =0.01μg/ml) and less than 55% HYP-PDT (IC_{50}=0.11μg/ml) needed to kill 50% of cells when used independently. When both HYP-PDT and VIN concentration increased in the combination (IC_{50} isoeffect level = 0.10μg/ml HYP-PDT and 0.004μg/ml VIN), less than additive interaction was observed. On the other hand, when HYP-PDT concentration was reduced and VIN concentration increased, synergistic interaction shifted toward less than additive interaction (IC_{50} isoeffect level = 0.02μg/ml HYP-PDT and 0.014μg/ml VIN).

All combinations of HYP-PDT+VIN concentration against HSC-3 cells gave additive effects (Figure 4.12b). For example, an additive combination (IC_{50} isoeffect level = 0.06μg/ml HYP-PDT and 0.0011μg/ml VIN) can result in 50% cell killing with approximately 30% of VIN (IC_{50}=0.0012μg/ml) and approximately 60% HYP-PDT (IC_{50}=0.10μg/ml) needed to kill 50% of cells when used independently.

In HSC-4, since combination of HYP-PDT+VIN with fixed HYP-PDT concentration of 0.02μg/ml and 0.06μg/ml did not kill more than 50% of cells, there was no IC_{50} data available (Appendix Table 9.1-Appendix Table 9.3). HYP-PDT with 0.10μg/ml concentration alone is approaching IC_{50} isoeffect level, therefore, all combination using fixed concentration 0.10μg/ml of HYP-

PDT will have to be evaluated at inhibitory concentration (IC) higher than IC_{50} isoeffect level. Since there is no IC_{90} data available for fixed HYP-PDT concentration 0.10μg/ml and above, the best options are evaluation at IC_{40} isoeffect level or IC_{70} isoeffect level. In this circumstance, IC_{40} isoeffect level is selected to perform evaluation.

All IC_{40} isoeffect level combinations gave synergistic effect (Figure 4.12c). For example, a synergistic combination (IC_{40}=0.06μg/ml HYP-PDT and 0.0004μg/ml VIN) can result in 40% cell killing with less than 20% of VIN (IC_{40}=0.0025μg/ml) and approximately 75% HYP-PDT (IC_{40}=0.08μg/ml) needed to kill 40% of cells when used independently.
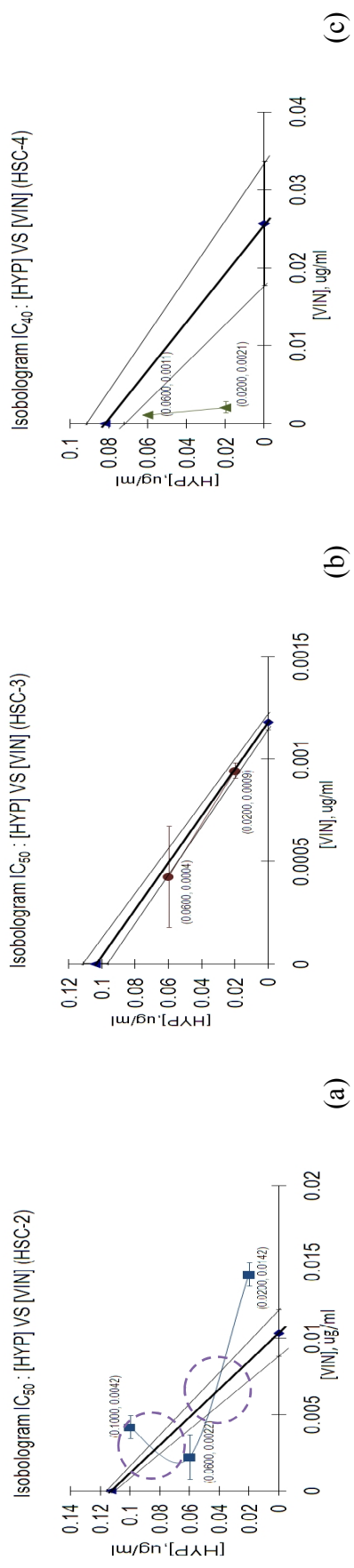
Figure 4.12(a-c) Isobolograms of HYP-PDT+VIN combination. Isobologram of HYP-PDT and VIN concentrations in combination treatments that kill 50% of HSC-2(a) and HSC-3(b), and 40% of HSC-4(c) cell line. Thick solid line represents line of 'additivity' bounded by standard error. The numbers in parentheses (Y,X) above refers to the concentration of DOX (X) and HYP-PDT (Y) in μg/ml.

4.2   Cell Killing Mode of Combination Treatment

4.2.1   Flow Cytometric Measurement of Phosphotidylserine

Externalisation

To reveal whether these combination of drugs concentration kill cells by apoptosis or necrosis, double staining flow cytometric analysis using FITC-Annexin V and PI was done on HSC-2, HSC-3 and HSC-4 cells treated with drug combinations which resulted in 40%, 50% or 90% cell killing in prior MTT assays.

4.2.1.1 Combination drug pair selection principle

From IC_{40}, IC_{50} and IC_{90} isoeffect level isobolographic analysis in section 4.1, one of the synergistic or additive drug pair was selected from each combination for further cell death analysis using flow cytometric method. The principle of selection is as follow,

1. It must be synergistic or additive combination. Less than additive or antagonistic drugs pairs are not worthy to further investigate.

2. If both IC_{50} and IC_{90} isoeffect level isobologram have additive and synergistic combination pairs, concentration of individual drug component in a combination to be selected must be lower than or equal to IC_{50} isoeffect level. This is to comply with objective of reducing drug concentration of both drug components in order to lower side

effect or drug toxicity. For example, HSC-4 treated with HYP-PDT+CIS (Figure 4.10(c) and Figure 4.10(f)), even though there are synergistic pairs in IC_{90} isobologram (Figure 4.10(f)) given by high concentration of HYP-PDT and low concentration of CIS or vice-versa, one of the drug components exceeded IC_{50} concentration limit, thus, they were not selected.

3. In the case where only IC_{50} isobologram showed additive or synergistic combination pairs and IC_{90} isobologram give all less than additive or antagonistic combination pairs (or vice-versa), and if and only if when these additive or synergistic combination pairs have one of the component drug concentration greater than IC_{50} isoeffect level, principle no. 2 can be ignored.

4. In the case where the synergistic combination pairs are resulted with one of the drug component with extremely low concentration (less than IC_{20} isoeffect level), this drug pair is not selected. These data was obtained from assay done with 96-well plate and further flow-cytometric analysis was to be done in 6-well plate. Volumetric scale up of very low drug concentration against cells growing in single layer might alter the actual effect of drug where the scale-up effect was in concern. For example, in figure 4.10(c), synergistic combination was not selected for scale-up analysis in this section.

4.2.2 HYP-PDT+CIS Treatment on HSC-2

HSC-2 treated with HYP-PDT+CIS was not subjected to flow cytometric test because observation from both IC_{50} and IC_{90} isobolograms (Figure 4.10) in section 4.1.5 exhibited less than additive (antagonistic) effect for all HYP-PDT+CIS combinations pairs.

4.2.3 HYP-PDT+CIS Treatment on HSC-3

Dot plots (divided by quadrants) of HSC-3 cells treated with HYP-PDT+CIS (additive combination; IC_{50} isoeffect level; 0.06μg/ml HYP-PDT and 0.39μg/ml CIS), recorded after phosphatidylserine redistribution assay, are shown in Figure 4.13.

Based on isobologram, this HYP-PDT+CIS concentration pair (additive combination; IC_{50} isoeffect level; 0.06μg/ml HYP-PDT and 0.39μg/ml CIS), gave additive effect. However, it did not produce apoptosis in HSC-3 cells. More than 80% of cells remained viable throughout 72 hours (Figure 4.13; Row I). At 1 hour post irradiation, 6.5% of cells appeared in the UL quadrant (Figure 4.13; Row I, Column A) and increased over time to 10.6% at 48 hours (Figure 4.13; Row I, Column F) and 6.6% at 72 hours (Figure 4.13; Row I, Column G). The amount of cells in the UL quadrant paralleled the results seen with the use of HYP-PDT alone (Figure 4.13; Row III), up to 24 hours. However, at 48 hours (Figure 4.13; Row I, Column F) and

72 hours (Figure 4.13; Row I, Column G), the percentage of cells in the UL quadrant was higher than cells treated with either CIS (Figure 4.13; Row II) or HYP-PDT alone (Figure 4.13; Row III).

CIS alone (0.39μg/ml) did not result in significant killing of HSC-3 and viable cells in LL quadrant were more than 90% throughout 72 hours (Figure 4.13; Row II). Treatment with HYP-PDT alone (0.06μg/ml) did not cause apoptosis and more than 80% of cells remained viable throughout 72 hours (Figure 4.13; Row III). Necrotic cell population of 6.5% was found in the UL quadrant at first hour (Figure 4.13; Row III, Column A) and increased up to 7.5% at 24 hours (Figure 4.13; Row III, Column E). Thereafter, population in UL quadrant dropped to 2.8% at 72 hours (Figure 4.13; Row III, Column G). For untreated HSC-3, the viable cells maintained at more than 95% in LL quadrant throughout 72 hours (Figure 4.13; Row IV).

HSC-3 Cells : HYP-PDT+CIS Combination

Time Points (hour)
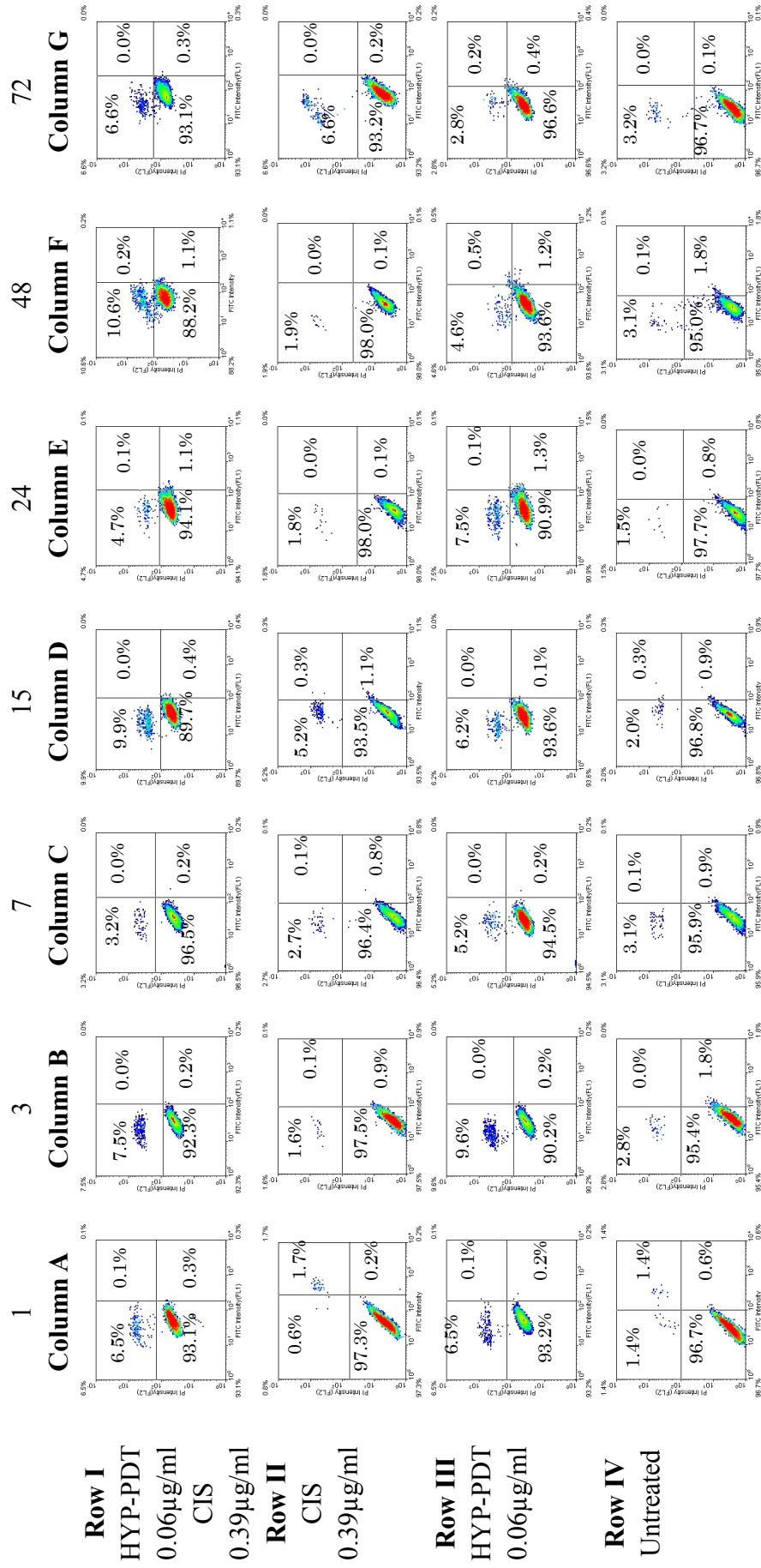
Figure 4.13   Mode of cell death with HYP-PDT+CIS treatment (additive combination; IC$_{50}$ isoeffect level; 0.06µg/ml HYP-PDT and 0.39µg/ml CIS) in HSC-3. Double staining of FITC-Annexin-V and PI was recorded as FL-1 and FL-2 at 1st, 3rd, 7th, 15th, 24th, 48th and 72nd hour.

4.2.4 HYP-PDT+CIS Treatment on HSC-4

Dot plots (divided by quadrants) of HSC-4 cells treated with HYP-PDT+CIS (additive combination; IC_{50} isoeffect level; 0.06μg/ml HYP-PDT and 0.35μg/ml CIS), recorded after phosphatidylserine redistribution assay, are shown in Figure 4.14.

HYP-PDT+CIS (additive combination; IC_{50} isoeffect level; 0.06μg/ml HYP-PDT and 0.39μg/ml CIS) did not kill more than 10% HSC-4 cells at early time points (Figure 4.14; Row I, Column A, B, C) but produced apoptosis in HSC-4 cells at 15 hours (Figure 4.14; Row I, Column D). Viable cells in LL quadrant decreased drastically from 94.3% at 7 hours (Figure 4.14; Row I, Column C) to 14.7% at 15 hours (Figure 4.14; Row I, Column D). At 15 hours, 80% of cells were found in LR quadrant. Apoptotic population decreased over the next few time points to 56% at 48 hours (Figure 4.14; Row I, Column F) and 54% at 72 hours (Figure 4.14; Row I, Column G). The proportion of apoptotic population from 15 hours onward was significantly more than the results seen with the use of CIS (Figure 4.14; Row II) and HYP-PDT (Figure 4.14; Row III) alone. The necrotic cells in the UL quadrant stayed below 5% until 24 hours (Figure 4.14; Row I, Columns A, B, C, D, E). At 48 hours (Figure 4.14; Row I, Column F), 17% necrotic cells were seen in UL quadrant and the percentage continued to increase up to 22% at 72 hours (Figure 4.14; Row I, Column G). The percentage of cells in the UL quadrant from 48 hours onward was higher than cells treated with either CIS (Figure 4.14; Row II) or HYP-PDT alone (Figure 4.14; Row III).

CIS alone (0.35µg/ml) did not result in significant killing of HSC-4 and viable cells in LL quadrant were more than 80% throughout 72 hours (Figure 4.14; Row II). Treatment with HYP-PDT alone (0.06µg/ml) also did not cause apoptosis and more than 80% of cells remain viable throughout 72 hours (Figure 4.14; Row III). Necrotic population of 9.6% were found in UL quadrant at first hour (Figure 4.14; Row III, Column A) and increased up to 13.8% at 72 hours (Figure 4.14; Row III, Column G). For untreated HSC-4, the viable cells maintained at approximately 95% in LL quadrant throughout 72 hours (Figure 4.14; Row IV).
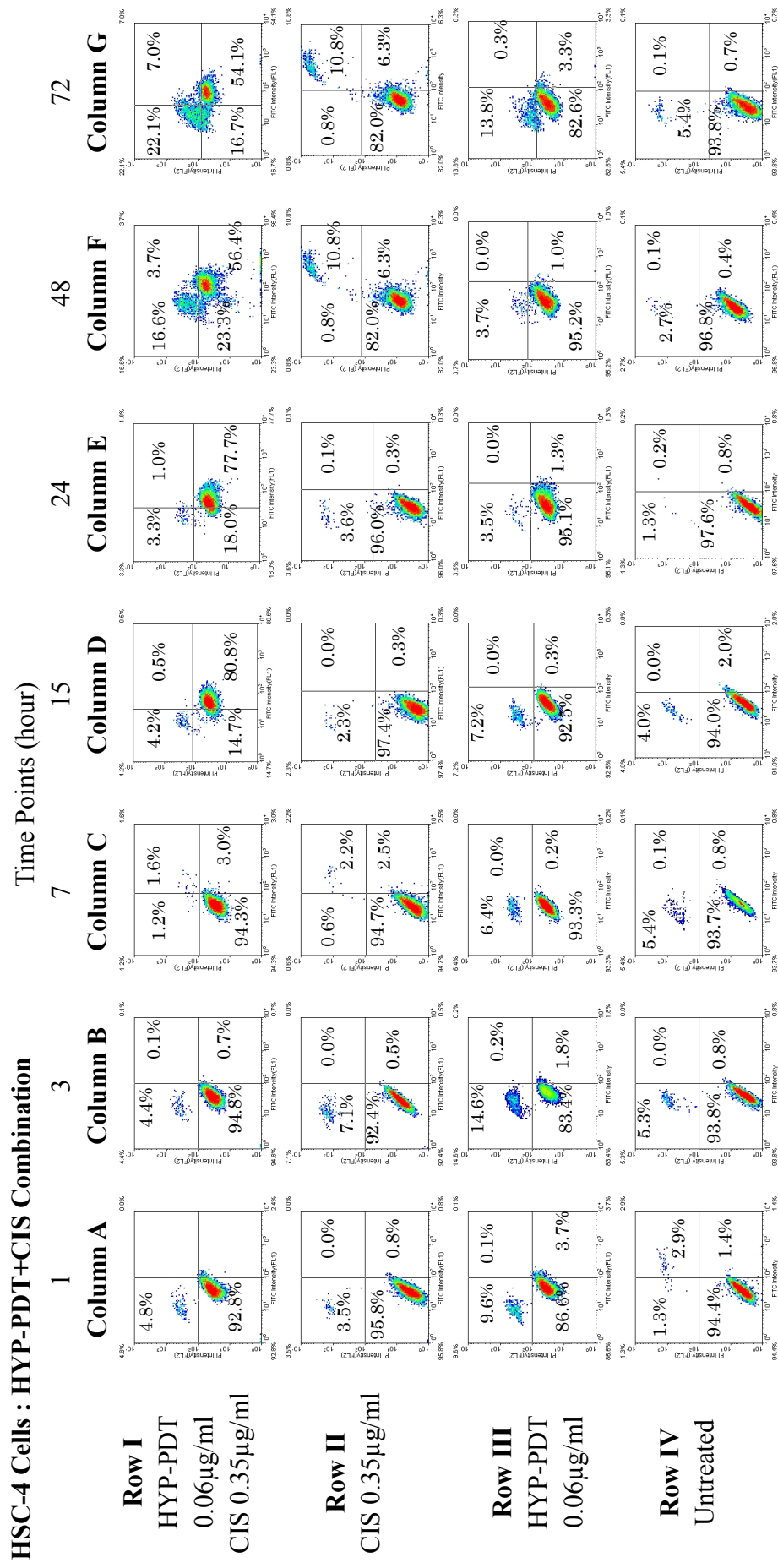
Figure 4.14 Mode of cell death with HYP-PDT+CIS treatment (additive combination; IC_{50} isoeffect level: 0.06μg/ml HYP-PDT and 0.35μg/ml CIS) in HSC-4. Double staining of FITC-Annexin-V and PI was recorded as FL-1 and FL-2 at 1st, 3rd, 7th, 15th, 24th, 48th and 72nd hour.

4.2.5 HYP-PDT+DOX Treatment on HSC-2

Dot plots (divided by quadrants) of HSC-2 cells treated with HYP-PDT+DOX (additive combination; $IC_{90;}$ 0.10μg/ml HYP-PDT and 0.45μg/ml DOX), recorded after phosphatidylserine redistribution assay, are shown in Figure 4.15.

HYP-PDT+DOX (additive combination; $IC_{90;}$ 0.10μg/ml HYP-PDT and 0.45μg/ml DOX) produced 85% apoptotic HSC-2 cells at 1 hour (Figure 4.15; Row I, Column A). This apoptotic population was more than those produced by either DOX (Figure 4.15; Row II, Column A) or HYP-PDT (Figure 4.15; Row III, Column A) alone at 1 hour. Apoptotic population decreased over the next few time points to 62% at 24 hours (Figure 4.15; Row I, Column E) and 6% at 48 hours (Figure 4.15; Row I, Column F). At 72 hours, apoptosis was absent (Figure 4.15; Row I, Column G).

There was 7% of necrotic population seen at 1 hour. This necrotic proportion (7%) is less than necrotic proportion of HSC-2 cells (42%) treated with HYP-PDT alone (0.10μg/ml) at 1 hour. However, cells in UL quadrant continued to increase over the next few time-point to 40% at 15 hours (Figure 4.15; Row I, Column D) and finally 97% at 72 hours (Figure 4.15; Row I, Column G).

DOX alone (0.45μg/ml) did not result in significant killing of HSC-2 and viable cells in LL quadrant were approximately 95% throughout 72 hours

(Figure 4.15; Row II). Treatment with HYP-PDT alone (0.10µg/ml) caused 1.5% apoptosis (less than HYP-PDT+DOX) and 19% necrosis (more than HYP-PDT+DOX) of HSC-2 cells at 1 hour (Figure 4.15; Row III, Column A). The cell death was not significantly different until 15 hours (Figure 4.15; Row III Column D) where the apoptotic population increased to 32.7% and necrotic population increased to 27.7%. Thereafter, necrotic population that might arise from secondary apoptosis continued to increased up to 93.3% at 72 hours (Figure 4.15; Row III Column G).

For untreated HSC-2, the viable cells maintained at approximately 95% in LL quadrant throughout 72 hours (Figure 4.15; Row IV). From these results, it can be observed that most of the effect can be attributed to HYP-PDT alone. The combination of HYP-PDT+DOX only produce earlier onset of apoptosis in HSC-2.
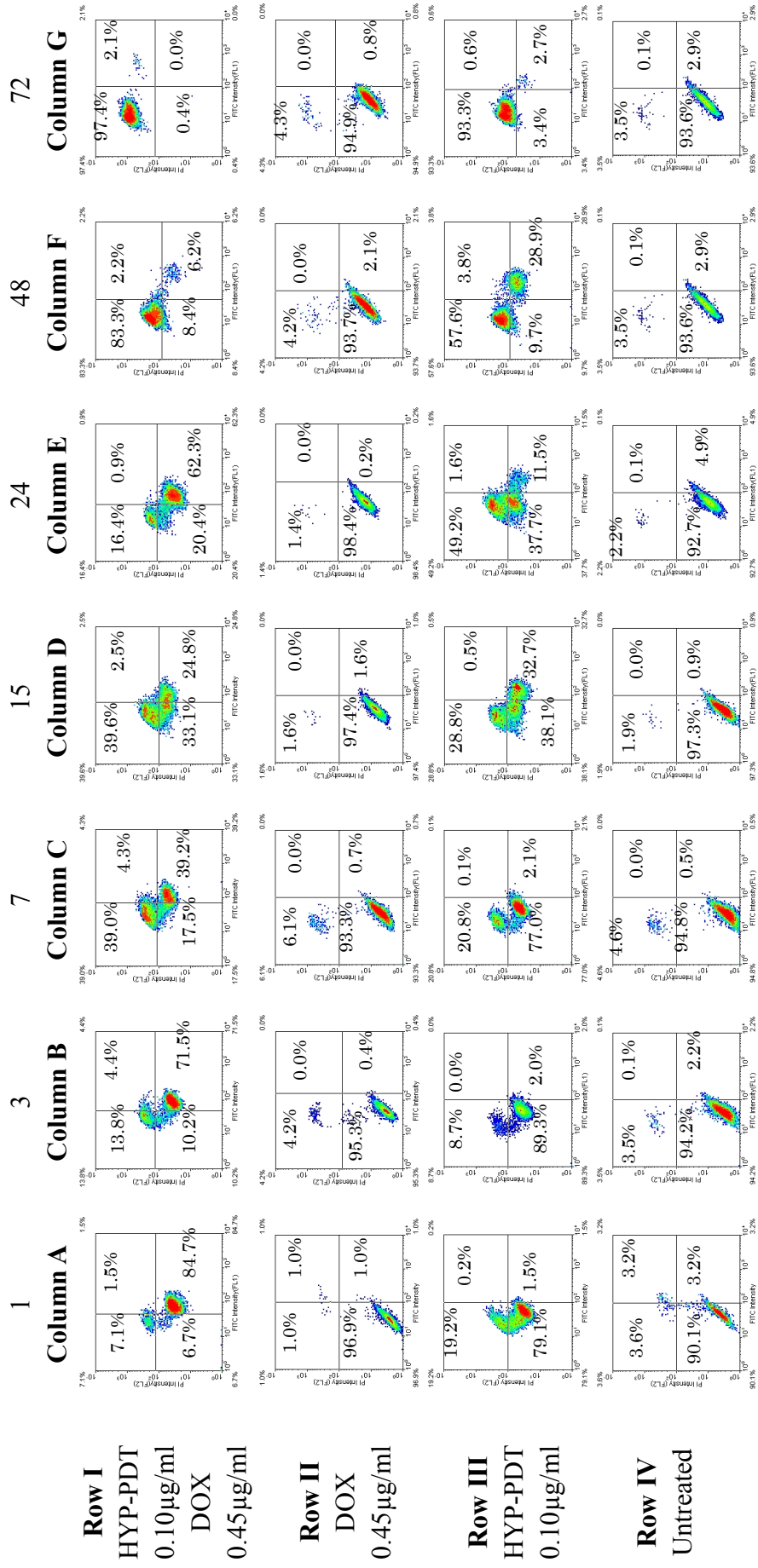
Figure 4.15 Mode of cell death with HYP-PDT+DOX treatment (additive combination; IC$_{90}$: 0.10μg/ml HYP-PDT and 0.45μg/ml DOX) in HSC-2. Double staining of FITC-Annexin-V and PI was recorded as FL-1 and FL-2 at 1st, 3rd, 7th, 15th, 24th, 48th and 72nd hour.

113

4.2.6 HYP-PDT+DOX Treatment on HSC-3

Dot plots (divided by quadrants) of HSC-3 cells treated with HYP-PDT+DOX (synergistic combination; $IC_{90;}$ 0.10µg/ml HYP-PDT and 0.22µg/ml DOX), recorded after phosphatidylserine redistribution assay, are shown in Figure 4.16.

HYP-PDT+DOX (synergistic combination; $IC_{90;}$ 0.10µg/ml HYP-PDT and 0.22µg/ml DOX) produced 63% apoptotic and 11% necrotic HSC-3 cells at 3 hours (Figure 4.16; Row I, Column B). Both of the percentages at this time-point were superior to HSC-3 cells treated with either DOX (0.22µg/ml) or HYP-PDT (0.10µg/ml) alone. The apoptotic population in LR quadrant was later increased to 77% at 15 hours (Figure 4.16; Row I, Column D) before decreasing to 33% at 48 hours (Figure 4.16; Row I, Column F) and 7 % at 72 hours (Figure 4.16; Row I, Column G). At the same time, necrotic population in UL quadrant increase steadily over the next few time-point to 55% at 48 hours (Figure 4.16; Row I, Column F) and 88% at 72 hours (Figure 4.16; Row I, Column G).

DOX alone (0.22µg/ml) did not result in significant killing of HSC-3 and viable cells in LL quadrant were approximately 95% throughout 72 hours (Figure 4.16; Row II). Treatment with HYP-PDT alone (0.10µg/ml) started to produced significant apoptosis (35%) at 15 hours (Figure 4.16; Row III, Column D), which was slower (HYP-PDT alone apoptosis seen at 15 hours; HYP-PDT+DOX apoptosis seen at 3 hours) and lesser in percentage (HYP-

PDT alone 35% at 15 hours; HYP-PDT+DOX 77% at 15 hours) than HYP-PDT+DOX combination. This apoptosis percentage remained around 35% from 15 hours to 48 hours (Figure 4.16; Row III, Column D, E, F) and then decreased to 3% at 72 hours (Figure 4.16; Row III, Column G). The necrotic population caused by HYP-PDT alone remained less than 10% until 7 hours (Figure 4.16; Row III, Column A, B, C). At 15 hours (Figure 4.16; Row III, Column D), necrotic population in UL quadrant increased to 34%. It was further increased to 68% at 72 hours (Figure 4.16; Row III, Column G). For untreated HSC-3, the viable cells maintained at approximately 95% in LL quadrant throughout 72 hours (Figure 4.16; Row IV).

Similar to the result in HSC-2, most of the effect can be attributed to HYP-PDT alone. Combination of HYP-PDT+DOX only helped to produce earlier onset of apoptosis in HSC-3.
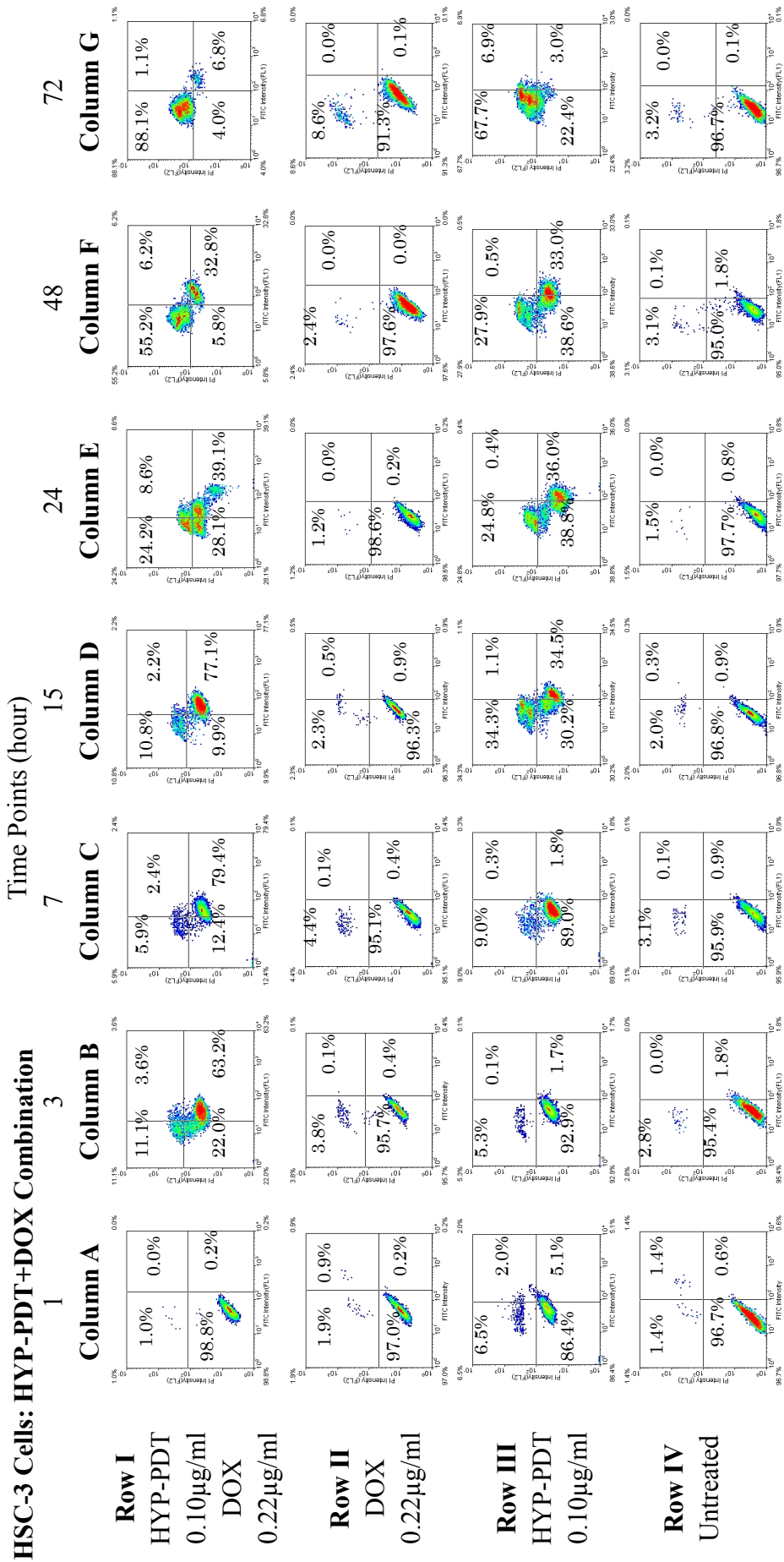
Figure 4.16   Mode of cell death with HYP-PDT+DOX treatment (synergistic combination; IC_{90}; 0.10μg/ml HYP-PDT and 0.22μg/ml DOX) in HSC-3. Double staining of FITC-Annexin-V and PI was recorded as FL-1 and FL-2 at 1st, 3rd, 7th, 15th, 24th, 48th and 72nd hour.

116

4.2.7 HYP-PDT+DOX Treatment on HSC-4

Dot plots (divided by quadrants) of HSC-4 cells treated with HYP-PDT+DOX (synergistic combination; $IC_{90;}$ 0.10μg/ml HYP-PDT and 0.26μg/ml DOX), recorded after phosphatidylserine redistribution assay, are shown in Figure 4.17.

HYP-PDT+DOX (synergistic combination; $IC_{90;}$ 0.10μg/ml HYP-PDT and 0.26μg/ml DOX) started to produce 10% necrotic HSC-4 cells early at 1 hour (Figure 4.17; Row I, Column A). The necrotic population in UL quadrant continued to increase up to 43% at 15 hours (Figure 4.17; Row I, Column D) and around 90% at 48 hours (Figure 4.17; Row I, Column F) and 72 hours (Figure 4.17; Row I, Column G). These percentages were superior to HSC-4 cells treated with either DOX (Figure 4.17; Row II, Column D) or HYP-PDT (Figure 4.17; Row III, Column D) alone at the same time-point. Apoptotic population (28%) only appeared at 15 hours (Figure 4.17; Row I, Column D). This percentage was superior to HSC-4 cells treated with either DOX (Figure 4.17; Row II, Column D) or HYP-PDT (Figure 4.17; Row III, Column D) alone at the same time-point. This percentage increased up to 59% at 24 hours (Figure 4.17; Row I, Column E) and then dropped to approximately 5% at 48 hours (Figure 4.17; Row I, Column F) and 72 hours (Figure 4.17; Row I, Column G). DOX alone (0.26μg/ml) did not result in significant killing of HSC-4 and viable cells in LL quadrant were approximately 95% throughout 72 hours (Figure 4.17; Row II).

Treatment with HYP-PDT alone (0.10μg/ml) started to produced significant apoptosis (37%) at 24 hours (Figure 4.17; Row III, Column E), which was slower (HYP-PDT alone, apoptosis seen at 24 hours; HYP-PDT+DOX apoptosis seen at 15 hours) and lesser in percentage (HYP-PDT alone 37% at 24 hours; HYP-PDT+DOX 59% at 24 hours) than HYP-PDT+DOX combination. This apoptosis percentage was later decreased to 19% at 48 hours (Figure 4.17; Row III, Column F) and 8% at 72 hours (Figure 4.17; Row III, Column G). The necrotic population was around 11-25% until 15 hours (Figure 4.17; Row III, Column A, B, C, D) but increased sharply to 40% at 24 hours (Figure 4.17; Row III, Column E) and 88% at 72 hours (Figure 4.17; Row III, Column G). For untreated HSC-4, the viable cells maintained at approximately 95% in LL quadrant throughout 72 hours (Figure 4.17; Row IV). Similar to the result in HSC-2 and HSC-3, most of the effect can be attributed to HYP-PDT alone. HYP-PDT+DOX only helped to produce earlier onset of apoptosis.
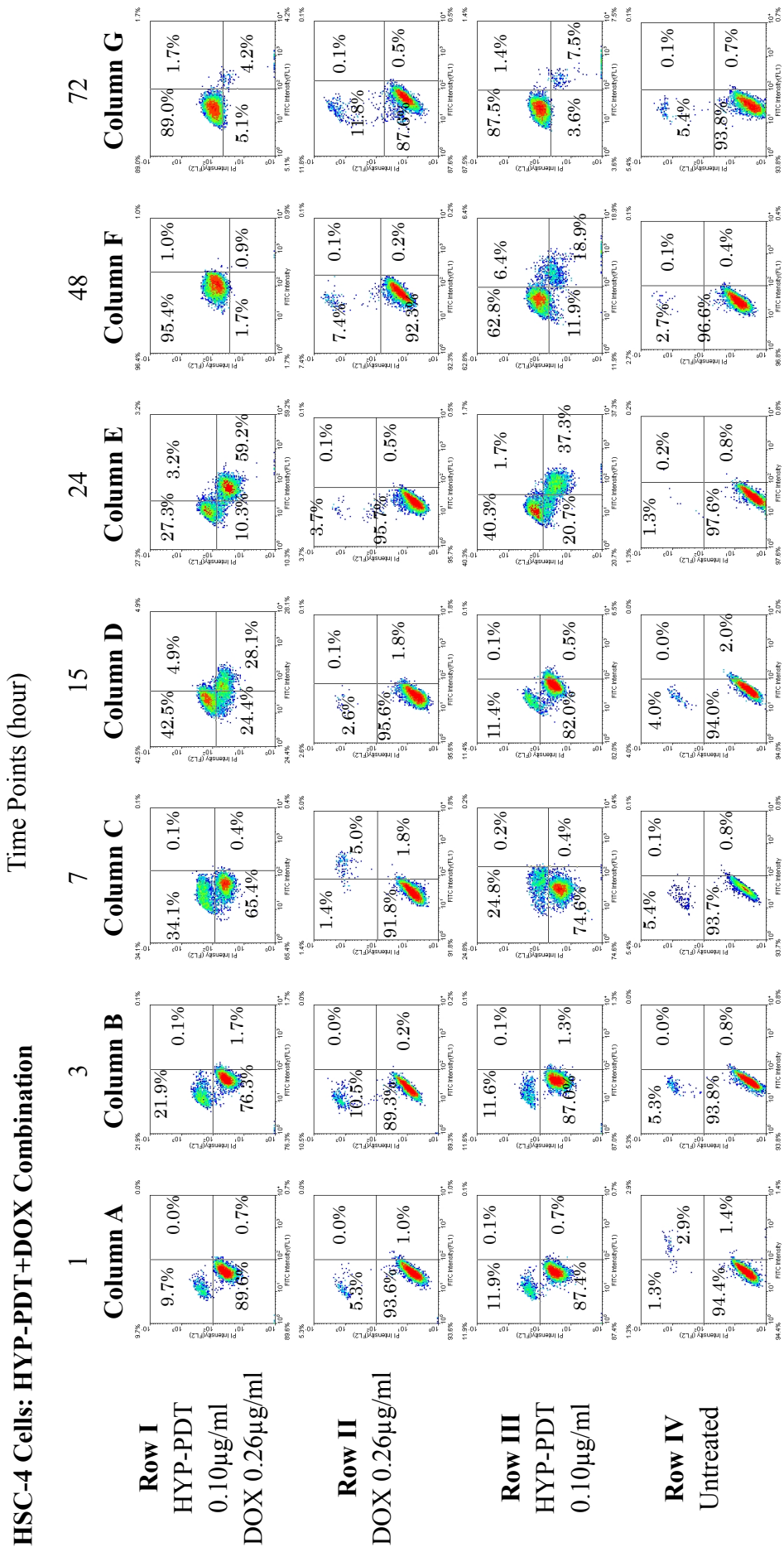
Figure 4.17　Mode of cell death with HYP-PDT+DOX treatment (synergistic combination; IC_{90}; $0.10\mu g/ml$ HYP-PDT and $0.26\mu g/ml$ DOX) in HSC-4. Double staining of FITC-Annexin-V and PI was recorded as FL-1 and FL-2 at 1st, 3rd, 7th, 15th, 24th, 48th and 72nd hour.

4.2.8 HYP-PDT+VIN Treatment on HSC-2

Dot plots (divided by quadrants) of HSC-2 cells treated with HYP-PDT+VIN (synergistic combination; IC_{50} isoeffect level; 0.06μg/ml HYP-PDT and 0.002μg/ml VIN), recorded after phosphatidylserine redistribution assay, are shown in Figure 4.18.

HYP-PDT+VIN (synergistic combination; IC_{50} isoeffect level; 0.06μg/ml HYP-PDT and 0.002μg/ml VIN) produced 78% apoptotic cells in HSC-2 cells early at 1 hour (Figure 4.18; Row I, Column A). This percentage was superior to HSC-2 cells treated with either VIN (Figure 4.18; Row II, Column A) or HYP-PDT (Figure 4.18; Row III, Column A) alone at the same time-point. The apoptotic population in LR quadrant was then decreased steadily to 55% at 24 hours (Figure 4.18; Row I, Column E) and around 4% at 72 hours (Figure 4.18; Row I, Column G). 8% of necrotic population was also seen in UL quadrant at 1 hour. The percentage increased steadily to 21% at 24 hours (Figure 4.18; Row I, Column E) and 94% at 72 hours (Figure 4.18; Row I, Column G). The percentage of necrotic population produced by HYP-PDT+VIN (Figure 4.18; Row I) was superior to HSC-2 cells treated with either VIN (0.002μg/ml) (Figure 4.18; Row II) or HYP-PDT (0.06μg/ml) (Figure 4.18; Row III) alone in all time-points.

Due to cytostatic properties, VIN alone (0.002μg/ml) did not result in significant killing of HSC-2 cells until 48 hours (Figure 4.18; Row II, Column F). At 48 hours, 23% of apoptotic cells in LR quadrant and 35% of necrotic

cells in UL quadrant were seen (Figure 4.18; Row II, Column F). Apoptotic population decreased to 19% at 72 hours while necrotic population increased to 48% at 72 hours (Figure 4.18; Row II, Column G).

Treatment with HYP-PDT alone (0.06µg/ml) only produced around 15% apoptosis from 24 hours to 72 hours (Figure 4.18; Row III, Column E, F, G). The onset of apoptosis was slower than HYP-PDT+VIN (apoptosis onset at 1 hour). The necrotic cells produced by HYP-PDT alone (0.06µg/ml) was less than 10% throughout 72 hours (Figure 4.18; Row III). For untreated HSC-2, the viable cells maintained at approximately 95% in LL quadrant throughout 72 hours (Figure 4.18; Row IV).
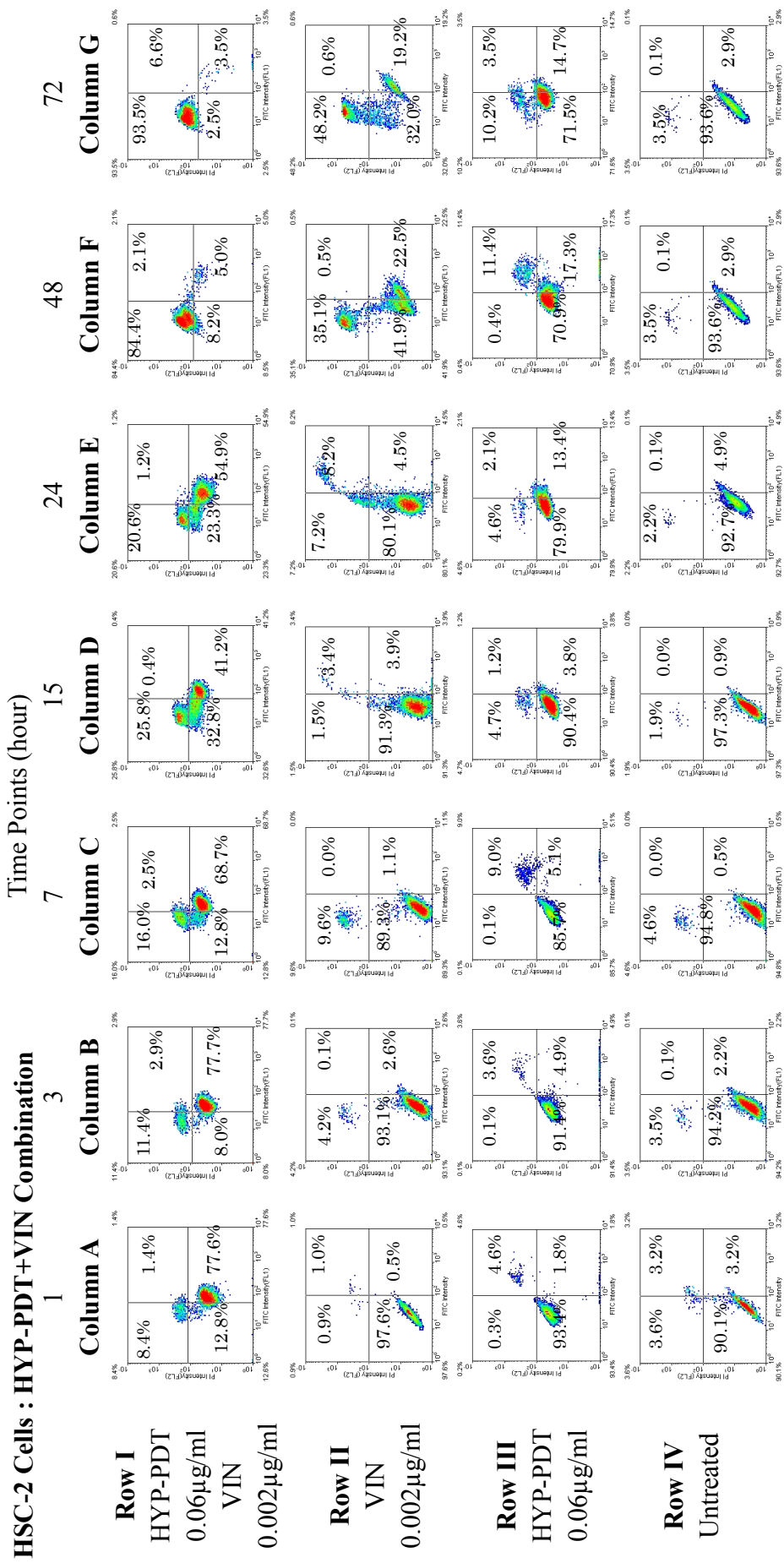
Figure 4.18 Mode of cell death with HYP-PDT+VIN treatment (synergistic combination; IC_{50} isoeffect level. $0.06\mu g/ml$ HYP-PDT and $0.002\mu g/ml$ VIN) in HSC-2. Double staining of FITC-Annexin-V and PI was recorded as FL-1 and FL-2 at 1st, 3rd, 7th, 15th, 24th, 48th and 72nd hour.

122

4.2.9 HYP-PDT+VIN Treatment on HSC-3

Dot plots (divided by quadrants) of HSC-3 cells treated with HYP-PDT+VIN (additive combination; IC_{50} isoeffect level; 0.06μg/ml HYP-PDT and 0.0004μg/ml VIN) recorded after phosphatidylserine redistribution assay, are shown in Figure 4.19.

HYP-PDT+VIN (additive combination; IC_{50} isoeffect level; 0.06μg/ml HYP-PDT and 0.0004μg/ml VIN) produced 19% necrotic cells in HSC-3 cells early at 1 hour (Figure 4.19; Row I, Column A). This percentage was superior to HSC-3 cells treated with either VIN (Figure 4.19; Row II, Column A) or HYP-PDT (Figure 4.19; Row III, Column A) alone at the same time-point. The necrotic population in UL quadrant was then increased to 71% at 15 hours (Figure 4.19; Row I, Column D) and decreased to 22% at 48 hours (Figure 4.19; Row I, Column F). At 72 hours, 87% necrotic cells were detected (Figure 4.19; Row I, Column G). Significant apoptosis caused by HYP-PDT+VIN only appeared from 24 hours (29%) (Figure 4.19; Row I, Column E). This figure is superior to apoptotic percentage of HSC-3 cells treated with either VIN (0.0004μg/ml) (Figure 4.19; Row II, Column E) or HYP-PDT (0.06μg/ml) (Figure 4.19; Row III, Column E) alone at the same time point.

VIN alone (0.002μg/ml) did not result in significant killing of HSC-3 cells until 15 hours (Figure 4.19; Row II, Column D). At 15 hours, 12% of apoptotic cells in LR quadrant and 21% of necrotic cells in UL quadrant were seen (Figure 4.19; Row II, Column D). Apoptotic population decreased to 36%

123

at 72 hours while necrotic population increased to 34% at 72 hours (Figure 4.19; Row II, Column G).

Treatment with HYP-PDT alone (0.06μg/ml) only produced less than 10% necrotic population and less than 2% apoptotic population throughout 72 hours (Figure 4.19; Row III). For untreated HSC-3, the viable cells maintained at approximately 95% in LL quadrant throughout 72 hours (Figure 4.19; Row IV).
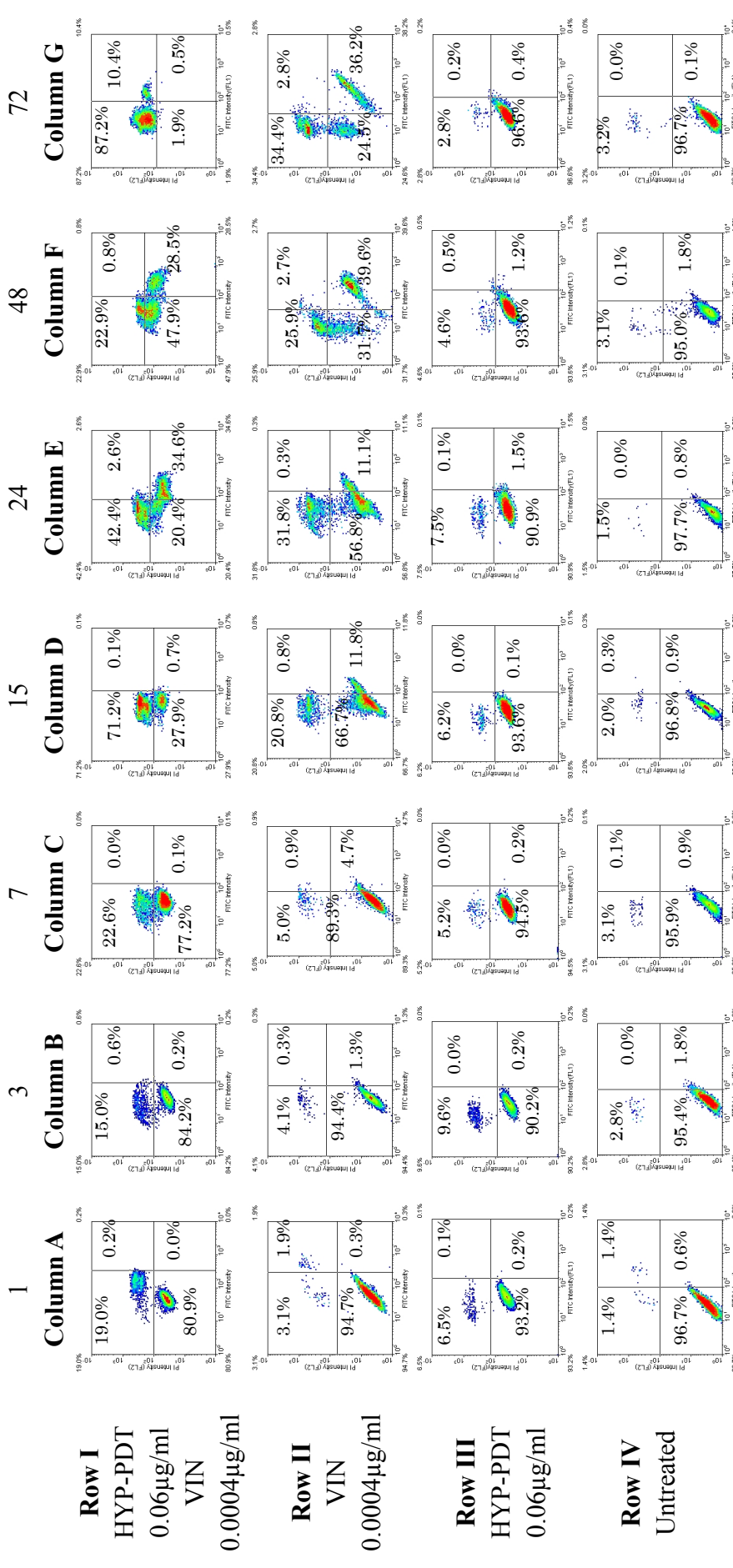
Figure 4.19   Mode of cell death with HYP-PDT+VIN treatment (additive combination; IC$_{50}$ isoeffect level: 0.06µg/ml HYP-PDT and 0.0004µg/ml VIN) in HSC-3. Double staining of FITC-Annexin-V and PI was recorded as FL-1 and FL-2 at 1st, 3rd, 7th, 15th, 24th, 48th and 72nd hour.

4.2.10 HYP-PDT+VIN treatment on HSC-4

Dot plots (divided by quadrants) of HSC-4 cells treated with HYP-PDT+VIN (synergistic combination; IC_{40} isoeffect level; 0.06μg/ml HYP-PDT and 0.00125μg/ml VIN) recorded after phosphatidylserine redistribution assay, are shown in Figure 4.20.

HYP-PDT+VIN (synergistic combination; IC_{40} isoeffect level; 0.06μg/ml HYP-PDT and 0.00125μg/ml VIN) only produced significant apoptotic population (71%) starting from 15 hours (Figure 4.20; Row I, Column D). The apoptotic population was later decreased to 29% at 48 hours (Figure 4.20; Row I, Column F) and 27% at 72 hours (Figure 4.20; Row I, Column G). The necrotic population was around 5% until 7 hours (Figure 4.20; Row I, Column C) and increased to 12% at 15 hours (Figure 4.20; Row I, Column D). At 72 hours, necrotic population was recorded aat 40% (Figure 4.20; Row I, Column G).

VIN alone (0.00125μg/ml) did not result in significant killing of HSC-4 cells until 48 hours (Figure 4.20; Row II, Column F). At 48 hours, 44% of apoptotic cells in LR quadrant and 20% of necrotic cells in UL quadrant were seen (Figure 4.20; Row II, Column F). Apoptotic and necrotic population increased to 48% and 28% respectively at 72 hours (Figure 4.20; Row II, Column G).

Treatment with HYP-PDT alone (0.06μg/ml) only produced less than

10% necrotic population and less than 5% apoptotic population throughout 72 hours (Figure 4.20; Row III). For untreated HSC-4, the viable cells maintained at approximately 95% in LL quadrant throughout 72 hours (Figure 4.20; Row IV).
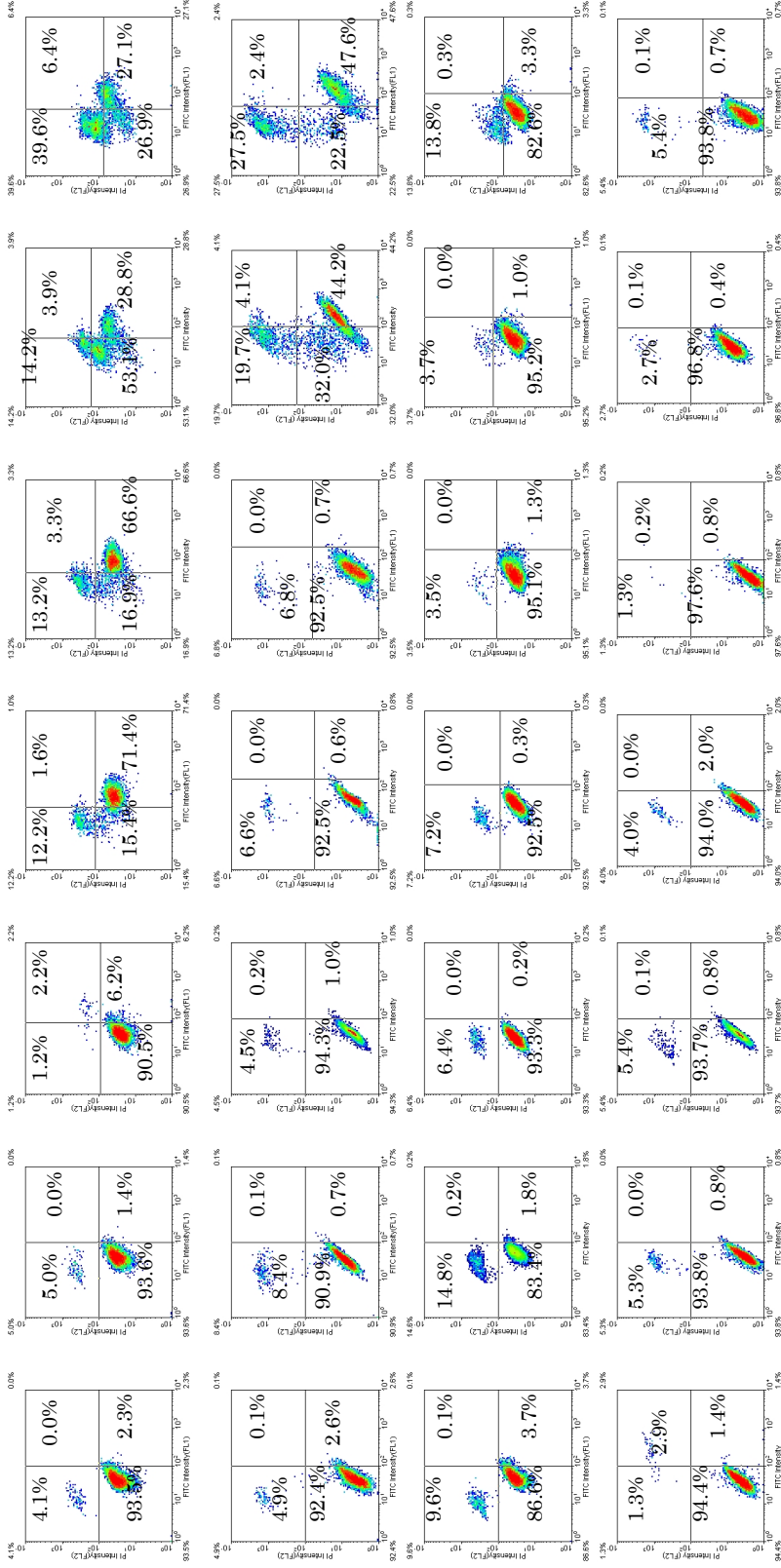
Figure 4.20   Mode of cell death with HYP-PDT+VIN treatment (synergistic combination; IC$_{40}$ isoeffect level; 0.06µg/ml HYP-PDT and 0.00125µg/ml VIN) in HSC-4. Double staining of FITC-Annexin-V and PI was recorded as FL-1 and FL-2 at 1st, 3rd, 7th, 15th, 24th, 48th and 72nd hour.

4.3   Morphological Study of Treatment Effect

Cells morphology was examined in a time course manner post-irradiation. The changes of cell morphology after exposed to combination treatments and independent drug treatment are reported below.

4.3.1   Morphology changes after different combination treatments in HSC-2

4.3.1.1 HYP-PDT+CIS treatment in HSC-2

Morphologiy study was not conducted for HYP-PDT+CIS treatment in HSC-2 because isobolographic reveal combination of both drugs at IC_{50} and IC_{90} isoeffect level gave less than additive effect.

4.3.1.2 HYP-PDT+DOX treatment in HSC-2

In HSC-2, when exposed to HYP-PDT+DOX treatment (additive combination; $IC_{90;}$ 0.10μg/ml HYP-PDT and 0.45μg/ml DOX), majority of HSC-2 cells became round shape (Figure 4.21a). At 3 hours, shrunken cells with apoptotic bodies appeared (Figure 4.21b). Apoptotic cells increased until 15 hours (Figure 4.21d). From 24 hours onward, necrotic cells were predominant and apoptotic cells could hardly be seen. In contrast, with DOX treatment alone (0.45μg/ml), HSC-2 cells remained viable (Figure 4.21l) and the cells' membrane remained intact until 48 hours.

HSC-2:HYP-PDT(0.10μg/ml)+DOX(0.45μg/ml), IC$_{50}$

DOX alone(0.45μg/ml)

(a)1 hour   (d)15 hours   (g)1 hour   (j)15 hours

(b)3 hours   (e)24 hours   (h)3 hours   (k)24 hours

(c)7 hours   (f)48 hours   (i)7 hours   (l)48 hours
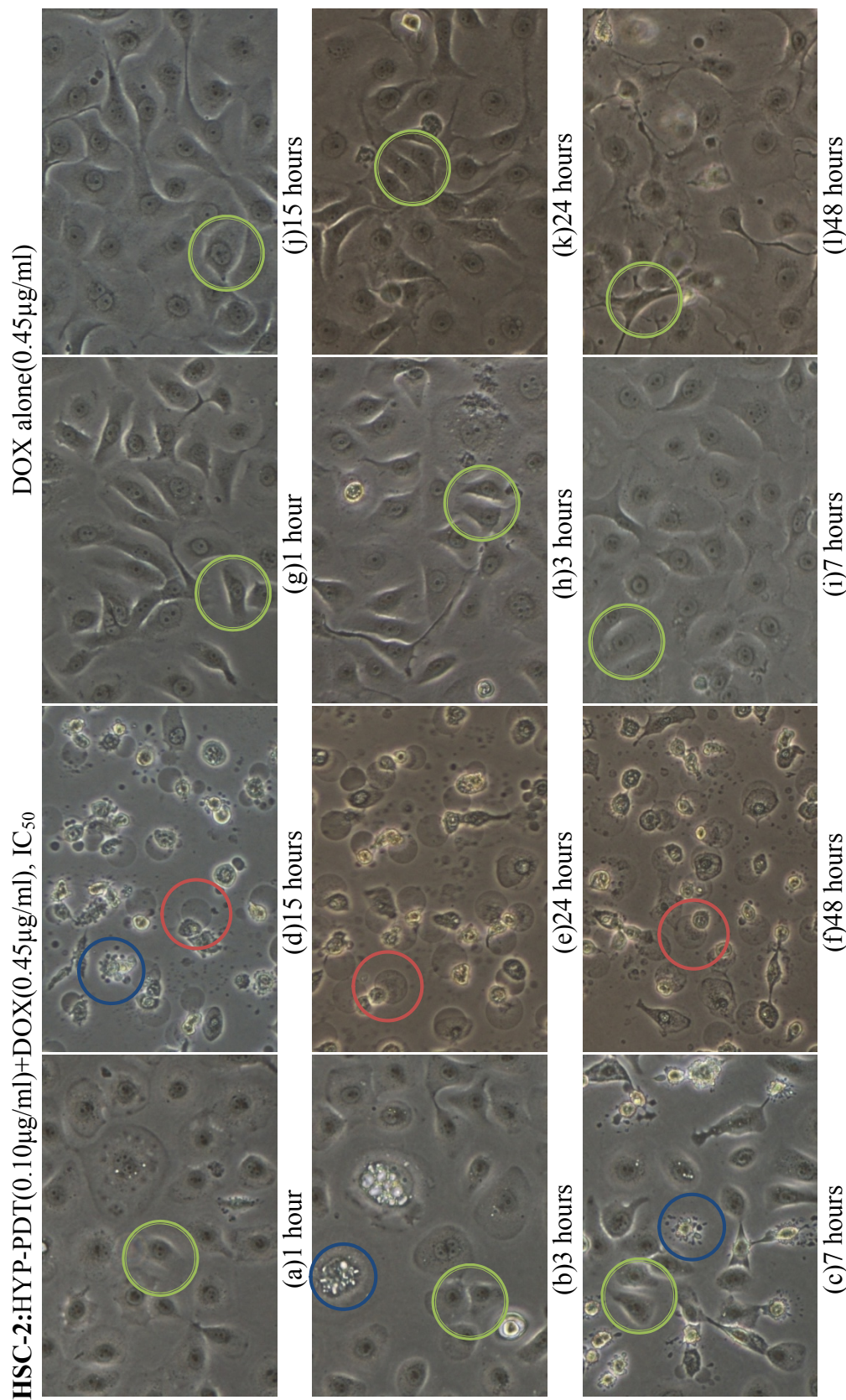
Figure 4.21   Morphological changes of HSC-2 treated with HYP-PDT+DOX and DOX alone at 1st, 3rd, 7th, 15th, 24th and 48th hour post-irradiation were shown above. ⃝ refers to viable cell; ⃝ refers to apoptotic cell; ⃝ refers to necrotic cells. Pictures magnification is 80X.

4.3.1.3 HYP-PDT+VIN treatment in HSC-2

When HSC-2 cells were exposed to HYP-PDT+VIN treatment (synergistic combination; IC_{50} isoeffect level; 0.06μg/ml HYP-PDT and 0.002μg/ml VIN), apoptotic bodies could be seen as early as in 3rd hour (Figure 4.22b). Cells with apoptotic morphology continued to increase until 15 hours (Figure 4.22d) where necrotic cells started to be seen. From 24 hours (Figure 4.22e) onward, necrotic cells is predominant in the culture.

When HSC-2 cells were treated with VIN alone (0.002μg/ml), other than increment in confluency, cells remained viable and no obvious morphological changes were observed from 1 hour (Figure 4.22g) to 48 hours (Figure 4.22l).

HSC-2:HYP-PDT(0.06μg/ml)+VIN(0.002μg/ml), IC$_{50}$

VIN alone(0.002μg/ml)

(a)1 hour

(b)3 hours

(c)7 hours

(d)15 hours

(e)24 hours

(f)48 hours

(g)1 hour

(h)3 hours

(i)7 hours

(j)15 hours

(k)24 hours

(l)48 hours
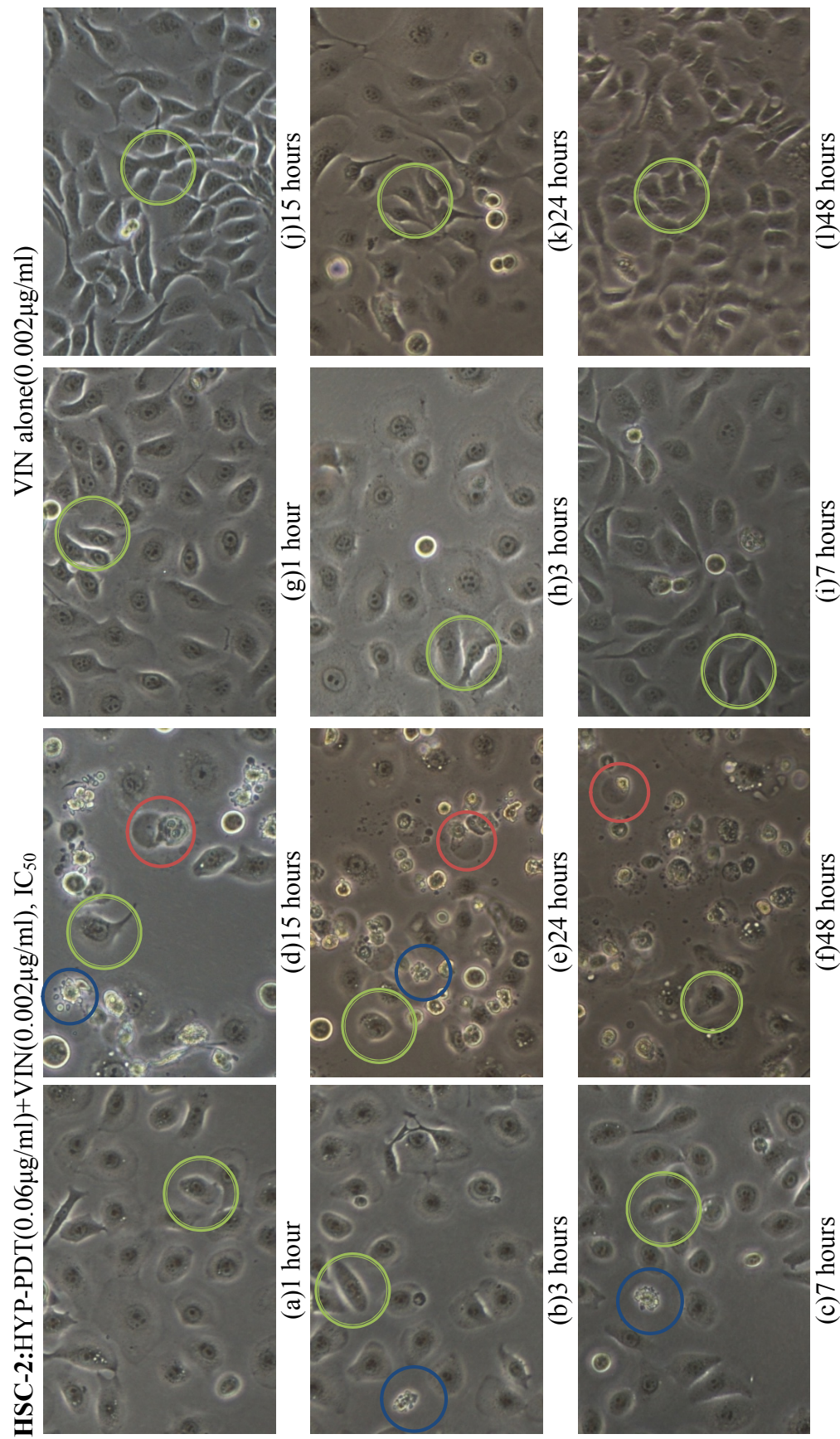
Figure 4.22   Morphological changes of HSC-2 treated with HYP-PDT+VIN and VIN alone at 1st, 3rd, 7th, 15th, 24th and 48th hour post-irradiation were shown above. ○ refers to viable cell; ○ refers to apoptotic cell; ○ refers to necrotic cells. Pictures magnification is 80X.

4.3.1.4 HYP-PDT treatment alone and negative control in HSC-2

When HSC-2 cells were treated with HYP-PDT alone (0.06μg/ml), cells remained viable and no obvious morphological changes were observed from 1 hour (Figure 4.23a) to 48 hours (Figure 4.23f).

In untreated HSC-2 cells, viable cells were observed from 1 hour (Figure 4.23g) to 48 hours (Figure 4.23l).

HSC-2: HYP-PDT alone (0.06μg/ml) Untreated control

(a)1 hour (d)15 hours (g)1 hour (j)15 hours

(b)3 hours (e)24 hours (h)3 hours (k)24 hours

(c)7 hours (f)48 hours (i)7 hours (l)48 hours
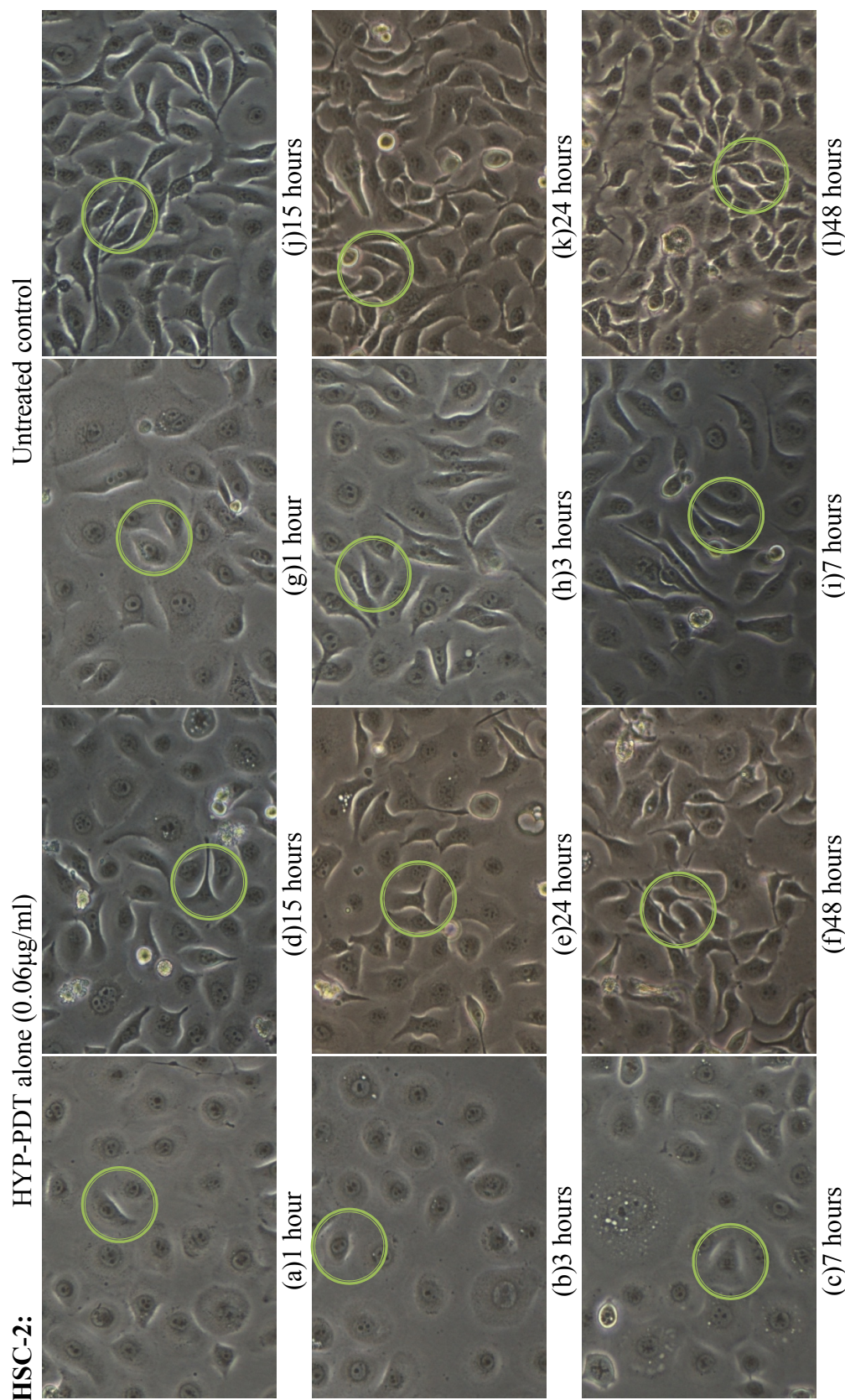
Figure 4.23   Morphological changes of HSC-2 treated with HYP-PDT alone and untreated control at 1st, 3rd, 7th, 15th, 24th and 48th hour post-irradiation were shown above.◯ refers to viable cell. Pictures magnification is 80X.

4.3.2   Morphology changes after different combination treatments in HSC-3

4.3.2.1 HYP-PDT+CIS treatment in HSC-3

When exposed to HYP-PDT+CIS treatment (additive combination; IC_{50} isoeffect level; 0.06µg/ml HYP-PDT and 0.39µg/ml CIS), HSC-3 cells (Figure 4.24) remained viable until 48 hours. No shrunken cells or apoptotic bodies were observed. When HSC-3 cells were treated with CIS alone (0.39µg/ml), cells remained viable and no obvious morphological changes were observed from 1 hour (Figure 4.24g) to 48 hours (Figure 4.24l). This is consistent with the result in section 4.2.2 where HYP-PDT+CIS additive combination did not create significant apoptosis or necrosis after the experiment being scaled up from 96-well plates to 60mm culture disc.

HSC-3:HYP-PDT(0.06μg/ml)+CIS(0.39μg/ml), IC_{50}
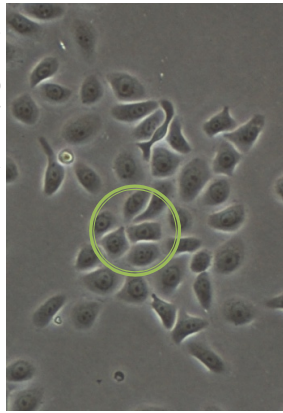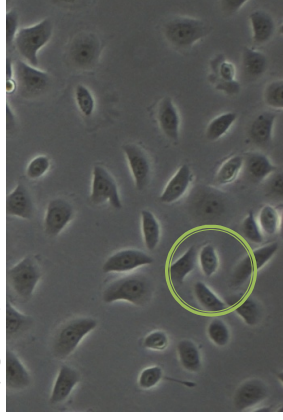
CIS alone(0.39μg/ml)

(a)1 hour

(b)3 hours

(c)7 hours

(d)15 hours

(e)24 hours

(f)48 hours

(g) 1 hour

(h)3 hours

(i)7 hours

(j)15 hours
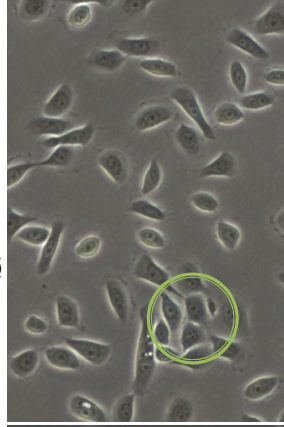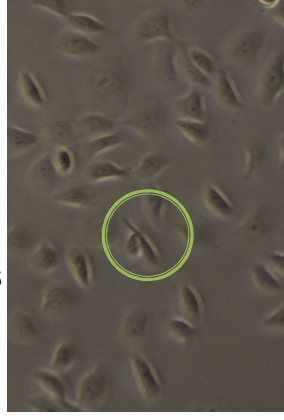
(k)24 hours
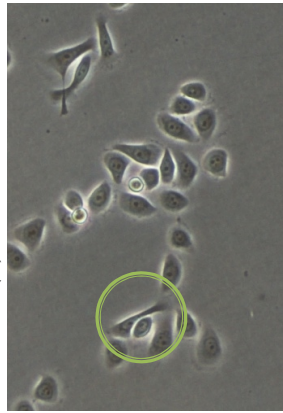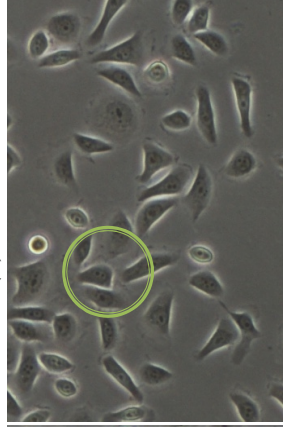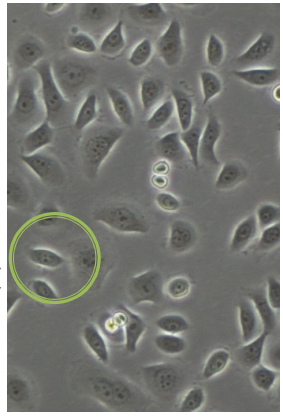
(l)48 hours

Figure 4.24   Morphological changes of HSC-3 treated with HYP-PDT+CIS and CIS alone at 1st , 3rd , 7th , 15th , 24th and 48th hour post-irradiation were shown above.◯ refers to viable cell. Pictures magnification is 80X.

4.3.2.2 HYP-PDT+DOX treatment in HSC-3

When HSC-3 cells (Figure 4.25) were treated with HYP-PDT+DOX (synergistic combination; IC_{90}; 0.10µg/ml HYP-PDT and 0.22µg/ml DOX), apoptotic bodies could be seen (Figure 4.25b) as early as in 3rd hour. At 7 hours, some viable cells could still be seen but the culture was littered with cell debris. Swollen necrotic cells with cytoplasmic contents leakage were present (Figure 4.25c). Although small amount of apoptotic cells could still be observed, necrotic cells were predominant thereafter until 48 hours (Figure 4.25e). In comparison, in HSC-3 treated with DOX alone, no necrotic cells or apoptotic bodies were seen throughout 48 hours. Viable cells could still be seen at 48 hours (Figure 4.25l).

HSC-3:HYP-PDT(0.10μg/ml)+DOX(0.22μg/ml), IC$_{90}$

(a)1 hour

(b)3 hours

(c)7 hours

(d)15 hours

(e)24 hours

(f)48 hours

DOX alone(0.22μg/ml)

(g)1 hour

(h)3 hours

(i)7 hours

(j)15 hours

(k)24 hours

(l)48 hours
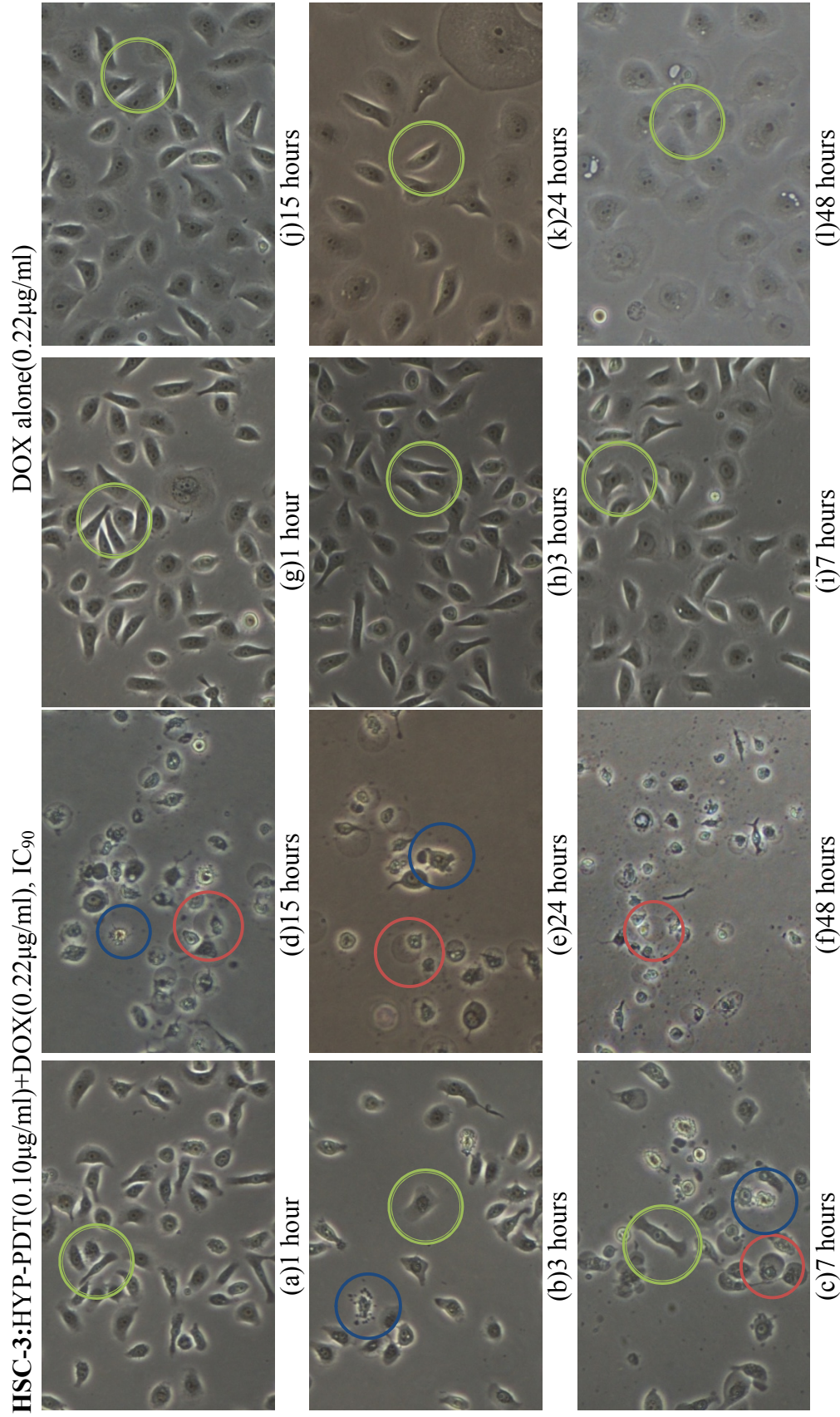
Figure 4.25   Morphological changes of HSC-3 treated with HYP-PDT+DOX and DOX alone at 1st, 3rd, 7th, 15th, 24th and 48th hour post-irradiation were shown above. ○ refers to viable cell; ○ refers to apoptotic cell; ○ refers to necrotic cells. Pictures magnification is 80X.

4.3.2.3 HYP-PDT+VIN treatment in HSC-3

For HSC-3 cells (Figure 4.26) exposed to HYP-PDT+VIN treatment (additive combination; IC_{50} isoeffect level; 0.06μg/ml HYP-PDT and 0.0004μg/ml VIN), small amount of apoptotic cells could be found at 7 hours (Figure 4.26c). The amount of cells with apoptosis morphology increased until 48 hours. Though, starting from 24 hours (Figure 4.26f), necrotic cells could be found in the culture.

When HSC-3 cells were treated with VIN alone (0.0004μg/ml), other than increment in confluency, cells remained viable and no obvious morphological changes were observed from 1 hour (Figure 4.26g) to 48 hours (circled in Figure 4.26l).

HSC-3:HYP-PDT (0.06μg/ml)+VIN(0.0004μg/ml), IC$_{50}$

VIN alone(0.0004μg/ml)

(a)1 hour

(b)3 hours

(c)7 hours

(d)15 hours

(e)24 hours

(f)48 hours

(g)1 hour

(h)3 hours

(i)7 hours

(j)15 hours

(k)24 hours

(l)48 hours
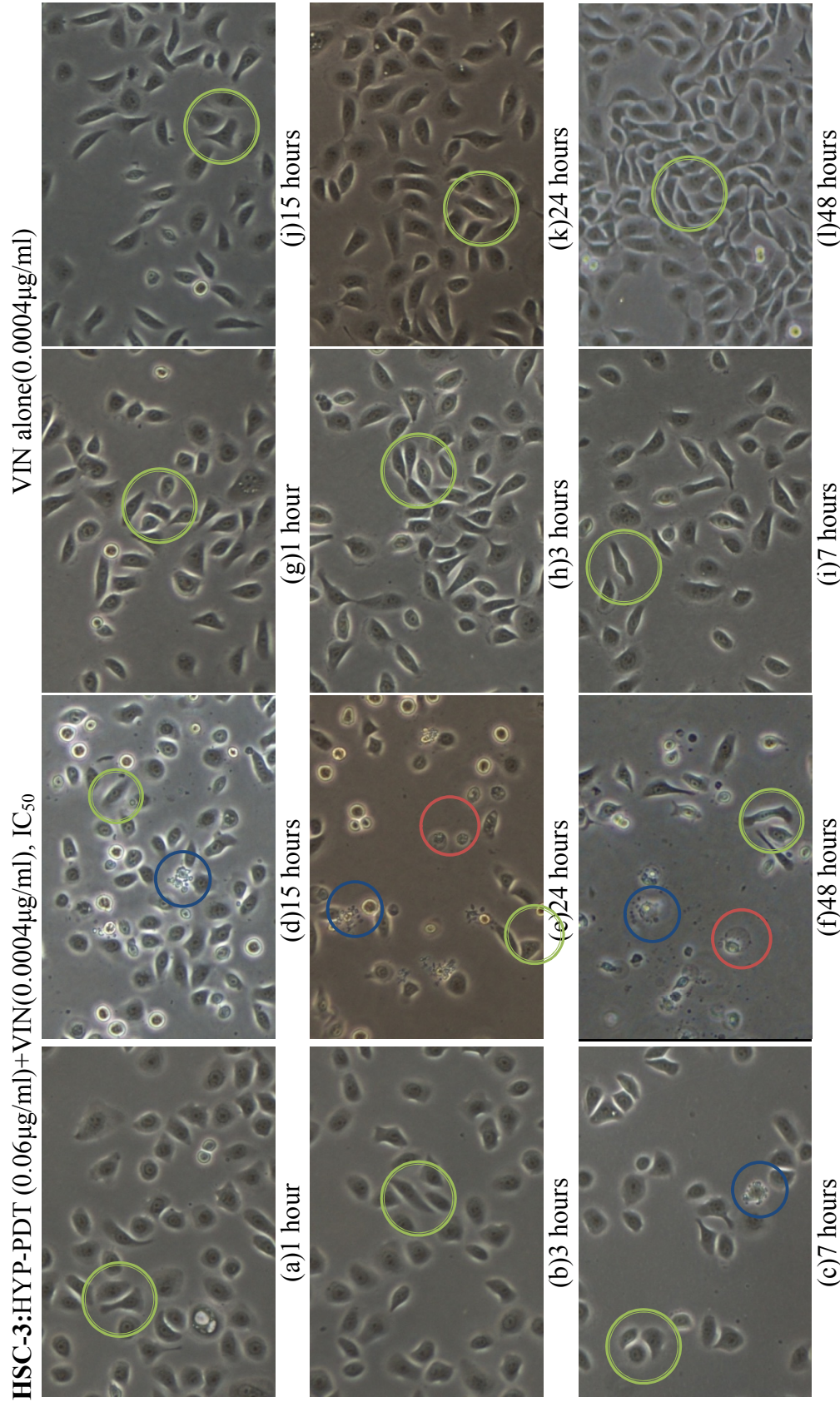
Figure 4.26   Morphological changes of HSC-3 treated with HYP-PDT+VIN and VIN alone at 1st, 3rd, 7th, 15th, 24th and 48th hour post-irradiation were shown above. ○ refers to viable cell; ○ refers to apoptotic cell; ○ refers to necrotic cells. Pictures magnification is 80X.

4.3.2.4 HYP-PDT treatment alone and negative control in HSC-3

When HSC-3 cells were treated with HYP-PDT alone (0.06μg/ml), cells remained viable and no obvious morphological changes were observed from 1 hour (Figure 4.27a) to 48 hours (Figure 4.27f).

Figure 4.27g to Figure 4.27l showed the negative control of untreated viable HSC-3 cells from 1 hour to 48 hours for comparison.

HSC-3:

Untreated control

HYP-PDT alone (0.06μg/ml)

(a)1 hour

(b)3 hours

(c)7 hours

(d)15 hours

(e)24 hours

(f)48 hours

(g)1 hour

(h)3 hours

(i)7 hours

(j)15 hours

(k)24 hours

(l)48 hours
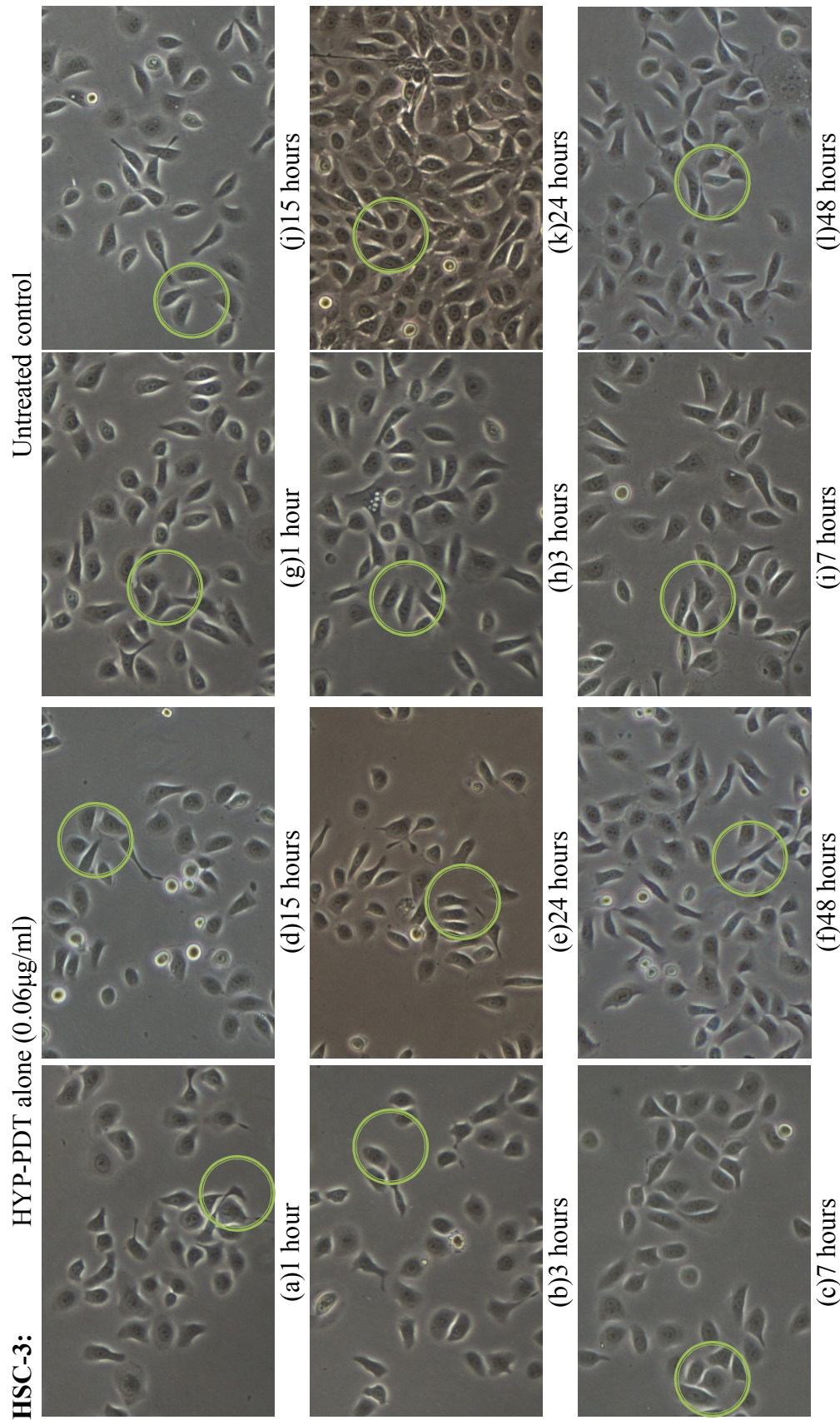
Figure 4.27   Morphological changes of HSC-3 treated with HYP-PDT alone treatments and untreated control at 1st, 3rd, 7th, 15th, 24th and 48th hour post-irradiation were shown above. ◯ refers to viable cell. Pictures magnification is 80X.

4.3.3 Morphology changes after different combination treatments in HSC-4

4.3.3.1 HYP-PDT+CIS treatment in HSC-4

For HSC-4 cells (Figure 4.28) treated with HYP-PDT+CIS (additive combination; IC_{50} isoeffect level; 0.06μg/ml HYP-PDT and 0.35μg/ml CIS), although majority of cells were still viable, shrunken cells with apoptotic bodies could be observed at the first hour (Figure 4.28a). The amount of shrunken cells with apoptotic bodies continued to increase until 7 hours (Figure 4.28c). At 15 hours, plenty of necrotic swollen necrotic cells with ruptured membrane appeared in view (Figure 4.28d). Necrotic cells continued to breakdown until 48 hours (Figure 4.28l).

When HSC-4 cells were treated with CIS alone (0.35μg/ml), cells remained viable and no obvious morphological changes were observed from 1 hour (Figure 4.28g) to 48 hours (Figure 4.28l).

HSC-4:HYP-PDT(0.06μg/ml)+CIS(0.35μg/ml), IC$_{50}$

CIS alone(0.35μg/ml)

(a)1 hour

(b)3 hours

(c)7 hours

(d)15 hours

(e)24 hours

(f)48 hours

(g)1 hour

(h)3 hours

(i)7 hours

(j)15 hours

(k)24 hours

(l)48 hours
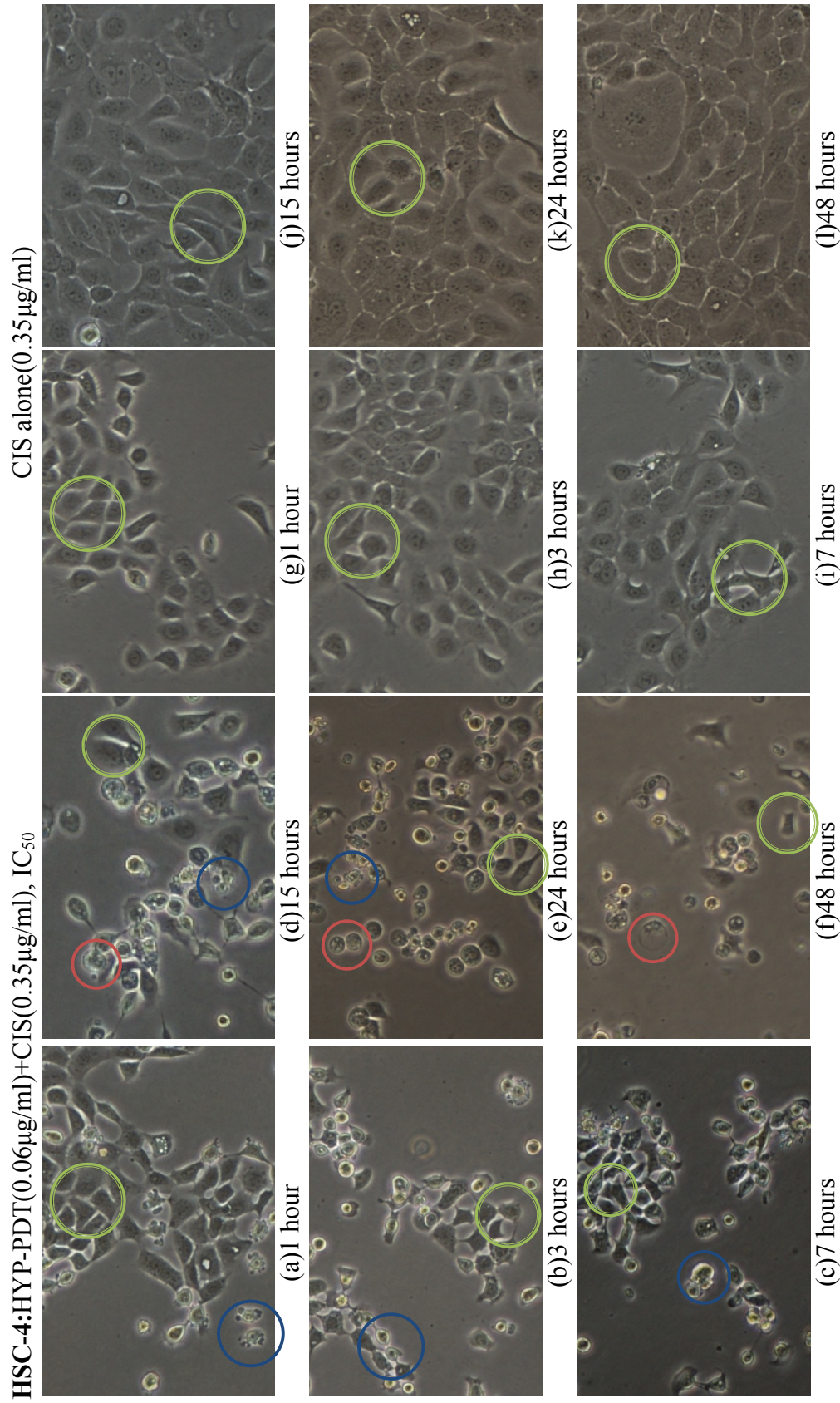
Figure 4.28   Morphological changes of HSC-4 treated with HYP-PDT+CIS and CIS alone at 1st, 3rd, 7th, 15th, 24th and 48th hour post-irradiation were shown above. ◯ refers to viable cell; ◯ refers to apoptotic cell; ◯ refers to necrotic cells. Pictures magnification is 80X.

144

4.3.3.2 HYP-PDT+DOX treatment in HSC-4

When HSC-4 cells (Figure 4.29) were treated with HYP-PDT+DOX (synergistic combination; $IC_{90;}$ 0.10μg/ml HYP-PDT and 0.26μg/ml DOX), cells started to shrink from each other forming isolated growing colonies at 1 hour (Figure 4.29a). At this time point, Some shrunken cells with apoptotic bodies could be observed but majority of cells were still viable. Amount of shrunken cells increased through 3 hours (Figure 4.29b) and 7 hours (Figure 4.29c). At 15 hours, other than shrunken cells, plenty of swollen cells were found floating in the culture. Membrane disruption and cell cytoplasmic contents leakage indicated the onset of necrosis (Figure 4.29d). From 24 hours onwards (Figure 4.29e and Figure 4.29f), only necrotic cells and debris could be observed.

When treated with DOX alone (0.26μg/ml), morphology of HSC-4 cells remained constantly and the cells were viable until 48 hours (Figure 4.29l).

HSC-4: HYP-PDT(0.10μg/ml)+DOX(0.26μg/ml), IC$_{90}$ DOX(0.26μg/ml)

(a)1 hour

(b)3 hours

(c)7 hours

(d)15 hours

(e)24 hours

(f)48 hours

(g)1 hour

(h)3 hours

(i)7 hours

(j)15 hours

(k)24 hours

(l)48 hours
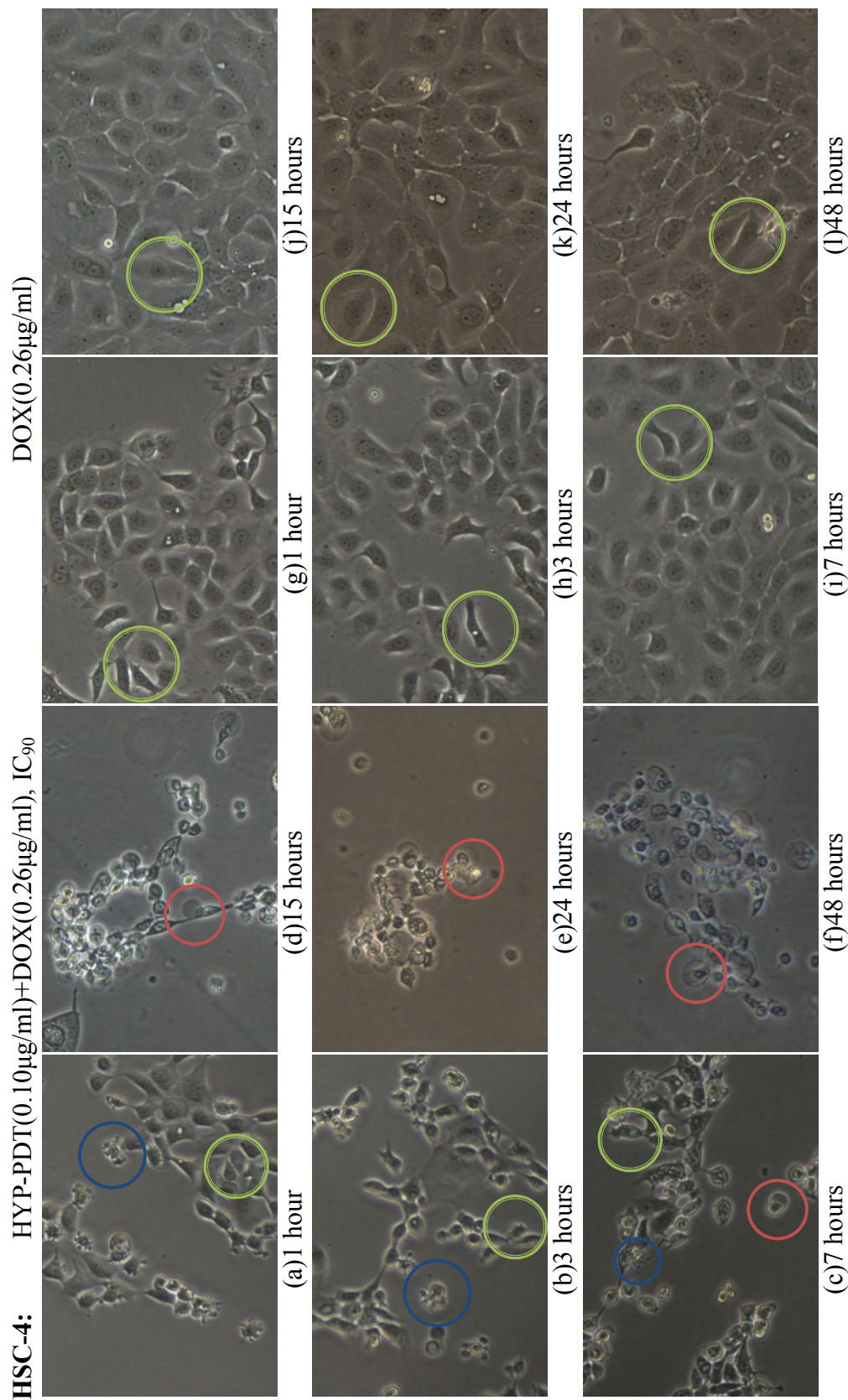
Figure 4.29   Morphological changes of HSC-4 treated with HYP-PDT+DOX and DOX alone at 1st, 3rd, 7th, 15th, 24th and 48th hour post-irradiation were shown above. ◯ refers to viable cell; ◯ refers to apoptotic cell; ◯ refers to necrotic cells. Pictures magnification is 80X.

4.3.3.3 HYP-PDT+VIN treatment in HSC-4

When HSC-4 cells were treated with HYP-PDT+VIN (synergistic combination; IC_{40} isoeffect level; 0.06μg/ml HYP-PDT and 0.00125μg/ml VIN), apoptotic cells started to appear at 3rd hour (Figure 4.30b). There was no necrotic population observed until 48 hours.

For comparison, HSC-4 cells were exposed to VIN alone (0.00125μg/ml). Other than increment in confluency, cells remained viable and no obvious morphological changes were observed from 1 hour (Figure 4.30g) to 48 hours (Figure 4.30l).

HSC-4:HYP-PDT (0.06μg/ml)+VIN(0.00125μg/ml), IC_{40}

VIN(0.00125μg/ml)

(a)1 hour (d)15 hours (g)1 hour (j)15 hours

(b)3 hours (e)24 hours (h)3 hours (k)24 hours

(c)7 hours (f)48 hours (i)7 hours (l)48 hours
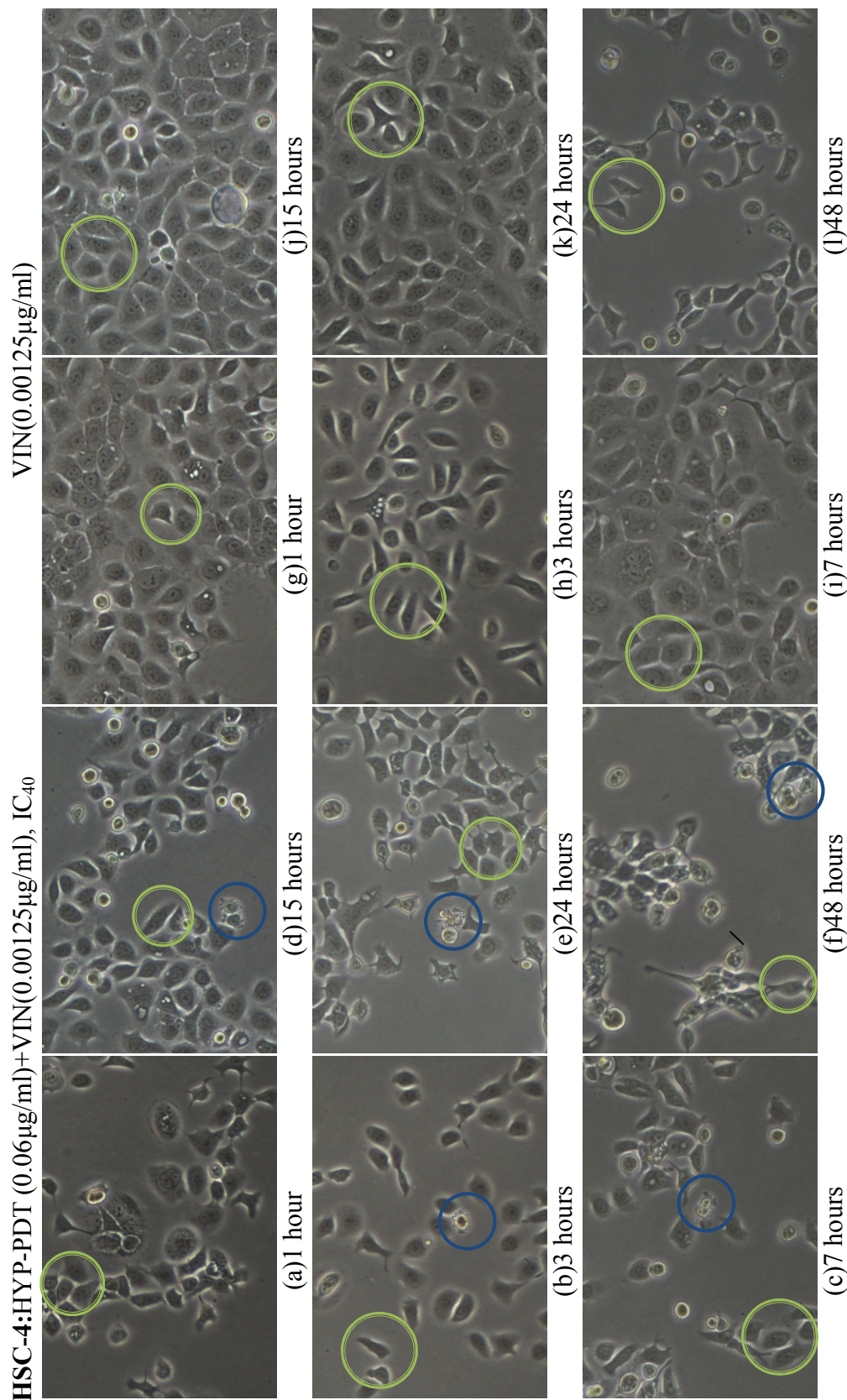
Figure 4.30 Morphological changes of HSC-4 treated with HYP-PDT+VIN and VIN alone at 1st, 3rd, 7th, 15th, 24th and 48th hour post-irradiation were shown above. ⭕ refers to viable cell; ⭕ refers to apoptotic cell. Pictures magnification is 80X.

4.3.3.4 HYP-PDT treatment alone and negative control in HSC-4

When HSC-4 cells were treated with HYP-PDT alone (0.06µg/ml), there was small amount of apoptotic cells discovered at 15 hours. However, most cells remained viable from 1 hour (Figure 4.31a) to 48 hours (Figure 4.31f).

In untreated HSC-4 cells, viable cells were observed from 1 hour (Figure 4.31g) to 48 hours (circled in Figure 4.31l).

HSC-4:

HYP-PDT alone (0.06μg/ml)   Untreated control

(a)1 hour   (d)15 hours   (g)1 hour   (j)15 hours

(b)3 hours   (e)24 hours   (h)3 hours   (k)24 hours

(c)7 hours   (f)48 hours   (i)7 hours   (l)48 hours
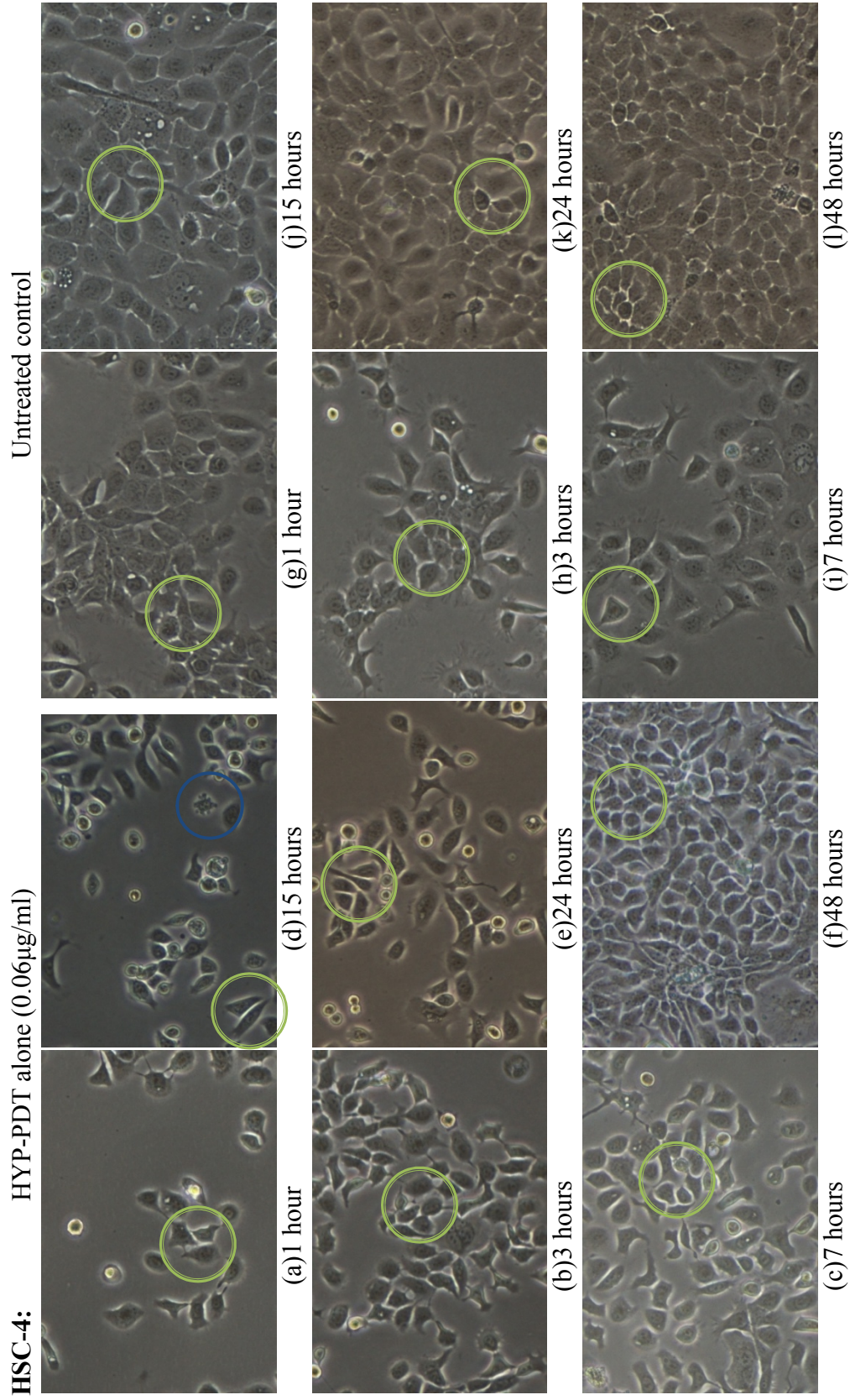
Figure 4.31   Morphological changes of HSC-4 treated with HYP-PDT alone and untreated control at 1st, 3rd, 7th, 15th, 24th and 48th hour post-irradiation were shown above. ⭘ refers to viable cell; ⭘ refers to apoptotic cell. Pictures magnification is 80X.

150

4.4   Investigation of Apoptotic Mediators

After quantification of apoptosis and necrosis and examination of morphological features, combination treatments were found able to induce earlier onset of apoptosis as well as more apoptosis death compared drugs or HYP-PDT used alone. The activities of several upstream and downstream caspases and apoptosis regulator Bcl-2 protein family members, Bax and Bcl-2 were analysed using Western blot method to characterize their involment.

Time-course expression of the selected proteins (including pro- & cleaved fragments) in was recorded using Western blot detection method after every treatment subjected to treatments in all cell lines reported in the section below. These proteins are listed in table 4.8.

Table 4.8   Summary of proteins (including fragments) being expressed and recorded using Western blot detection method after treatments in three different cell lines.

Protein Name	Size of Protein or Fragment(s), kDa
Bax	21kDa
Bcl-2	26kDa
Caspase-8, consists of,	
Procaspase-8	55kDa
Cleaved caspase-8	36kDA and 23kDa
Caspase-9, consists of,	
Procaspase-9	46kDa
Cleaved caspase-9	37kDA and 25kDa
Caspase-7, consists of,	
Procaspase-7	37kDa
Cleaved caspase-7	19kDA
Actin (control)	42kDa

4.4.1 Expression after combination treatments in HSC-2

The time-point expression profile of tested proteins after HSC-2 was treated with HYP-PDT+DOX and HYP-PDT+VIN was shown in Figure 4.32.

Cell line : HSC-2

	HYP-PDT+DOX	HYP-PDT+VIN	Untreated	Molecular weight
	Hour	Hour	Hour	(kDa)
	3 7 15 24	3 7 15 24	3 7 15 24	
Bax			N/A	21kD
Bcl-2				26kD
Casp-8				55kDa 36kDa 23kDa
Casp-9				46kDa 37kDa 25kDa
Casp-7				37kDa 19kDa
Actin				42kD
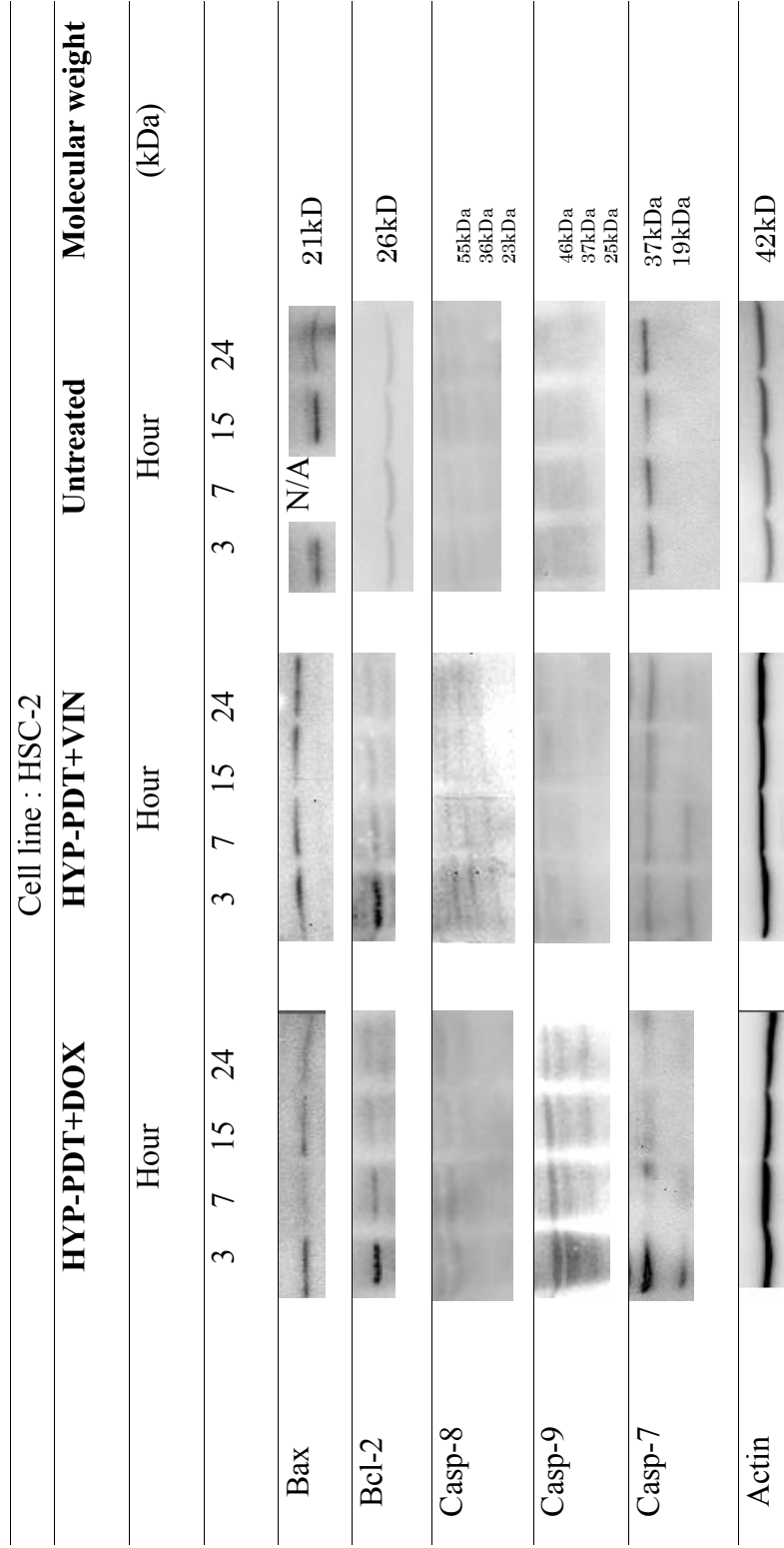
Figure 4.32   The level of Bax (21kDa), Bcl-2 (26kDa), caspase-9 (3 bands; procaspase-8 = 55kDa; cleaved caspase-8 = 36kDA and 23kDa),caspase-9 (3 bands; procaspase-9 = 46kDa; cleaved caspase-9 = 37kDA and 25kDa), caspase-7 (2 bands; procaspase-7 = 37kDa; cleaved caspase-7 = 19kDA) and actin(control, 42kDa)   in HSC-2 after various combination treatments recorded at 3rd, 7th, 15th and 24th hour. Untreated control is provided for comparison. The control band at 7 hour for Bax was unavailable.

154

4.4.1.1 HYP-PDT+CIS in HSC-2

The expression of cell death protein for HYP-PDT+CIS combination treatment was not further tested because isobologram analysis of both IC_{50} and IC_{90} data observed after combination treatments gave less than additive (antagonistic) effect as shown in section 4.1.5.

4.4.1.2 HYP-PDT+DOX in HSC-2

After HSC-2 was treated with HYP-PDT+DOX (additive combination; $IC_{90;}$ 0.10μg/ml HYP-PDT and 0.45μg/ml DOX), both Bax and Bcl-2 proteins decreased in HSC-2 cells from 3 hours to 24 hours. Cleaved caspase-8 could not be detected in HSC-2 throughout 24 hours. However, caspase-9 and cleaved caspase-7 could be detected at 3 hours.

4.4.1.3 HYP-PDT+VIN in HSC-2

After HSC-2 was treated with HYP-PDT+VIN (synergistic combination; IC_{50} isoeffect level; 0.06μg/ml HYP-PDT and 0.002μg/ml VIN), Bcl-2 was decreasing starting at 3 hour. The level of Bax remained unchanged at a relatively higher level compared to Bcl-2 from 3 hours to

24 hours. Cleaved caspase-9 could not be detected in HSC-2 throughout 24 hours. However, cleaved caspase-8 and cleaved caspase-7 could be detected at 3 hours.

4.4.1.4 Controls in HSC-2

Level of actin (protein quantity control) remains constant (Figure 4.32) after all treatments. This verified the up-regulation or down-regulation of tested proteins due to drugs effect but not due to different amount of protein loaded in Western blotting assay.

In untreated HSC-2 cells (Figure 4.32), Bax was constantly expressed but Bcl-2 expression is minimal and constant. Procaspase-8 and procaspase-9 or its cleaved counterparts were not detected. Procaspase-7 can be seen constant throughout 24 hours.

4.4.2 Expression after combination treatments in HSC-3

The time-point expression profile of tested proteins after HSC-3 was treated with HYP-PDT+CIS, HYP-PDT+DOX and HYP-PDT+VIN was shown in Figure 4.33.

156
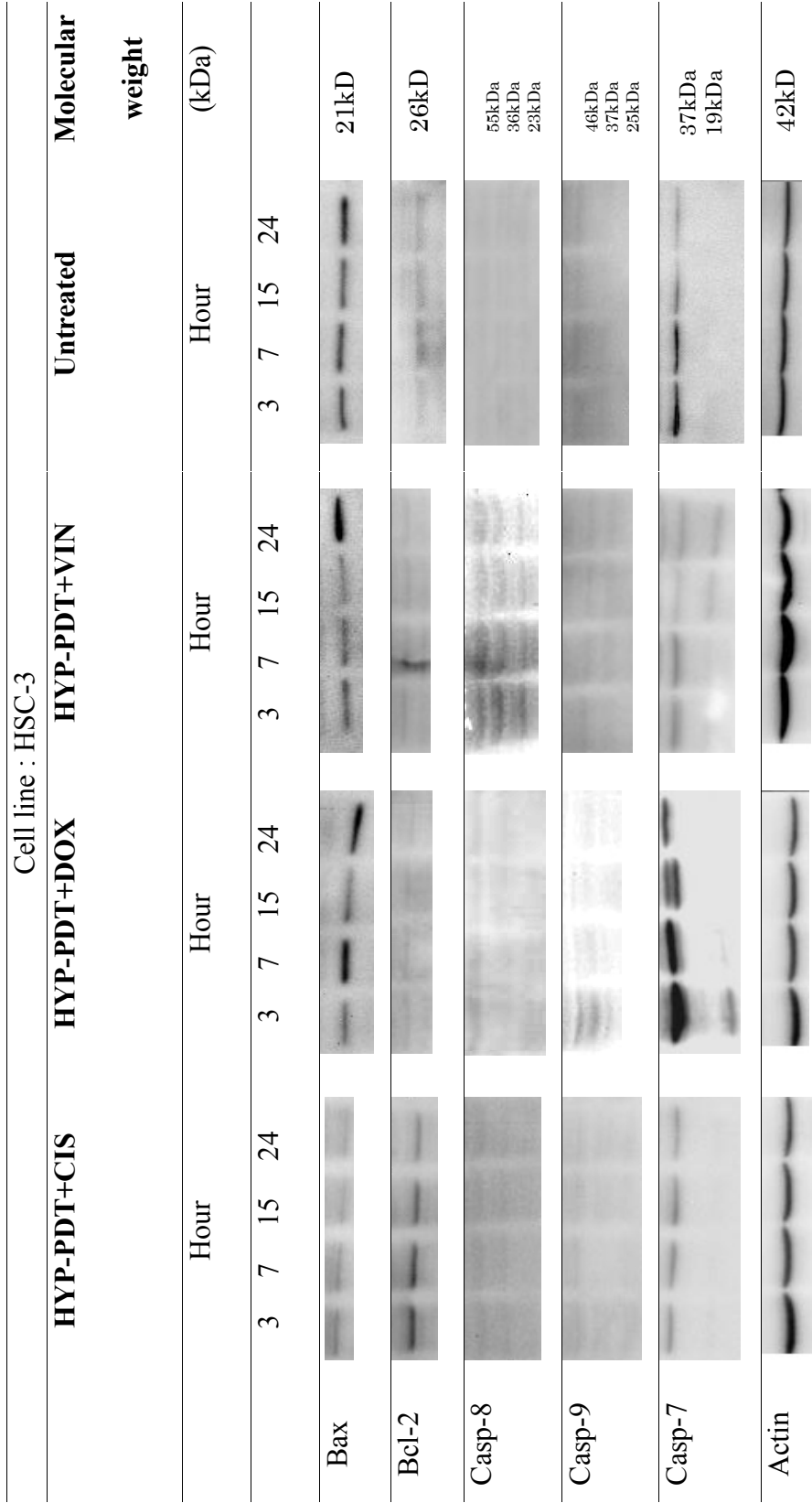
Figure 4.33   The level of Bax (21kDa), Bcl-2 (26kDa), caspase-8(3 bands; procaspase-8 = 55kDa; cleaved caspase-8 = 36kDA and 23kDa),caspase-9 (3 bands; procaspase-9 = 46kDa; cleaved caspase-9 = 37kDA and 25kDa), caspase-7 (2 bands; procaspase-7 = 37kDa; cleaved caspase-7 = 19kDA) and actin(control, 42kDa) in HSC-3 after various combination treatments recorded at 3rd, 7th, 15th and 24th hour. Untreated control is provided for comparison.

4.4.2.1 HYP-PDT+CIS in HSC-3

After HSC-3 was treated with HYP-PDT+CIS (additive combination; IC_{50} isoeffect level; 0.06μg/ml HYP-PDT and 0.39μg/ml CIS), Bax was observed to decrease from 1 hour to 24 hours. Bcl-2 level was relatively higher than Bax and also decreased from 3 to 24 hours. Cleaved caspase-8 and cleaved caspase-9 could not be detected in HSC-3 throughout 24 hours. There was no cleaved caspase-7 detected in all time-points as well.

4.4.2.2 HYP-PDT+DOX in HSC-3

After HSC-3 was treated with HYP-PDT+DOX (synergistic combination; IC_{90}; 0.10μg/ml HYP-PDT and 0.22μg/ml DOX), Bcl-2 level remained unchanged from 3 to 24 hours. Bax level increased from 3 to 24 hours. Cleaved caspase-8 could not be seen in all time-points. Cleaved caspase-9 and cleaved caspase-7 could be detected at 3 hours.

4.4.2.3 HYP-PDT+VIN in HSC-3

After HSC-3 was treated with HYP-PDT+VIN (additive combination; IC_{50} isoeffect level, 0.06µg/ml HYP-PDT and 0.0004µg/ml VIN), Bcl-2 level remained unchanged at a relatively lower level compared to Bax from 3 to 24 hours. Bax level remained unchanged at a relatively higher level compared to Bcl-2 from 3 to 15 hours and then increased at 24 hours. Cleaved caspase-8 could be detected starting from 3. Cleaved caspase-9 could not be detected throughout 24 hours. Cleaved caspase-7 could be detected at 15 and 24 hours.

4.4.2.4 Controls in HSC-3

Level of actin (protein quantity control) remains constant (Figure 4.33) after all treatment, this validified the upregulation or downregulation of tested proteins due to drugs effect but not due to different amount of protein loaded in Western blotting assay.

In untreated HSC-3 cells (Figure 4.33), Bax was constantly expressed but Bcl-2 expression is minimal and constant. Procaspase-8 and procaspase-9 or its cleaved counterparts were not detected. Procaspase-7 can be seen decreasing throughout 24 hours.

159

4.4.3 Expression after combination treatments in HSC-4

The time-point expression profile of tested proteins after HSC-4 was treated with HYP-PDT+CIS, HYP-PDT+DOX and HYP-PDT+VIN was shown in Figure 4.34.

Cell line : HSC-4

	HYP-PDT+CIS	HYP-PDT+DOX	HYP-PDT+VIN	Untreated	Molecular Weight (kDa)
	Hour	Hour	Hour	Hour	
	3 7 15 24	3 7 15 24	3 7 15 24	3 7 15 24	
Bax					21kD
Bcl-2					26kD
Casp-8					55kDa 36kDa 23kDa
Casp-9					46kDa 37kDa 25kDa
Casp-7					37kDa 19kDa
Actin					42kD
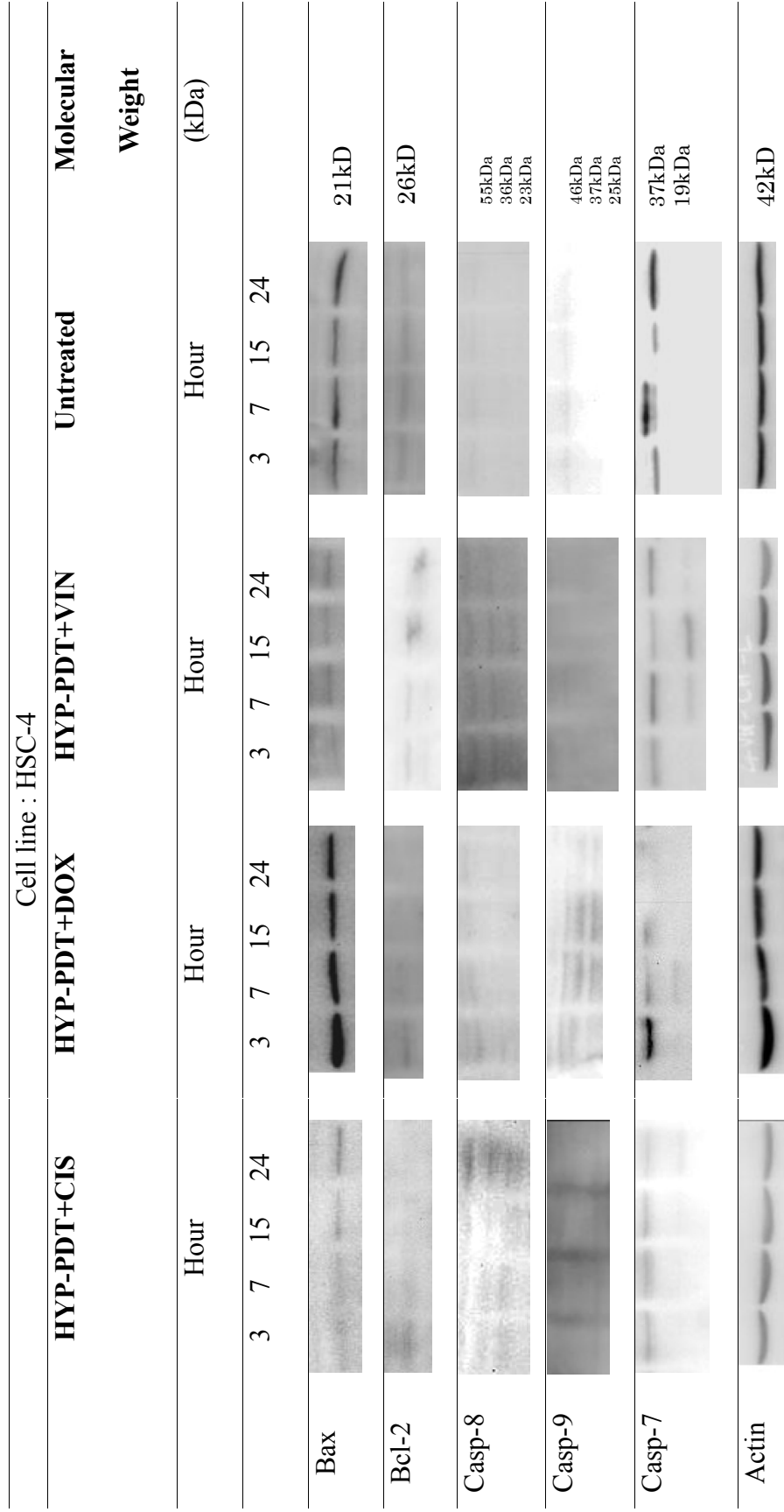
Figure 4.34   The level of Bax (21kDa), Bcl-2 (26kDa), caspase-8(3 bands; procaspase-8 = 55kDa; cleaved caspase-8 = 36kDA and 23kDa),caspase-9 (3 bands; procaspase-9 = 46kDa; cleaved caspase-9 = 37kDA and 25kDa), caspase-7 (2 bands; procaspase-7 = 37kDa; cleaved caspase-7 = 19kDA) and actin(control, 42kDa) in HSC-4 after various combination treatments recorded at 3rd , 7th , 15th and 24th hour. Untreated control is provided for comparison.

4.4.3.1 HYP-PDT+CIS in HSC-4

After HSC-4 was treated with HYP-PDT+CIS (additive combination; IC_{50} isoeffect level; 0.06μg/ml HYP-PDT and 0.35μg/ml CIS), Bax levels increased over 24 hours while Bcl-2 levels decreased from 3 to 24 hours. Cleaved caspase-8 and cleaved caspase-7 could be seen at 24 hours. There was no cleaved caspase-9 detected throughout 24 hours.

4.4.3.2 HYP-PDT+DOX in HSC-4

In HSC-4 treated with HYP-PDT+ DOX (synergistic combination; IC_{90}; 0.10μg/ml HYP-PDT and 0.26μg/ml DOX), Bcl-2 level decreased from 3 to 24 hours. Bax level decreased from 3 to 7 hours and then remained at a relatively high level compared to Bcl-2 until 24 hours. Cleaved caspase-8 could not be seen in all time-points. Cleaved caspase-9 and cleaved caspase-7 could be detected at 7 hours.

4.4.3.2 HYP-PDT+VIN in HSC-4

After HSC-4 was treated with HYP-PDT+VIN (synergistic combination; IC_{40} isoeffect level; 0.06μg/ml HYP-PDT and 0.00125μg/ml VIN), Bcl-2 level decreased from 15 hours to 24 hours. Bax level increased from 3 to 24 hours. Cleaved caspase-8 and cleaved caspase-7 could be

detected at 15 hours. Cleaved caspase-9 could not be detected in all time-points.

4.4.3.4 Controls in HSC-4

Level of actin (protein quantity control) remains constant (Figure 4.34) after all treatment, this validified the upregulation or downregulation of tested proteins due to drugs effect but not due to different amount of protein loaded in Western blotting assay.

In untreated HSC-4 cells (Figure 4.34), Bax was constantly expressed but Bcl-2 expression is minimal and constant. Procaspase-8 and procaspase-9 or its cleaved counterparts were not detected. Procaspase-7 can be seen throughout 24 hours.

CHAPTER 5

DISCUSSION

5.1   Combination of PDT and Chemotherapy

Several studies had shown that doxorubicin, cisplatin, vinblastine and HYP-PDT induced apoptosis in various cell line models (Ali, Chee, Yuen & Olivo, 2001; Mizutani, Tada-Oikawa, Hikaru, Kojima & Kawanishi, 2005; Duan, Sterba, Kolomeichuk, Kim, Brown & Chambers, 2007; Xu, Huang, Pan, Zhang, Liu & Zhang,2007). Early studies have already shown that drug regimens consisting of doxorubicin, cisplatin and vinblastine induced apoptosis in mouse cancer models (Zhang, Jin & Takenaka, 1998). In view of HYP-PDT photodynamic properties that allow selective activation at tumor sites, the combination of these clinically approved apoptosis-inducing drugs with HYP-PDT may lead to treatment synergism or reduced concentration-related side effects of those cytotoxic drugs.

5.2   Drugs Interaction of HYP-PDT+CIS

Isobolographic analysis (Figure 4.10) revealed that HYP-PDT+CIS combination exhibited less than additive interaction in HSC-2 (Figure 4.10d), additive interaction in HSC-3 (Figure 4.10e) and synergistic interaction in HSC-4 (Figure 4.10f). Especially in HSC-4 (Figure 4.10f), synergistic effect

could be seen when high concentration HYP-PDT was combined with low concentration CIS or high concentration CIS was combined with low concentration HYP-PDT. This result suggested that HYP-PDT+CIS combination is superior in killing HSC-4 cells compared to single drugs alone. This may involve two signal pathways or two different drug targets, in which one of the signal pathways or targets has to be disturbed in greater degree (one of the components in combination has to be in high concentration) in order for the synergism to occur. In similar studies using L5178Y lymphoma cells, the combination of photofrin and cisplatin gave enhanced apoptotic cell death, most probably due to an additive or less than additive interaction but not synergistic interaction. The authors suggested that there might be two signal pathways responsible for apoptotic cell death, one associated with PDT and the other associated with CIS (Nonaka, Ikeda & Inokuchi, 2002).

Another group of researchers suggested that PDT-Cisplatin combination worked in a way that PDT targeted plasma membranes and mitochondria while CIS inhibited DNA repair processes by inactivation of DNA polymerase (Uehara, Inokuchi & Ikeda, 2006). Previous study showed that HYP-PDT localized at the plasma membrane and pernuclear area of cells (Agostinis *et al*., 2002). Thus, HYP-PDT most probably damaged membrane or organelles outside nucleus but not the DNA. In contrast, CIS disturbed DNA replication bounded by nucleus membrane. Since the target of both drugs are mutually exclusive (separated by nucleus membrane), reduction in drugs interaction could be expected. Therefore, this may explain why there was no synergism seen in HSC-2 (Figure 4.10d) and HSC-3 (Figure 4.10e)

with HYP-PDT+CIS treatment. This may also explain why HSC-4 (Figure 4.10f) synergism occurred only when either one of the combination components is higher in concentration (more than IC70). It is probably that when both drugs attack mutually exclusive targets (separated by organnelle membrane), either one of the components must break the separate "defense threshold" of its target to allow the other component with lesser concentration to now exert its effect to increase cell killing. If both of the components used were in moderate concentrations (Figure 4.10f; 0.12μg/ml HYP-PDT and 1.55μg/ml CIS; each component alone is less than IC70), none of the thresholds were broken, obscuring synergism interaction. However, further investigation is needed to confirm this.

In the other way round, the timing of drug application may be related with the outcome. If CIS is applied at the time HYP-PDT is light activated, CIS and HYP-PDT may compromise the effect of each other by increasing the expression of defensive protein but if CIS is allowed to act on cells for certain period before HYP-PDT light activation, induction of defensive protein may be reduced to a lower level. In one study, researchers found that applying CIS three hours prior to PDT light irradiation produced better cell killing effect than CIS applied one hour or immediately after PDT (Uehara, Inokuchi & Ikeda, 2006). In a different study, researchers also found that application of CIS before PDT gave better treatment effect in mice bearing leukemia (Canti, Nicolin, Cubeddu, Taroni, Bandieramonte & Valentini, 1998). These findings are consistent with the current study, especially for combination treatment of HYP-PDT+CIS in HSC-3 and HSC-4, whereby CIS is applied four hours

before light activation of HYP-PDT. Application of CIS 4 hours prior to HYP-PDT light activation might have strengthened or activated certain unknown pro-cell death factors that produced additive or synergistic effect in HSC-3 (Figure 4.10e) and HSC-4 (Figure 4.10f).

However, the timing of CIS application is unable to explain the less than additive phenomena found in HSC-2 cells treated with HYP-PDT+CIS. Thus, it might be due to genetic background of the cell lines itself. In other research using same cell lines, Akita and colleagues found that HSC-2 is a cyclooxygenase (COX)-2 high expresser, whereby HSC-4 is a COX-2 non-expresser (Akita, Kozaki, Nakagawa, Saito, Ito & Tamada, 2004). Consistent with that, Terakado and colleagues demonstrated that approximately 30% higher radiation concentration was required to achieve 90% cell killing in HSC-2 if compared with HSC-3 and HSC-4. They showed that it was due to constitutive COX-2 expression in HSC-2 (Terakado *et al*.,2004). COX-2 is an inducible form of COX protein involved in catalyzing arachidonic acid to produce prostaglandins E2 that can stimulate epithelial cell proliferation and motility, resulting in tumorgenesis in vitro (Park, Han, Kim & Kim, 2006). Other researchers also indicated that COX-2 expressing tumor was shown to be more aggressive than non-expressing tumor (Park,Han,Kim & Kim, 2006). Since HSC-2 is high COX-2 expresser, in HSC-2, there is a possibility when a combination drug pair consist of a high concentration component (more than IC70) and a low concentration component (less than IC70) was used, especially for the lower concentration component, may stimulate the expression of COX-2 (or other unknown defensive proteins) until these

defensive protein gradually masked and overtaken the killing effect. Eventually, this resulted in an increment in the level of "defense threshold", abolishing drugs synergism. This could be a hypothesis to explain less than additive interaction in HSC-2.

5.3   Drugs Interaction of HYP-PDT+DOX

PDT-DOX combination was shown in several studies to be superior in cell killing than its components alone, in various cell types. In a study using δ-aminolevulinic acid (ALA)-based PDT and DOX, researchers showed that inhibition of tumour growth was significantly enhanced by combined treatment when low concentrations of DOX was used (Casas, Fukuda, Riley & Batlle, 1997). In H-MESO-1 human malignant mesothelioma cell line, Photofrin II and DOX were found to produce greater tumor killing than PDT alone (Brophy & Keller, 1992). In lung carcinoma in vivo, the authors found that Photohem and DOX combination could produce synergistic cell killing (Streckyte *et al*., 1999).

In the present study, isobolographic analysis revealed that HYP-PDT+DOX combination at IC90 isoeffect level exhibited synergistic interaction in HSC-2 (Figure 4.11d), HSC-3 (Figure 4.11e) and HSC-4 (Figure 4.11f). These isobograms suggested a threshold of synergism. The cell killing strength of HYP-PDT component in combination might have to overcome a certain threshold in order to yield a synergistic effect. For example, in Figure

4.11d, e, f, only when high HYP-PDT concentration (>IC50 isoeffect level) was combined with low concentration of DOX (<IC50 isoeffect level), synergistic outcomes were observed. In contrast, when low HYP-PDT concentration (<IC50 isoeffect level) was combined with high concentration of DOX (>IC50 isoeffect level),, the synergistic effect gradually diminished as DOX concentration increased. This is especially obvious when IC_{50} isoeffect level isobolograms (Figure 4.11a,b,c) for HYP-PDT+DOX combination were evaluated. All combinations in all cell lines tested with HYP-PDT+DOX at IC50 isoeffect level gave less than additive effect. Again, this supported the hypothesis that the strength of HYP-PDT has to overcome certain threshold of defense in order to give a synergistic combination outcome. Based on this observation, it is reasonable to suggest that the threshold of synergism for HYP-PDT+DOX may fall in between IC50 isoeffect level and IC90 isoeffect level, at least for HSC-2, HSC-3 and HSC-4 cells. This may also suggest that other anthracycline antibiotic with similar mechanism of action, such as epirubicin and valrubicin, has possibility to work with high concentration HYP-PDT in a combination to yield synergistic treatment outcome.

The action and role of low DOX concentration might be able to explain the occurrence of threshold of synergism. At the IC90 isoeffect level (Figure 4.11d, e, f), synergism only occurred when high HYP-PDT concentrations (more than IC50) were used to combine with low DOX concentrations (less than IC50 in HSC-4 and less than IC30 in HSC-2 and HSC-3). Such low concentration of DOX may induce depletion of intracellular antioxidants prior to HYP-PDT activation while avoiding the increment in production of

defensive proteins. When HYP-PDT was light activated 4 hours later, HYP-PDT generated excessive ROS. With lower level of intracellular antioxidants at the time of HYP-PDT activation, HYP-PDT ROS activity may encounter less quenching effect by cellular antioxidant defense and more cells could be killed. In consistent with this view, Streckyte and colleagues had found that administration of DOX induces decrease in the activity of glutathione peroxidase, superoxide dismutase and catalase (intracellular antioxidants) (Streckyte *et al*., 1999). In an earlier study, researchers also mentioned that DOX toxicity is probably due to the generation of reactive oxygen species such as peroxide and hydroxyl radical. The impairment of the antioxidant levels and antioxidant enzyme activities caused by ROS generated by low concentration DOX may make cells more susceptible to photodynamic damage (Casas, Fukuda, Riley & Batlle, 1997).

In some studies, DOX was also shown to be affected by COX-2 upregulation (Notabartolo, Poma, Perri, Dusonchet, Cervello & D'Allesandro,2005; Wijngaarden *et al*., 2007; Wijngaarden *et al*., 2007). In addition, Akita and colleagues found that HSC-2 is a cyclooxygenase (COX)-2 high expresser, whereby HSC-4 is a COX-2 non-expresser (Akita, Kozaki, Nakagawa, Saito, Ito & Tamada, 2004). In this study, when DOX was used alone, higher concentrations were needed to kill HSC-2 cells (COX-2 expresser) than HSC-4 cells (COX-2 non-expresser). However, when HYP-PDT and DOX were used in combinations, the isobolograms were similar for HSC-2, HSC-3 and HSC-4 (Figure 4.10d, e, f). A hypothesis arose from this observation where it might be related to the use of low concentration DOX

(defined here as less than IC50 in HSC-4 and less than IC30 in HSC-2 and HSC-3) in combination which may not be sufficient to trigger COX-2 up-regulation or in the opposite way, enough to control the effect of COX-2 expression. When HYP-PDT was activated four hours later, excessive ROS production may have overcome COX-2 protection threshold. Thus, synergistic interactions occurred at similar concentration among all three cell lines.

Fluorescence microscopy showed that HYP-PDT localized at the plasma membrane and perinuclear area of cells (Agostinis *et al*., 2002). This may indicate that the ROS produced by HYP-PDT attacks plasma membrane and organelles surrounding nucleus. Since DOX may also localize in cell cytoplasm, the ROS produced by DOX may also attack the same targets. Similar targets (ROS produced by both drugs may attack the same organelle in cytoplasm) of HYP-PDT and DOX may eventually lead to synergism. Furthermore, when both drugs localize and target the same area in cells, enhance drugs interaction may occur. For example, it has been shown that localization of DOX to membrane and mitochondria may increase the uptake of photosensitizer (Casas, Fukuda, Riley & Batlle, 1997).

5.4   Drug Interaction of HYP-PDT+VIN

In HYP-PDT+VIN combination, additive interaction could be seen in HSC-3 (Figure 4.12b) and synergistic interactions were observed in HSC-2 (Figure 4.12a) and HSC-4 (Figure 4.12c).

Synergism occurred when low concentration HYP-PDT (less than IC50) and low concentration VIN (less than IC50) were used. According to Piette *et al*., low concentration PDT can cause damage on unpolymerized form of microtubule constituents (for example, tubulin subunit). Low concentration PDT is defined as treatment when any one of light, oxygen or photosensitizer is limiting. For example, HYP-PDT that is activated with light energy that leads to less than 20% cell killing may be considered as low concentration PDT (Piette, Volantia, Vantieghem, Matroule, Habraken & Agostinis, 2003). In the current study, HYP-PDT concentrations (0.06μg/ml) used in all HYP-PDT+VIN resulted in approximately 75% cell survival when used alone. Therefore, it may be considered as "low concentration PDT" which possibly damaged tubulin.

Furthermore, HYP-PDT was shown to be able to accumulate intracellularly in cytoplasm (Agostinis *et al*., 2002). Since VIN can attack microtubule, it will have to be localized within cytoplasm as well. Therefore, similar targets of both HYP-PDT and VIN may be another reason for enhanced drug interaction. VIN is a mitotic arresting drug that can depolymerize microtubule into tubulin, a monomeric form that is more sensitive to HYP-PDT. Thus, when used in combination it is hypothesized that VIN first depolimerizes microtubules and then HYP-PDT-generated ROS causes secondary photodamage on the tubulin upon light activation. In consistent with this suggestion, an earlier study had shown that combination of a non-toxic concentration of vincristine and TPPS2a-mediated PDT gave

additive effect against mammary tumor in mice only if vincristine was applied six hours prior to PDT. Similar with vinblastine, being a member of vinca alkaloid, vincristine can depolymerize mitotic spindle microtubule and eventually forms tubulin paracrystals which could be attacked by PDT (Ma, Berga, Danielsen, Kaalhus, Iani & Moan, 1996).

5.5   Mode of cell death for HYP-PDT+CIS

By using relatively low cost and rapid MTT assay, combination pairs resulted in additive effect (can reduce dosage) or synergistic effect (kill more with less dosage) were determined. However, due to certain limitations, MTT assay can tell the percentage of dead and viable cells but it is unable to tell whether the cells die through apoptosis or necrosis. Furthermore, once initiated, apoptosis is an irreversible process and it takes time for biochemical and morphological changes until the cells finally die (mitochondria inactive). Within certain time frame after apoptosis is initiated, mitochondria are still functioning. Since MTT assay relies on mitochondria dehydrogenase activity, it may have included some apoptotic population as viable cells. To reveal whether these combination drugs kill cells by apoptosis or necrosis, double staining flow cytometric analysis using FITC-Annexin V and PI was done by using the results from MTT assay to select the concentration of drugs in combination that kill either 50% or 90% of cells.

In HYP-PDT-CIS (additive combination; IC50 isoeffect level;

0.06μg/ml HYP-PDT and 0.39μg/ml CIS) treatment, HSC-3 (Figure 4.13; Row 1) only showed minor necrosis (5-10%) but not apoptosis within 72 hours post irradiation. In contrast, with HYP-PDT+CIS (additive combination; IC50 isoeffect level; 0.06μg/ml HYP-PDT and 0.35μg/ml CIS) treatment, apoptosis (80%) occurred in HSC-4 (Figure 4.14; Row 1) at 15 hours. The lack of apoptosis in HSC-3 can be explained by absence of caspases cleavage and the decrement in Bax:Bcl-2 ratio (Figure 4.35; Column B). In HYP-PDT+CIS combination treatment, although both Bax and Bcl-2 were decreasing from 1st hour to 24th hour in HSC-3, the Bax:Bcl-2 ratio appeared to favor Bcl-2, which is anti-apoptotic. This is consistent with the results seen in phophatidylserine redistribution analysis that showed that HYP-PDT+CIS did not cause apoptosis in HSC-3 cells. On the other hand, cleavage of initiator Caspase-8 and effector Caspase-7 together with high Bax:Bcl-2 ratio (Figure 4.35; Column C) could explain the onset of apoptosis in HSC-4.

Bax/Bcl-2 ratio was proven to be a key mediator of apoptosis in previous study (Schelman, Andres, Sipe, Kang and Weyhenmeyer,2004). Generally, when the ratio favors to Bax (pro-apoptotic protein), apoptosis is promoted and when the ratio favors to Bcl-2, apoptosis is suppressed.

Detection of cleaved caspase-8 in HSC-4 may indicate activation of pro-caspase-8 and can be linked to death-receptor-mediated pathway. Researchers have linked caspase-8-dependant caspases cascade with death-receptor-mediated pathway (Reed, 2003; Kim, 2005). Apart from that, caspase-8 may also be activated by unligated β-1-integrin from cytoplasmic

domain. Unligated β-1-integrin induces recruitment of caspase-8 to cell membrane where it is activated. This process is death receptor independent (Sheng *et al.*, 2008). Yet, these hypothesis remained to be investigated and has to be confirmed by simultaneous increment in level of death receptor pathway-related proteins or intergrin-mediated pathway such as tumour necrosis factor alpha (TNF-α) or unligated β-1-integrin.

Other than that, in contrast, the observation of high Bax:Bcl-2 ratio may indicate relationship with another pathway called mitochondria-mediated pathway. A link may have occurred between these two pathways. One possibility is through the Bcl-2 family protein, Bid. Several groups of scientists have described that activated caspase-8 can cleave Bid into truncated-Bid (tBid), which may later interfere with mitochondria permeability. tBid then interfere mitochondria permeability by facilitating Bax oligomerisation and insertion into mitochondria outer membrane. This will then initiate dimerisation of Bax that form a cytochrome c-permeable channel (Kirkin, Joos & Zőrnig, 2004; Sharpe, Arnoult & Youle, 2004; Skommer, Wlodkowic & Deptala, 2007). However, whether this mechanism is related to what happened in HSC-2 treated with HYP-PDT+CIS remains to be elucidated. Although Bax ratio was found higher than Bcl-2 in this study, the level of tBid has to be further validated.

The intracellular localization of photosensitizer may give clues as to the mechanism employed to cause cell death. Similarly, the mode of cell death may also indirectly indicate intracellular localization of photosensitizer. For

example, localization of HYP-PDT in perinuclear area in HSC-4 cells may suggest apoptosis because photosensitizer localized at mitochondria causes apoptosis, while photosensitizers that target plasma membrane or lysosomes caused mainly necrosis due to direct damage to the phospholipid bilayet and release of cytolytic enzymes (Agostinis *et al.*, 2002). Generally, the ER is regarded as the primary site for HYP-PDT with resultant mitochondrial involvement leading to apoptosis (Moor, 2000). At the same time, HYP-PDT may also localize in plasma membrane and lysosomes in different cell type, leading to necrosis (Davids, Kleemann, Kacerovská, Pizinger & Kidson, 2008).

5.6   Mode of cell death for HYP-PDT+DOX

In HYP-PDT+DOX treatment (additive combination; IC90 isoeffect level; 0.10μg/ml HYP-PDT and 0.45μg/ml DOX) for HSC-2, apoptosis (85%) and necrosis (7%) occurred at 1 hour. Apoptotic population (LR quadrant) and necrotic population (UL quadrant) were recorded as early as one hour post-irradiaton in HSC-2 treated with HYP-PDT+DOX, indicating membrane phosphatidylserine (PS) externalization might occur before morphological and biochemical changes could be detected. For HSC-3 treated with HYP-PDT+DOX (synergistic combination; IC90 isoeffect level; 0.10μg/ml HYP-PDT and 0.22μg/ml DOX), apoptosis (63%) and necrosis (11%) occurred at 3 hours. Obviously, in both cell lines, apoptosis is predominant at early time point. In contrast, HSC-4 cells treated with HYP-PDT+DOX (synergistic combination; IC90 isoeffect level; 0.10μg/ml HYP-PDT and 0.26μg/ml DOX)

encountered only necrosis at early time points (10% at 1 hour; 22% at 3 hours). Apoptosis was only detected later at 15 hours (28%), the point where necrosis already increased to 43%.

For all cell lines treated with HYP-PDT+DOX, Bax/Bcl-2 balance was altered and favorable to apoptosis. High Bax:Bcl-2 ratio (Figure 4.37; Row 1 and Row 2) throughout 24 hours may explained the reason of apoptosis occurrence. The reason for earlier onset of apoptosis in HSC2 and HSC-3 may be explained by analysing the onset of caspase cleavage. In HSC-2 and HSC-3, both caspase-9 and caspase-7 were shown to be cleaved as early at 3 hours, leading to early apoptosis. In HSC-4, caspase-9 and caspase-7 was only cleaved later at 7 hours and 15 hours. This is in consistent with the result in flow cytometric phophatidylserine redistribution analysis (Figure 4.17).

Since caspase-9 was found cleaved, it may indicate that pro-caspase-9 has been activated. At the same time, high Bax:Bcl-2 ratio also help to alter mitochondria permeability. Therefore, the apoptosis caused by HYP-PDT+DOX may be related to intrinsic mitochondria-mediated pathway. Other study had shown that caspase-7 can be activated directly by apoptosome complex (Twiddy, Cohen, Macfarlane and Cain, 2006). This may also infer that apoptosis induced by combination treatments went through intrinsic mitochondria pathway.

Other crucial factors in determining mode of cell death, especially apoptosis or necrosis after PDT are concentration of photosensitizer, activation

light concentration, oxygen level and photosensitizer subcellular localization. For example, in HYP-PDT+DOX combination (Figure 4.11d,e,f), synergism only occurred in all three cell lines when high concentration HYP-PDT (more than IC50) were used to combine with low DOX concentrations (less than IC50 in HSC-4 and less than IC30 in HSC-2 and HSC-3). Predominance of necrosis in HYP-PDT+DOX combination may be due to the use of high concentration HYP-PDT (more than IC50). Agotinis and colleagues observed a shift of mode of cell death from apoptosis to necrosis by increasing HYP-PDT concentration and/or the activation light concentration in human and murine cancer cell lines. These increments of HYP-PDT concentration or light concentration relatively determined the amount of ROS produced (Agostinis *et al*., 2002).

When ROS was produced in excessive amounts, death by necrosis is favoured. This may explain the overall predominance of necrosis in HYP-PDT+DOX (all three cell lines) and HYP-PDT+VIN (HSC-2 and HSC-3). HYP-PDT and DOX are both able to generate ROS (Casas, Fukuda, Riley & Batlle, 1997; Agostinis *et al*., 2002). Thus, DOX first caused oxidative damage to cell and eliminated antioxidant molecules, and photodynamic action of HYP-PDT caused more oxidative damage to the cells, resulting in rapid necrosis soon after the light activation. Due to photobleaching of HYP-PDT within irradiation period (Streckyte *et al*., 1999), ROS production may be reduced over the irradiation time and the cells accumulated lesser damage may be arrested in cell cycle (Piette, Volantia, Vantieghem, Matroule, Habraken & Agostinis, 2003) with apoptosis as a consequence much later.

Incomplete apoptosis may be another reason for necrosis to be predominant at early time-points in HSC-4. For example, with phase contrast microscopy, small amount of apoptotic bodies could be observed at 1 hour in HSC-4 treated with HYP-PDT+DOX. Yet, majority of cells started to swell at 15 hours, leading to necrosis morphology in 24 hours. HYP-PDT ability to inhibit PKC bII may be another reason to cause early necrosis in HSC-4 as suggested by Lavie et at.(1999). Their study showed that HYP-PDT induced necrosis in some leukemic cell lines may be due to an incomplete apoptosis, characterized by DNA degradation to oligonucleosomes in the absence of nuclear fragmentation, followed by necrosis. HYP-PDT's ability to inhibit protein kinase C (PKC) bII inside the cells may favor cell death toward necrosis. Inhibition of PKC bII interferes with lamin phosphorylation and therefore preventing nuclear fragmentation during apoptosis (Lavie, *et al.*, 1999). However, more studies have to be done to show that it is relevant in HSC series cell lines.

5.7   Mode of cell death for HYP-PDT+VIN

HYP-PDT+VIN treatment (additive combination; IC50 isoeffect level; 0.06μg/ml HYP-PDT and 0.0004μg/ml VIN) in HSC-3 produced only necrosis (19% at 1 hour; up to 71% at 15 hours) until 15 hours. Apoptosis (35%) occurred later at 24 hours. Similar to this, for HSC-4 treated with HYP-PDT+VIN (synergistic combination; IC40 isoeffect level; 0.06μg/ml HYP-PDT and 0.001μg/ml VIN), apoptosis also occurred late at 15 hours. In

contrast, HSC-2 cells treated with HYP-PDT+VIN treatment (synergistic combination; IC50 isoeffect level; 0.06μg/ml HYP-PDT and 0.002μg/ml VIN), showed that apoptosis (78%) and necrosis (8%) occurred as early at 1 hour post irradiation.

First, for all cell lines treated with HYP-PDT+VIN, high Bax:Bcl-2 ratio (Figure 4.38; Row 1 and Row 2) throughout 24 hours may favor the cells toward apoptosis. Although caspase-8 was found cleaved early at 3 hours, caspase-7 in HSC-3 (Figure 4.38; Row 5, Column B) was only cleaved later at 15 and 24 hours; caspase-7 in HSC-4 (Figure 4.38; Row 5, Column C) was also cleaved later at 7 and 15 hours. This is in consistent with phosphatidylserine redistribution assay where apoptosis occurred late in HSC-3 (24 hours) (Figure 4.19; Row 1, Column E) and HSC-4 (15 hours) (Figure 4.20; Row 1, Column D). In contrast, caspase-7 can be seen cleaved early at 3 hours in HSC-2. This may lead to earlier apoptosis occurrence in HSC-2 and this is proven by phosphatidylserine redistribution assay where HSC-2 showed apoptosis as early at 1 hour (Figure 4.18; Row 1, Column A).

Cleavage of caspase-8 suggests that apoptosis induced by HYP-PDT+VIN is partly mediated by components of the extrinsic pathway. Caspase-8-dependant caspases cascade is related to death-receptor-mediated activation (Reed, 2003; Kim, 2005). However, since Bax levels were also elevated, this may indicate that the intrinsic mitochondria-mediated pathway may be enhanced by caspase-8 activity.

Cells treated with VIN, a microtubule inhibitor, were arrested in the

cell cycle and encountered apoptosis at late time-points. At the same time, "low concentration PDT" used in this study may also cause cell cycle arrest (Ma, Berga, Danielsen, Kaalhus, Iani & Moan, 1996; Piette, Volantia, Vantieghem, Matroule, Habraken & Agostinis, 2003). Therefore, both VIN and HYP-PDT may act together to disturb mitosis, causing apoptosis to occur late in HSC-3 and HSC-4.

Confluence-dependant resistance may be one of the factors affecting the mode of cell death. For example, in HSC-2, HYP-PDT+DOX treatment caused more necrotic death at early time point if compared to HYP-PDT+VIN treatment. DOX is a cytotoxic drug but VIN is a cytostatic drug. At early time point, DOX may kill the cells while VIN will only arrest the cells without killing them. When cells were killed earlier by DOX, cell confluency reduced, and more cells surface was exposed to culture medium (drugs and photosensitizer). Thereby, more damage could be accumulated, leading to necrosis. In contrast, VIN did not kill cells in early time point, therefore, cell confluency was relatively higher, lesser cell surface was exposed to accumulate drugs. Thus, fewer damage was accumulated, leading to apoptosis. This is supported by a prior study in which the researchers found that monolayer of cells in low density were more responsive to PDT than confluent cell culture. Therefore, for same photosensitizer concentration, adherent cells in higher density (high conflueny) may be accounted for confluence-dependent resistance (Kleban *et al.*, 2006).

5.8 Clinical value on oral cancer

Oral cancers are excellent candidates for PDT because the oral cavity can be very easily accessed by light irradiation tools when photodynamic therapy (PDT) is to be carried out, either for in vivo or clinical investigation (Allison, Cuenca, Downie, Camnitz, Brodish & Sibata, 2005). Currently, PDT is available for use in oral cancer clinically. The treatments of patients with clinically approved photosensitizers like Photofrin®, Foscan®, 5-aminolevulinic acid are reported with excellent results (Allison, Downie, Cuenca, Hu, Childs & Sibata, 2004). However, multifactorial working requirements have limited PDT to be used as conservative or back-up treatments. For PDT to work as desired, several interdependent factors such as the type of sensitizer, its extracellular and intracellular localization, the total concentration administered, the total light exposure concentration, light fluence rate, oxygen availability, and the time between the administration of the drug and light exposure have to be determined (Dolmans, Fukumura & Jain, 2003). Despite discovery of photosensitizer that can penetrate deeper into tissue and light irradiation tools that helps to irradiate tumor located under skin, clinical PDT treatment is still limited in treating early stage of oral cancer or late stage, recurrent oral cancer patients who are unsuitable for other standard treatment (Allison, Downie, Cuenca, Hu, Childs & Sibata, 2004; Pichi, Ruscito, Pellini, Manciocco & Spriano, 2009; Chen *et al.*, 2010). Due to uncertainty in PDT multifactorial requirements, in most cases, PDT is used in combination with chemotherapy as the last resolution or savage treatment after the patients failed to response to previous chemotherapy (Allison, Cuenca,

Downie, Camnitz, Brodish & Sibata, 2005; Yano, Muto, Minashi, Ohtsu & Yoshida, 2005).

These concerns can be solved by looking for and using only the combination drug pairs with a "threshold of synergism". For example, in current study, a "threshold of synergism" can be found in HYP-PDT+DOX treatments in all three cell lines (Figure 4.11 d, e, f) at fixed light exposure concentration and light fluence rate. Animal trials have to be conducted to confirm this finding. If these ranges of combination pairs located under the "threshold of synergism" is proved under animal models and can act as a guideline for choosing tolerable yet effective concentrations for clinical treatment, it is going to eliminate the doubt and uncertainty in choosing suitable dosage.

CHAPTER 6

FUTURE STUDY

Other than Bcl-2 and Bax which had been evaluated in this study, there are several other apoptosis regulating factors with may be upregulated or downregulated during combination treatments. By identifying these proteins, more drugable targets can be detected and be incorporated into current combination treatments. Two dimensional SDS-PAGE is a relevant way to reveal these proteins. Other than Bcl-2 and Bax, COX-2 was also mentioned in other study that it will influence apoptosis outcome. Therefore, investigation of COX-2 involvement in the cell killing of combination treatments may shed light on the mechanism of action.

HYP-PDT+CIS combination is one which produced less than additive outcome in oral cancer cell lines. Investigation of HYP-PDT combination with other platinum-based cytotoxic drugs such as oxaliplatin, tetraplatin and carboplatin may reveal whether metal-based anticancer drug is suitable as a candidate for combination with HYP-PDT-PDT.

HYP-PDT+CIS and HYP-PDT+VIN treatments resulted in caspase-8 activation in HSC-2, HSC-3 and HSC-4, which may be related to death-receptor-mediated apoptosis. Therefore, further investigation can be carried out to confirm the involvement of death receptors in apoptosis. At the same time, due to ambiguitiness of the bands for upstream caspases such as caspase-

8 and caspase-9 in current Western Blot data, confirmation of these ambiguities should be carried out before any other future work is to be performed. More supporting evidences have to be collected from *in vivo* study in order to validate the efficacy of these drug combinations involving HYP-PDT.

In current study, although downstream effector caspase-7 can be a proof of apoptosis occurrence, further study on the involvement of another downstream effector, caspase-3 will help to describe the cell death pathways of combination treatment. In addition, caspase-2 is a unique caspase that can act as initiator (with long pro-domain) or effector (having VDVAD substrate Specificity). Other studies have revealed that caspase-2 resides primarily in Golgi complex and it is constitutively pooled in nucleus (Boris & Sten, 2005). Therefore, study of caspase-2 may indicate whether Golgi complex and nucleus can be the primary target site for the combination treatments.

Kramarenko and colleagues (2006) reported that ascorbate could decrease toxicity by converting highly reactive singlet oxygen to less reactive hydrogen peroxide, which could increase apoptotic rate. They demonstrated that ascorbate increases hydrogen peroxide production in verterporfin-PDT. Thus, in combination treatment causing more necrotic cell death, for example, HYP-PDT+DOX treatment in HSC-4, existence of ascorbate during light activation may help to convert necrotic cell death into apoptotic cell death.

Other than apoptosis, another outcome of combination treatment is

necrosis. For instance, several protein complexes such as FAS, FAD, FADD may act together with RIP and cause necrosis. The mechanism involved in inducing necrosis should also be studied.

CHAPTER 7

CONCLUSION

In this study, HYP-PDT was combined with CIS, DOX and VIN respectively and killing rate against HSC-2, HSC-3 and HSC-4 was evaluated. In HYP-PDT+CIS treatments, synergistic cell killing was seen in HSC-4 and may have involved caspase-8-mediated activity of mitochondria apoptotic pathway. In HYP-PDT+DOX treatments, synergistic drugs interaction could be seen in all cell lines when concentration of drugs were chosen to give 90% cell killing (IC_{90} isoeffect level). HYP-PDT+DOX killed cells by necrosis and apoptosis mediated by caspase-9 and high Bax:Bcl-2 ratio. HYP-PDT+VIN showed synergistic drugs interaction in HSC-2 and HSC-4. Besides necrosis, this combination may also kill cells through extrinsic apoptotic pathway. This study demonstrated that combination treatments increase Bax:Bcl-2 ratio. At the same time, the onset and the degree of apoptosis or necrosis in selected drugs pairs (additive or synergistic pairs) were shown to be greater than the drugs used alone. Therefore, instead of being an alternative or salvage treatment, PDT has great potential to be used together with clinically approved cisplatin, doxorubicin and vinblastine as standard treatment in oral cancer. At the same time of giving better synergistic treatment outcome, combination of PDT and chemotherapy in combating oral cancer may also help to reduce the working dosage and side effect of conventional high-concentration chemotherapy.

REFERENCES

Ackroyd, R., Kelty, C., Brown, N. & Reed, M. (2001). The history of photodetection and photodynamic therapy. Photochemistry and Photobiology, vol. 74(5), pp. 56–669.

Adams, J. M. & Cory, S. (2001). Life-or-death decisions by the Bcl-2 protein family. Trends in Biochemical Sciences, vol. 26(1), pp. 61-66.

Adelstein, D. J. , Tan, E. H. & Lavertu, P. (1996). Treatment of head and neck cancer: the role of chemotherapy. Critical Reviews in Oncology/Hematology, vol. 24, pp. 97-116.

Agostinis, P., Vantieghem, A., Merlevede, W. & de Witte, P. A. M. (2002). Hypericin in cancer treatment: more light on the way. The International Journal of Biochemistry & Cell Biology, vol. 34, pp. 221–241.

Akita, Y., Kozaki, K., Nakagawa, A., Saito, T., Ito, S., Tamada, Y., Fujiwara, S., Nishikawa, N., Uchida, K., Yoshikawa, K., Noguchi, T., Miyaishi, O., Shimozato, K., Saga, S. & Matsumoto, Y. (2004). Cyclooxygenase-2 is a possible target of treatment approach in conjunction with photodynamic therapy for various disorders in skin and oral cavity. British Journal of Dermatology, vol. 151(2), pp. 472-480.

Akita, Y., Kozaki, K., Takeo, T., Ohmura, M., Nakagawa, A., Yanagishita, T., Kazaoka, Y., Nozaki, T., Yokoo, K., Shinohara, M., Watanabe, D., Kawai, T., Yamada, S., Tamada, Y., Ohura, K. & Matsumoto, Y. (2006). Enhancement of the photodynamic effects on human oral squamous cell carcinoma cell lines by treatment with calcipotriol. Journal of Dermatological Science Supplement vol. 2, pp. S57—S64.

Ali, S. M., Chee, S. K., Yuen, G. Y., & Olivo, M. (2001). Hypericin and hypocrellin induced apoptosis in human mucosal carcinoma cells. Journal of Photochemistry and Photobiology B: Biology, vol. 65(1), pp. 59-73.

Allison, R. R., Downie, G. H., Cuenca, R., Hu, X., Childs, C. J. H. & Sibata, C. H. (2004). Photosensitizers in clinical PDT. Photodiagnosis and Photodynamic Therapy, vol. 1, pp. 27-42.

Allison, R. R., Mota, H. C. & Sibata, C. H. (2004). Clinical PD/PDT in North America: an historical review. Photodiagnosis and Photodynamic Therapy, vol. 1(4), pp. 263-277.

Allison, R. R., Cuenca, R. E., Downie, G. H., Camnitz, P., Brodish, B., Sibata, C. H. (2005). Clinical photodynamic therapy of head and neck cancers——A review of applications and outcomes. Photodiagnosis and Photodynamic Therapy, vol. 2, pp. 205-222.

Assefa, Z., Vantieghem, A., Declercq, W., Vandenabeele, P., Vandenheede, J. R., Merlevede, W., de Witte, P. & Agostinis, P. (1999). The activation of the c-Jun N-terminal kinase and p38 mitogen-activated protein kinase signaling pathways protects HeLa cells from apoptosis following photodynamic therapy with hypericin. The Journal of Biological Chemistry, vol. 274(13), pp. 8788-8796.

Bamias, A., Aravantinos, G., Deliveliotis, C., Bafaloukos, D., Kalofonos, C., Xiros, N., Zervas, A., Mitropoulos, D., Samantas, E., Pectasides, D., Papakostas, P., Gika, D., Kourousis, C., Koutras, A., Papadimitriou, C., Bamias, C., Kosmidis, P. & Dimopoulos, M. A. (2004). Docetaxel and cisplatin with granulocyte colony-stimulating factor (G-CSF) versus MVAC with G-CSF in advanced urothelial carcinoma: a multicenter, randomized, phase III study from the hellenic cooperative oncology group. Journal of Clinical Oncology, vol. 22(2), pp. 220-228.

Barr, L., Cowan, R. & Nicolson, M. (1997). Churchill's Pocketbook of Oncology. In chapter 4 : Managing Specific Tumor – Tumours of Head and Neck –Carcinoma of Oral Cavity, pp.112-114.

Belusic-Gobic, M., Car, M., Juretic, M., Cerovic, R., Gobic, D., Golubovic, V. (2007). Risk factors for wound infection after oral cancer surgery. Oral Oncology, vol. 43, pp.77– 81.

Bernier, J., Hall, E. J. & Giaccia, A. (2004). Radiation oncology: a century of Achievements. Nature review cancer, vol.4, pp. 737-747.

Berr, F., Tannapfe, A., Lamesch, P., Pahernik, S., Wiedmann, M., Halm, U., Goetz, A. E., Mossner, J. & Hauss, J.(2000). Neoadjuvant photodynamic therapy before curative resection of proximal bile duct carcinoma. Journal of Hepatology, vol. 32, pp. 352-357.

Biel, M. A. (2002). Photodynamic therapy in head and neck cancer. Current Oncology Reports, vol. 4(1), pp. 87-96.

Binahmed, A., Nason, R. W & Abdoh, A. A. (2007). The clinical significance of the positive surgical margin in oral cancer. Oral Oncology, vol. 43, pp. 780-784.

Bonnett, R. (2000). Chemical Aspects of Photodynamic Therapy. Gordon and Breach Science Publishers, Singapore.

Boris, Z. & Sten, O. (2005). Caspase-2 function in response to DNA damage. Biochemical and Biophysical Research Communications, vol. 331(3), pp. 859-867.

Bouchet, B. P., Fromentel, C. C., Puisieux, A. & Galmarini, C. N. (2006). p53 as a target for anti-cancer drug development. Critical Reviews in Oncology/Hematology, vol. 58(3), pp. 190-207.
Boyer, M. J. & Tannock, I. F. (2005). Cellular and molecular basis of drug treatment for cancer. In: The basic science of oncology. Editors: Tannock, I. F., Hill, R. P., Bristow, R. G. & Harrington, L., pp. 349-375. McGraw Hill, USA.

Brophy, P. F. & Keller, S. M. (1992). Adriamycin enhanced in vitro and in vivo photodynamic therapy of mesothelioma. Journal of Surgical Research, vol. 52(6), pp. 631-634.

Brown, S. B., Brown, E. A. & Walker, I. (2004). The present and future role of photodynamic therapy in cancer treatment. Lancet Oncology, vol. 5, pp. 497-508.

Canti, G., Nicolin, A., Cubeddu, R., Taroni, P., Bandieramonte, G. & Valentini, G. (1998). Antitumor efficacy of the combination of photodynamic therapy and chemotherapy in murine tumors. Cancer Letters, vol. 125(1-2), pp. 39-44.

Cao, W., Ma, S. L., Tang, J., Shi, J. & Lu, Y. (2006). A combined treatment TNF-α/Doxorubicin alleviates the resistance of MCF-7/Adr cells to cytotoxic treatment. Biochimica et Biophysica Acta, vol.1763, pp. 182-187.

Casas, A., Fukuda, H., Riley, P. & Batlle, A. M. C. (1997). Enhancement of aminolevulinic acid based photodynamic therapy by adriamycin. Cancer Letters, vol. 121, pp. 105-113.

Chabner, B. A. & Roberts, Jr. T. G. (2005). Chemotherapy and the war on cancer. Nature Reviews Cancer, vol. 5, pp. 65-72.

Chatterjee, D. K., Fong, L. S. & Zhang, Y. (2008). Nanoparticles in photodynamic therapy: An emerging paradigm. Advanced Drug Delivery Reviews, vol. 60(15), pp. 1627-1637.

Chen, H. M., Chiang, C. P. & Kuo, M. Y. P. (2005). Effect of photodynamic therapy plus chemotherapy on oral cancer cell lines. Oral Oncology Supplement, vol. 1(1), pp. 189.

Chen, H., Yu, C., Lin, H., Yang, H., Kuo, R., Kuo, Y. & Chiang, C. (2010). Successful treatment of an early invasive oral squamous cell carcinoma with topical 5-minolevulinic acid-mediated photodynamic therapy. Journal of Dentistry Science, vol. 5(1), pp. 36-40.

Chevalier, T. Le. & Soria, J. C. (2004). Status and trends of chemotherapy for advance NSCLC. European Journal of Cancer Supplements, vol. 2(4), pp. 26-33.

Choi, E. H., Chang, H. J., Cho, J. Y. & Chun, H. S. (2007). Cytoprotective effect of anthocyanins against doxorubicin-induced toxicity in H9c2 cardiomyocytes in relation to their antioxidant activities. Food and Chemical Toxicology, vol. 45(10), pp. 1873-1881.

Choi, H. R. K., Luo, Y., Li, G. & Kessel, D. (1999). Enhanced apoptotic response to photodynamic therapy after Bcl-2 transfection. Cancer Research, vol.59, pp. 3429-3432.

Christiansen, S. & Autschbach, R.(2006). Doxorubicin in experimental and clinical heart failure. European Journal of Cardio-thoracic Surgery, vol. 30, pp. 611-616.

Clurman, B. E. & Roberts, J. M. (2002). Cell cycle control: An overview. In The Genetic Basis of Human Cancer, 2nd Edition, pp. 145-161, McGraw-Hill, USA.

Corti, L., Skarlatos, J., Boso, C., Cardin, F., Kosma, L., Koukourakis, M. I., Giatromanolaki, A., Norberto, L., Shaffer, M. & Beroukas, K. (2000). Outcome of patients receiving photodynamic therapy for early esophageal cancer. International Journal of Radiation Oncology • Biology • Physics, vol. 47(2), pp. 419-424.

Coultas, L. & Strasser, A. (2003). The role of the Bcl-2 protein family in cancer. Seminars in Cancer Biology, vol. 13, pp. 115-123.

Crescenzi, E., Varriale, L., Lovino, M., Chiavello, A., Veneziani, M. B. & Palumbo, G. (2004). Photodynamic therapy with indocyanine green complements and enhances low-dose cisplatin cytotoxicity in MCF-7 breast cancer cells. Molecular Cancer Therapeutics, vol. 3(5), pp. 537-544.

Davids, L. M., Kleemann, B., Kacerovská, D., Pizinger, K. & Kidson, S. H. (2008). Hypericin phototoxicity induces different modes of cell death in melanoma and human skin cells. Journal of Photochemistry and Photobiology B: Biology, vol. 91(2-3), pp. 67-76.

Debefve, E., Pegaz, B., Ballini, J. P., Konan, Y. N. & van den Bergh, H. (2006). Combination therapy using aspirin-enhanced photodynamic selective drug delivery. Vascular Pharmacology, vol. 46, pp. 171-180.

del Carmen, M. G., Rizvi, I., Chang, Y., Moor, A. C., Oliva, E., Sherwood, M., Pogue, B. & Hasan, T. (2005). Synergism of epidermal growth factor receptor-targeted immunotherapy with photodynamic treatment of ovarian cancer in vivo. Journal of the National Cancer Institute, vol. 97(20), pp. 1516-1524.

Delaey, E., Vandenbogaerde, A., Merlevede, W. & de Witte, P. (2000). Photocytotoxicity of hypericin in normoxic and hypoxic conditions Journal of Photochemistry and Photobiology B: Biology, vol. 56, pp. 19-24.

Deppert, W. (2007). Mutant p53: from guardian to fallen angel? Oncogene, vol. 26, pp. 2142-2144.

DeRosa, M. C. & Crutchley, R. J. (2002). Photosensitized singlet oxygen and its applications. Coordination Chemistry Reviews, vol. 233/234, pp. 351-371.

Dilkes, M. G., DeJode, M. L., Rowntree-Taylor, A, McGilligan, J. A., Kenyon, G. S. & McKelvie, P. (1996). m-THPC photodynamic therapy for head and neck cancer. Lasers in Medical Science, vol. 11(1), pp. 23-29.

Dinshaw, K. A., Agarwal, J. P., Ghosh-Laskar, S. , Gupta, T. , Shrivastava, S. K. (2006). Radical radiotherapy in head and neck squamous cell carcinoma: an analysis of prognostic and therapeutic factors. Clinical Oncology, vol. 18, pp. 383-389.

Dolmans, D. E. J. G. J., Fukumura, D. & Jain, R. K. (2003). Photodynamic therapy for cancer. Nature Reviews Cancer, vol. 3, pp.380-386.

Donovan, M. & Cotter, T. G. (2004). Control of mitochondrial integrity by Bcl-2 family members and caspase-independent cell death. Biochimica et Biophysica Acta, vol.1644, pp. 133-147.

Dowdy, S. C., Boardman, C. H., Wilson, T. O., Podratz, K. C., Hartmann, L. C., & Long, H. J. (2002). Multimodal therapy including neoadjuvant methotrexate, vinblastine, doxorubicin, and cisplatin (MVAC) for stage IIB to IV cervical cancer. American Journal of Obstetrics & Gynecology, vol. 186, pp. 1167-1173.

Duan, L. L, Sterba, K., Kolomeichuk, S., Kim, H., Brown, P. H. & Chambers, T. C. (2007). Inducible overexpression of c-Jun in MCF-7 cells causes resistance to vinblastine via inhibition of drug-induced apoptosis and senescence at a step subsequent to mitotic arrest. Biochemical Pharmacology, vol. 7(3), pp. 481-490.

Edinger, A. L. & Thompson, C. B. (2004). Death by design: apoptosis, necrosis and autophagy. Current Opinion in Cell Biology, vol.16, pp. 663-669.

Fanidi, A., Harrington, E. A. & Evan, G. I. (1992). Cooperative interaction between c-myc and bcl-2 proto-oncogenes. Nature, vol. 348, pp. 331-333.

Fernandez, J. M., Bilgin, M. D. & Grossweiner, L. L. (1997). Singlet oxygen generation by photodynamic agents. Journal of Photochemistry and Photobiology B: Biology. vol. 37, pp. 131-140.

Ferry, K. V., Hamilton, T. C. & Johnson S. W. (2000). Increased nucleotide excision repair in cisplatin-resistant ovarian cancer cells: role of ERCC1-XPF. Biochemical Pharmacology, vol. 60(9), pp. 1305-1315.

Festjens, N., Berghe, T. V. & Vandenabeele, P. (2006). Necrosis, a well-orchestrated form of cell demise: Signalling cascades, important mediators and concomitant immune response. Biochimica et Biophysica Acta, vol. 1757, pp. 1371-1387.

Finlay, C. A., Hinds, P. W., Levine, A. J. (1989). The p53 proto-oncogene can act as a suppressor of transformation. Cell, vol. 57(7), pp.1083–1093.

Fisher, A. M. R., Rucker, N., Wong, S. & Gomer, C. J. (1998). Differential photosensitivity in wild-type and mutant p53 human colon carcinoma cell lines. Journal of Photochemistry and Photobiology B: Biology, vol. 42(2), pp. 104-107.

Forshaw, M. J., Gossage, J. A., Chrystal, K., Cheong, K., Atkinson, S., Botha, A., Harper, P. G., Mason, R. C. (2006). Neoadjuvant chemotherapy for locally advanced carcinoma of the lower oesophagus and oesophago-gastric junction. European Journal of Surgical Oncology, vol. 32, pp. 1114-1118.

Foster, I. (2007). Cancer: A cell cycle defect, Radiography, vol. 14(2), pp. 144-149.

Frebourg, T., Kassel, J., Lam, K. T., Gryka, M. A., Barbier, N., Andersen, T. I., Borresen, A. U. & Friend, S. H. (1992). Germ-line mutations of the p53 tumor suppressor gene in patients with high risk for cancer inactivate the p53 protein. Proceedings of the National Academy of Sciences of the United States of America, vol. 89, pp. 6413-6417.

Frei, E. 3rd., Karon, M., Levin, R. H., Freireich, E. J., Taylor, R. J., Hananian, J., Selawry, O., Holland, J. F., Hoogstraten, B., Wolman, I. J., Abir, E., Sawitsky, A., Lee, S., Mills, S. D., Burgert, E. O. Jr., Spurr, C. L., Patterson, R. B., Ebaugh, F. G., James, G. W. 3rd. & Moon, J. H. (1965). The effectiveness of combinations of antileukemic agents in inducing and maintaining remission in children with acute leukemia. *Blood*, vol. 26(5), pp. 642-656.

Friedman, P. N., Chen, X. B., Bargonetti, J. & Prives, C. (1993). The p53 protein is an unusually shaped tetramer that binds directly to DNA. Proceedings of the National Academy of Sciences of the United States of America, vol. 90, pp. 3319-3323.

Gajewski, E., Gaur, S., Akman, S. A., Matsumoto, L., Balgooy, J. N. A. & Doroshow, J. H. (2007). Oxidative DNA base damage in MCF-10A breast epithelial cells at clinically achievable concentrations of doxorubicin. Biochemical Pharmacology, vol. 73(12), pp. 1947-1956.

Gartel, A. L. & Kandel, E. S. (2006). RNA interference in cancer. Biomolecular Engineering, vol.23, pp.17-34.

Gebski, V., Burmeister, B., Smithers, B. M., Foo, K., Zalcberg, J. & Simes, J. (2007). Survival benefits from neoadjuvant chemoradiotherapy or chemotherapy in oesophageal carcinoma: a meta-analysis. Lancet Oncology, vol. 8, pp.226-234.

Geh, J. I. (2002). The use of chemoradiotherapy in oesophageal cancer. European Journal of Cancer, vol.38, pp. 300-313.

Golstein, P. & Kroemer, G. (2006). Cell death by necrosis: towards a molecular definition. Trends in Biochemical Sciences, vol. 32(1), pp. 37-43.

Gossage, L. & Madhusudan, S. (2007). Current status of excision repair cross complementing-group 1 (ERCC1) in cancer. Cancer Treatment Reviews, vol. 33(6), pp. 565-577.

Gottschlich, S. & Ambrosch, P. (2004). Laser microsurgery of oral cavity cancer. Operative Techniques in Otolaryngology, vol. 15, pp. 252-255.

Gougeon, M. L. & Montagnier, L., (1993). Apoptosis in AIDS. Science, vol. 260, pp. 1269-1270.

Gressner, P. K. (1995). Isobolographic analysis of interactions: an update on applications and utility. Toxicology, vol. 105, pp. 161-179.

Guedes, R. C., & Eriksson, L. A. (2005). Theoretical study of hypericin. Journal of Photochemistry and Photobiology A: Chemistry, vol. 172, pp. 293-299.

Hadjur, C., Richard, M. J., Parat, M. O., Favier, A. & Jardon, P. (1995). Photodynamically induced cytotoxicity of hypericin dye on human fibroblast cell line MRC5. Journal of Photochemistry and Photobiology B: Biology, vol. 27(2), pp. 139-146.

Hail Jr. N., Carter, B. Z., Konopleva, M. & Andreeff, M. (2006). Apoptosis effector mechanisms: A requiem performed in different keys. Apoptosis, vol. 11(6), pp. 889-904.

Hait, W. N., Rubin, E., Alli, E. & Goodin, S. (2007). Tubulin Targeting Agents. Update on cancer therapeutics, vol. 2, pp. 1-18.

Hanahan, D. & Weinberg, R. A. (2000). The Hallmarks of Cancer. Cell, vol. 100, pp. 57-70.

Hanlon, J. G., Adams, K., Rainbow, A. J., Gupta, R. S. & Singh, G. (2001). Induction of Hsp60 by Photofrin-mediated photodynamic therapy. Journal of Photochemistry & Photobiology B, vol. 64(1), pp.55-61.

Harrington,K.J.(2007). Biology of cancer, Medicine, vol. 36(1), pp. 1-4.

Holdenrieder, S. & Stieber, P. (2004). Apoptotic markers in cancer. Clinical Biochemistry, vol. 37, pp. 605-617.

Hopper, C. (2000). Photodynamic therapy: a clinical reality in the treatment of cancer. The Lancet Oncology, vol.1, pp. 212-219.

Horch, H. H. & Deppe, H. (2005). New aspects of lasers in oral and craniomaxillofacial surgery. Medical Laser Application, vol. 20, pp. 7-11.

Imal, S., Kajihara, Y., Munemori, O., Kamei, T., Mori, T., Handa, T., Akisada, K. & Orita, Y. (1995). Superselective cisplatin (CDDP)-carboplatin (CBDCA) combined infusion for head and neck cancersEuropean Journal of Radiology, vol. 21, pp. 94-99.

Johnson, I. S., Armstrong, J. G., Goman, M. & Burnett J. P. Jr. (1963). The vinca alkaloids : a new class of oncolytic agents. Cancer Research, vol. 23, pp. 1390-1427.

Jackman, A. L., Kaye, S. & Workman, P. (2004). The combination of cytotoxic and molecularly targeted therapies – can it be done? Drug Discovery Today: Therapeutic Strategies, vol. 1(4), pp. 445-454.

Kaneski, C. R., Constantopoulos, G. & Brady, R. O. (1991). Effect of dimethylsulfoxide on the proliferation and glycosaminoglycan synthesis. Prostate, vol.18, pp. 47-58.

Kao, J., Lavaf, A., Teng, M. S., Huang, D. & Genden, E. M. (2008). Adjuvant radiotherapy and survival for patients with node-positive head and neck cancer : an analysis by primary site and nodal stage. International Journal of Radiation Oncology • Biology • Physics, vol. 71(2), pp. 362-370.

Katabami, M., Fijita, H., Haneda, H., Akita, H., Kuzumaki, N., Miyamoto, H. & Kawakami, Y. (1992). Reduced drug accumulation in a newly established human lung squamous-carcinoma cell line resistant to cis-diamminedichloroplatinum(II). Biochemical Pharmacology, vol. 44(2), pp. 394-397.

Kavallaris, M., Verrills, N. M. & Hill, B. T. (2001). Anticancer therapy with novel tubulin-interacting drugs. Drugs Resistance Updates, vol. 4, pp. 392-401.

Kelley, E. E., Domann, F. E., Buettner, G. R., Oberley, L. W. & Burns, C. P. (1997). Increased efficacy of in vitro Photofrin photosensitization of human oral squamous cell carcinoma by iron and ascorbate. Journal of Photochemistry and Photobiology B: Biology, vol. 40, pp. 273-277.

Kerr, J. F., Wyllie, A. H. & Currie, A. R. (1972). Apoptosis: a basic biological phenomenon with wide-ranging implications in tissue kinetics. British Journal of Cancer, vol. 26, pp. 239-257.

Kessel, D. (2004). Photodynamic therapy: from the beginning. Photodiagnosis and Photodynamic Therapy, vol. 1, pp.3-7.

Khdair, A, Chen, D., Patil, Y., Ma, L, Dou, Q. P., Shekhar, M. P. V. & Panyam, J. (2009). Nanoparticle-mediated combination chemotherapy and photodynamic therapy overcomes tumor drug resistance. Journal of Controlled Release, vol. 141(2), pp. 137-144.

Kim, R.(2005). Recent advances in understanding the cell death pathways activated by anticancer therapy. Cancer, vol. 103(8), pp. 1551-1559.

Kinzler, W. K. & Vogelstein, B. (2002). Introduction. In The Genetic Basis of Human Cancer, 2nd Edition, pp. 3-6, McGraw-Hill, USA.

Kirkin, V., Joos, S. & Zőrnig, M. (2004). The role of Bcl-2 family members in tumorigenesis. Biochimica et Biophysica Acta, vol. 1644, pp. 229-249.

Kleban, J., Szilardiova, B., Mikes, J., Horvath, V., Sackova, V., Brezani, P., Hofmanova, J., Kozubık, A., Fedorocko, P. (2006). Pre-treatment of HT-29 cells with 5-LOX inhibitor (MK-886) induces changes in cell cycle and increases apoptosis after photodynamic therapy with hypericin. Journal of Photochemistry and Photobiology B: Biology, vol. 84, pp. 79-88.

Knudson, A. G. (1971). Mutation and cancer: statistical study of retinoblastoma. Proceedings of the National Academy of Sciences of the United States of America, vol. 68(4), pp. 820-823.

Kostron, H., Obwegeser, A. & Jakober, R. (1996). Photodynamic therapy in neurosurgery: a review. Journal of Photochemistry and Photobiology B: Biology, vol.36, pp.157-168.

Kostron, H., Fiegele, T. & Akatuna, E. (2006). Combination of FOSCAN mediated fluorescence guided resection and photodynamic treatment as new therapeutic concept for malignant brain tumors. Medical Laser Application, vol.21, pp. 285-290.

Kramarenko, G. G., Wilke, W. W., Dayal, D., Buettner, G. R. & Schafer, F. Q. (2006). Ascorbate enhances the toxicity of the photodynamic action of Verteporfin in HL-60 cells.Free Radical Biology and Medicine, vol. 40(9), pp. 1615-1627.

Kuczyk, M. A., Zimmermann, R., Merseburger, A., Anastasiadis, A., Corvin, S., Hartmann, J. T. & Stenzl, A. (2004). Chemotherapy in locally advanced and metastatic bladder cancer. European Urology, Supplements 3, pp.79-88.

Kulka, U., Schaffer, M., Siefert, A., Schaffer, P. M., Olsner, A., Kasseb, K., Hofstetter, A., Duhmke, E. & Jori, G. (2003). Photofrin as a radiosensitizer in an in vitro cell survival assay. Biochemical and Biophysical Research Communications, vol. 311, pp. 98-103.

Kuriu, A., Ikeda, H., Kanakura, Y., Griffin, J. D., Druker, B., Yagura, H., Kitayama, H., Ishikawa, J., Nishiura, T., Kanayama, Y., Yonezawa, T. & Tarui, S. (1991). Proliferation of human myeloid leukemia cell line associated with the tyrosine-phosphorylation and activation of the proto-oncogene c-kit product. Blood, vol.78(11), pp. 2834-2840.

Land, H., Chen, A. C., Morgenstern, J. P., Parada, L. F. & Weinberg, R. A. (1986). Behaviour of MYC and RAS oncogenes in transformation of rat embryo fibroblasts. Molecular and Cellular Biology, vol. 6(6), pp. 1917-1925.

Lane, D. P. (1992). p53, guardian of the genome. Nature, vol. 358 (6381), pp. 15-16.

Lavie, G., Kaplinsky, C., Toren, A., Aizman, I., Meruelo, D., Mazur, Y. & Mandel, M. (1999). A photodynamic pathway to apoptosis and necrosis induced by dimethyl tetrahydroxyhelianthrone and hypericin in leukaemic cells: possible relevance to photodynamic therapy. British Journal of Cancer. vol. 79(3/4), pp. 423-432.

Levine, A. J., Momand, J. & Finlay, C. A. (1991). The p53 tumour suppressor gene. Nature, vol. 351(6326), pp. 453-456.

Leunig, A., Mehlmann, M., Betz, C., Stepp, H., Arbogast, S., Grevers, G. & Baumgartner, R. (2001). Fluorescence staining of oral cancer using a topical application of 5-aminolevulinic acid: fluorescence microscopic studies. Journal of Photochemistry and Photobiology B: Biology, vol. 60, pp. 44-49.

Li, L. Y., Luo, X. & Wang, X. (2001). Endonuclease G is an apoptotic DNase when released from mitochondria. Nature, vol. 412, pp. 95-99.

Lim, G. C. C., Yahaya, H. (2003). Second report of the National Cancer Registry : Cancer incidence in Malaysia. National Cancer Registry, Malaysia.

Lim, G. C. C. (2002). Overview of cancer in Malaysia. Japanese Journal of Clinical Oncology, vol. 32 (S1), pp. S37-42.

Lind, M. J. (2007). Principles of cytotoxic chemotherapy. Medicine, vol. 36(1), pp. 19-23.

Llano, J., Raber, J. & Eriksson, L. A. (2003). Theoretical study of phototoxic reactions of psoralens. Journal of Photochemistry and Photobiology A: Chemistry, vol. 154, pp. 235–243.

Llesuy, S. & Arnaiz, S. (1990). Hepatoxicity of mitoxantrone and doxorubicin. Toxicology, vol. 63, pp. 187-198.

Long, H. J., Monk, B. J., Huang, H. Q., Grendys, Jr. E. C., McMeekin, D. S., Sorosky, J., Miller, D. S., Eaton, L. A. & Fiorica, J. V. (2006). Clinical results and quality of life analysis for the MVAC combination (methotrexate, vinblastine, doxorubicin, and cisplatin) in carcinoma of the uterine cervix: A Gynecologic Oncology Group study. Gynecologic Oncology, vol. 100, pp. 537-543.

Lucchi, M., Fontanini, G., Mussi, A., Vignati, S., Ribechini, A., Menconi, G. F., Bevilacqua, G. & Angeletti, C. A. (1997). Tumor angiogenesis and biologic markers in resected stage I NSCLC. European Journal of Cardio-thoracic Surgery, vol. 12 , pp. 535-541.

Luksiene, Z., Kalvelyte, A. & Supino, R.(1999). On the combination of photodynamic therapy with ionizing radiation. Journal of Photochemistry and Photobiology B: Biology, vol. 52, pp. 35-42.

Ma, L. W., Berga, K., Danielsen, H. E., Kaalhus, O., Iani, V. & Moan, J. (1996). Enhanced antitumour effect of photodynamic therapy by microtubule inhibitors. Cancer Letters, vol. 109, pp. 129-139.

Magrath, I. & Litvak, J. (1993). Cancer in developing countries: opportunity and challenge. Journal of the National Cancer Institute, vol. 85(11), pp. 862-874.

Makin, G. & Dive, C. (2001). Apoptosis and cancer chemotherapy. Trends in Cell Biology, vol. 11(11), pp. S22-S26.

Margolis, R. L., Chuang, D. M. & Post, R. M. (1994). Programmed cell death : Implications for neuropsychiatric disorders. Biological Psychiatry, vol. 35(12), pp. 946-956.

Maria, P. L. S., Sader, C., Preston, N. J. M. & Fisher, P. H. (2007). Neck dissection for squamous cell carcinoma of the head and neck. Otolaryngology–Head and Neck Surgery, vol. 136, pp. S41-S45.

Martin, W. M. C. (1998). Cancer in developing countries: Part I - cancer burden, resources, epidemiology, aetiology and clinical practice. Clinical Oncology, vol.10, pp. 219-225.

Martinez-Irujo, J. J., Villahermosa, M. L., Alverdi, E. & Santiago, E. (1996). A checkerboard method to evaluate interactions between drugs. Biochemical Pharmacology, vol. 51, pp. 635-644.

Martinez-Poveda, B., Quesada, A. R. & Medina, M. A. (2005). Hypericin in the dark inhibits key steps of angiogenesis in vitro. European Journal of Pharmacology, vol. 516, pp. 97-103.

McConkey, D. J., Zhivotovsky, B. & Orrenius, S. (1996). Apoptosis -- molecular mechanisms and biomedical implications. Molecular Aspect of Medicine, vol. 17(1), pp. 1-110.

McGurk, M. G., Fan, K. F. M., MacBean, A. D. & Putcha, V. (2007). Complications encountered in a prospective series of 182 patients treated surgically for mouth cancer. Oral Oncology, vol. 43, pp. 471-476.

McLaughlin, J. R. & Boyd, N. F. (1998). Epidemiology of cancer. In The Basic Science of Oncology, 3rd Edition, pp. 6-25. McGraw-Hill, USA.

Meadows, S. L., Gennings, C., Carter, Jr. H. & Bae, D. (2002). Experimental designs for mixtures of chemicals along fixed ratio rays. Environmental Health Perspectives, vol. 10(6), pp. 979-983.

Michi, Y., Morita, I., Amagasa, T & Murota, S. (2000). Human oral squamous cell carcinoma cell lines promote angiogenesis via expression of vascular endothelial growth factor and upregulation of KDR/flk-1 expression in endothelial cells. Oral Oncology, vol. 36(1), pp. 81-88.

Mihara, M., Shintani, S., Nakashiro, K. & Hamakawa, H.(2003). Flavopiridol, a cyclin dependent kinase (CDK) inhibitor, induces apoptosis by regulating Bcl-x in oral cancer cells. Oral Oncology, vol. 39(1), pp. 49-55.

Mitton, D. & Ackroyd, R. (2005). History of photodynamic therapy in Great Britain. Photodiagnosis and Photodynamic Therapy, vol. 2, pp. 239-246.

Mizutani, H. Tada-Oikawa, S., Hiraku, Y., Kojima, M. & Kawanishi, S. (2005). Mechanism of apoptosis induced by doxorubicin through the generation of hydrogen peroxide. Life Sciences, vol. 76(13), pp. 1439-1453.

Mosmann, T. (1983). Rapid colorimetric assay for cellular growth and survival: Application to proliferation and cytotoxicity assays. Journal of Immunological Methods, vol. 65(1-2), pp. 55-63.

Mountz, J. D., Wu, J., Cheng, J. & Zhou, T. (1994). Autoimmune disease: a problem of defective apoptosis. Arthritis & Rheumatism, vol. 37, pp. 1415-1420.

Moxley, J. H. 3rd., De-Vita, V. T., Brace, K. & Frei, E. 3rd. (1967). Intensive combination chemotherapy and X-irradiation in Hodgkin's Disease, Cancer Research, vol. 27, pp. 1258-1263.

National Cancer Institute (NCI), (2004). What you need to know about oral cancer : Booklet. National Cancer Institute, USA.

Nielsen, D., Maare, C. & Skovsgaard, T. (1996). Cellular resistance to anthracyclines. General Pharmacology, vol. 27(2), pp. 251-255.

Nonaka, M., Ikeda, H. & Inokuchi, T. (2002). Effect of combined photodynamic and chemotherapeutic treatment on lymphoma cells *in vitro*. Cancer Letters, vol. 184, pp. 171-178.

Notabartolo, M., Poma, P., Perri, D., Dusonchet, L., Cervello, M. & D'Alessandro, N.(2005). Antitumor effects of curcumin, alone or in combination with cisplatin or doxorubicin, on human hepatic cancer cells. Analysis of their possible relationship to changes in NF-kB activation levels and in IAP gene expression. Cancer Letters, vol. 224, pp. 55-65.

Nyst, H. J., Tan, I. B., Stewart, F. A. & Balm, A. J. M. (2009). Is photodynamic therapy a good alternative to surgery and radiotherapy in the treatment of head and neck cancer? Photodiagnosis and Photodynamic Therapy, vol. 6, pp. 3-11.

Oakford, M. & Keohane, S. (2005). The use of photodynamic therapy prior to MOHS surgery to limit size of the excision defect. Journal of the American Academy of Dermatology, Poster P3107, pp. P208.

Ochsner, M. (1997). Photophysical and photobiological processes in the photodynamic therapy of tumours. Journal of Photochemistry and Photobiology B: Biology, vol. 39, pp. 1-18.

Ord, R. A., Kolokythas, A., & Reynolds, M. A. (2006). Surgical salvage for local and regional recurrence in oral cancer. Journal of Oral and Maxillofacial Surgery, vol. 64, pp. 1409-1414.

Oster, S., Penn, L. & Stambolic, V. (2005). Oncogenes and tumor suppressor genes. In. The Basic Science of Oncology, 4th Ed. Editors: Tannock,I.F., Hill, R.P., Bristow, R.G., Harrington, L.. pp. 123-141. McGraw Hill, USA.

Otani, N., Kumamoto, Y., Tsukamoto, T., Miyao, N., Iwabe, H., Yanase, M., Takahashi, A. & Masumori, N. (1991). Clinical efficacy of modified M-VAC chemotherapy for advanced urothelial carcinoma and influence of squamous cell carcinoma-associated antigen on efficacy of the chemotherapy. The Japanese Journal of Urology, vol. 82(5), pp. 786-791.

Park, D. S., Stefanis, L. & Greene, L. A. (1997). Ordering the multiple pathways of apoptosis. Trends in Cardiovascular Medicine, vol. 7(8), pp. 294-301.

Park, K., Han, S., Shin, E., Kim, H. J. & Kim, J. Y. (2006). Cox-2 expression on tissue microarray of breast cancer. European Journal of Surgical Oncology, vol. 32(10), pp. 1093-1096.

Pectasides, D., Pectasides, M. & Economopoulos, Th. (2006). Systemic chemotherapy in locally advanced and/or metastatic bladder cancer. Cancer Treatment Reviews, vol. 32, pp. 456-470.

Pelengaris, S. & Khan, M. (2006). Oncogenes. In: The molecular biology of cancer. Editors: Pelengaris, S. & Khan, M., pp. 158-218. McGraw Hill, USA.

Peters, G. Jj., van-der-Wilt, C. L., van-Moorsel, C. J., Kroep, J. R., Bergman, A. M. & Ackland, S. P. (2000). Basis for effective combination cancer chemotherapy with antimetabolites. Pharmacology & Therapeutics, vol. 87, pp. 227-253.

Pfaffel-Schubart, G., Scalfi-Happ, C. & Rück, A. (2008). Early and late apoptotic events induced in human glioblastoma cells by Hypericin PDT. Medical Laser Application, vol. 23(1), pp. 25-30.

Pichi, B., Ruscito, O., Pellini, R., Manciocco, V. & Spriano, G. (2009). Foscan mediated photodynamic therapy (Foscan-PDT) as palliative treatment in recurrent carcinoma of oral cavity. Our experience. Oral Oncology Supplement, vol.3(1), pp. 193-194.

Piette,J., Volantia,C., Vantieghem,A., Matroule, J., Habraken, Y. & Agostinis, P. (2003). Cell death and growth arrest in response to photodynamic therapy with Membrane-bound photosensitizers. Biochemical Pharmacology, vol. 66(8), pp. 1651-1659.

Pisani, P., Parkin, D. M, Bray, F. & Ferlay, J. (1999). Estimates of the worldwide mortality from 25 cancers in 1990. International Journal of Cancer, vol. 83(1), pp. 18-29.

Planas-Silva, M. D. & Weinberg, R. A. (1997). The restriction point and control of cell proliferation. Current Opinion in Cell Biology, vol. 9, pp. 768-772.

Potten, C. S. & Loeffler, M. (1990). Stem cells: attributes, cycles, spirals, pitfalls and uncertainties lessons for and from the Crypt. Development, vol. 110, pp. 1001-1020.

Proskuryakov, S. Y., Konoplyannikov, A. G. & Gabai, V. L. (2003). Necrosis: a specific form of programmed cell death? Experimental Cell Research, vol. 283, pp. 1-16.

Puri, P. L., MacLachlan, T. K., Levrero, M. & Giordano, A. (1999). The intrinsic cell cycle: From yeast to mammals. In The Molecular Basis of Cell Cycle and Growth Control, pp. 1-15, Wiley-Liss, USA.

Rabik, C. A. & Dolan, M. E. (2007). Molecular mechanisms of resistance and toxicity associated with platinating agents. Cancer Treatment Reviews, vol. 33, pp. 9-23.

Radu, A., Grosjeana, P., Jaqueta, Y., Pilloud, R., Wagnieresb, G., van-den-Bergh, H. & Monniera, Ph. (2005). Photodynamic therapy and endoscopic mucosal resection as minimally invasive approaches for the treatment of early esophageal tumors: Pre-clinical and clinical experience in Lausanne. Photodiagnosis and Photodynamic Therapy, vol. 2, pp. 35-44.
Reed, J. C. (2003). Apoptosis-targeted therapies for cancer. Cancer Cell, vol.3, pp. 17-22.

Revis, N. & Marasic, N. (1978). Glutathione peroxidase activity and selenium concentration in the heart of doxorubicin-treated rabbits. Journal of Molecular Cell Card, vol. 10, pp. 945-951.

Ris, H. (2005). Photodynamic therapy as an adjunct to surgery for malignant pleural mesothelioma. Lung Cancer, vol. 49(S1), pp. S65-S68.

Rosenberg, B., Van-Camp, L. & Krigas, T. (1965). Inhibition of cell division in *Escherichia coli* by electrolysis products from a platinum electrode. Nature vol. 205, pp. 698-699.

Roussel, M. (2006). Tumor suppressor gene. In, The molecular biology of cancer. Editors: Pelengaris, S. & Khan, M.. pp, 219-250. Blackwell Publishing, USA.

Rudin, C. M. & Thompson, C. B. (2002). Apoptosis and cancer. In The Genetic Basis of Human Cancer, 2nd Edition, pp. 163-171, McGraw-Hill, USA.

Sarkar, F. H. & Li, Y. (2009). Harnessing the fruits of nature for the development of multi-targeted cancer therapeutics. Cancer Treatment Reviews, vol. 35(7), pp. 597-607.

Schelman, W. R., Andres, R. D., Sipe, K. J., Kang, E. & Weyhenmeyer, J. A. (2004). Glutamate mediates cell death and increases the Bax to Bcl-2 ratio in a differentiated neuronal cell line. Brain Research : Molecular Brain Research, vol. 128(2), pp. 160-169.

Schmidt-Erfurth, U. & Hasan, T. (2000). Mechanisms of action of photodynamic therapy with Verteporfin for the treatment of age-Related macular degeneration. Survey of Ophthalmology, vol. 45(3), pp. 195-214.

Sharman, W. M., Allen, C. M. & Lier, J. E. (1999). Photodynamic therapeutics:basic principles and clinical applications. Drug Discovery Today, vol. 4(11), pp. 507-517.

Sharpe, J. C., Arnoult, D. & Youle, R. J. (2004). Control of mitochondrial permeability by Bcl-2 family members. Biochimica et Biophysica Acta, vol.1644, pp. 107-113.

Sheng, Z., Cao, X., Peng, S., Wang, C., Li, Q., Wang, Y. & Liu, M. (2008). Ofloxacin induces apoptosis in microencapsulated juvenile rabbit chondrocytes by caspase-8-dependent mitochondrial pathway. Toxicology and Applied Pharmacology, vol. 226, pp. 119-127.

Sherr, C. J. & Roberts, J. M. (2004). Living with or without cyclins and cyclin-dependent kinases. Genes & Developments, vol. 18, pp. 2699-2711.

Skommer, J., Wlodkowic, D. & Deptala, A. (2007). Larger than life: Mitochondria and the Bcl-2 family. Leukemia Research, vol. 31, pp. 277-286.

Soloway, M. S., Ishikawa, S., Taylor, T. & Ezell, G. (2006). M- VAC or MVC for the treatment of advanced transitional cell carcinoma: Metastatic, induction, and adjuvant. Journal of Surgical Oncology, vol. 42(S1), pp. 40-45.

Spikes, J. D. (1997). Photodynamic Action: From Paramecium to Photochemotherapy. Photochemistry and Photobiology, vol. 65s, pp. 142s-147s.

Sprick, M. R. & Walczak, H. (2004). The interplay between the Bcl-2 family and death receptor-mediated apoptosis. Biochimica et Biophysica Acta, vol. 1644, pp. 125-132.

Srivastava, M., Ahmad, N., Gupta, S. & Mukhtar, H. (2001). Involvement of Bcl-2 and Bax in photodynamic therapy mediated apoptosis. Journal of Biological Chemistry, vol. 276, pp. 15481-15488.

Stables, G. I. & Ash, D. V. (1995). Photodynamic therapy. Cancer Treatment Review, vol. 21, pp. 311-323.

Stephelin, D., Varmus, H. E., Bishop, J. M. & Vogt, P. K. (1976). DNA related to the transforming gene(s) of avian sarcoma viruses is present in normal avian DNA. Nature, vol. 260, pp. 170-173.
Stewart, F., Baas, P. & Star, W. (1998). What does photodynamic therapy have to offer radiation oncologists(or their cancer patients)? Radiotherapy and Oncology, vol. 48, pp. 233-248.

Streckyte, G., Didziapetriene, J., Grazeliene, G., Prasmickiene, G., Sukeliene, D., Kazlauskaite, N., Characiejus, D., Griciute, L. & Rotomskis, R. (1999). Effects of photodynamic therapy in combination with Adriamycin. Cancer Letters, vol. 146, pp. 73-86.

Sugiyama, T., Nishida, T., Hasuo, Y., Fujiyoshi, K. & Yakushiji, M. (1998). Neoadjuvant intraarterial chemotherapy followed by radical hysterectomy and/or radiotherapy for locally advanced cervical cancer. Gynecologic Oncology, vol.69, pp.130-136.

Symonds, R. P. & Foweraker, K.(2006). Principles of chemotherapy and radiotherapy. Current Obstetrics & Gynaecology, vol. 16(2), pp. 100-106.

Szeimies, R. M., Hein, R., Baumler, W., Heine, A. & Landthaler, M. (1994). A possible new incoherent lamp for photodynamic treatment of superficial skin lesions. Acta Dermato-Venereologica (Stockholm), vol. 74, pp. 117-119.

Szygula, M., Pietrusa, A., Adamek, M., Wojciechowski, B., Kawczyk-Krupka, A., Cebula, W., Duda, W. & Sieron, A. (2004). Combined treatment of urinary bladder cancer with the use of photodynamic therapy (PDT) and subsequent BCG-therapy: a pilot study. Photodiagnosis and Photodynamic Therapy, vol. 1, pp. 241-246.

Terakado, N., Shintani, S., Yano, J., Li, C. N., Mihara, M., Nakashiro, K. I. & Hamakawa, H. (2004). Overexpression of cyclooxygenase-2 is associated with radioresistance in oral squamous cell carcinoma. Oral Oncology, vol. 40(4), pp. 383-389.

Tallarida, R. J. & Raffa, R. B. (1996). Testing for synergism over a range of fixed ratio drug combinations: replacing the isobologram. Pharmacology Letters, vol. 58(2), pp. PL23-PL28.

Tei, K., Maekawa, K., Kitada, H., Ohiro, Y., Yamazaki, Y. & Totsuka, Y. (2007). Recovery from postsurgical swallowing dysfunction in patients with Oral Cancer. Journal of Oral and Maxillofacial Surgery, vol. 65, pp.1077-1083.

Termrungruanglert, W., Tresukosol, D., Vasuratna, A., Sittisomwong, T., Lertkhachonsuk, R. & Sirisabya, N. (2005). Neoadjuvant gemcitabine and cisplatin followed by radical surgery in (bulky) squamous cell carcinoma of cervix stage IB2. Gynecologic Oncology, vol.97, pp.576-581.

Thomas, A. L., Sharma, R. A. & Steward, W. P. (2006). Treatment of Cancer: Chemotherapy and Radiotherapy. In: The molecular biology of cancer. Editors: Pelengaris,S. & Khan,M., pp. 444-463. Blackwell Publishing, USA.

Torkarska-Schlattner, M., Zaugg, M., Zuppinger, C., Wallimann, T., Schlattner, U. (2006). New insights into doxorubicin-induced cardiotoxicity: The critical role of cellular energetic. Journal of Molecular and Cellular Cardiology, vol. 41, pp. 389-405.

Twiddy, D., Cohen, G. M., MacFarlane, M. & Cain, K. (2006). Caspase-7 is directly activated by the approximately 700-kDa apoptosome complex and is released as a stable XIAP-caspase-7 approximately 200-kDa complex. Journal of Biological Chemistry, vol.281, pp. 3876-3888.

Uehara, M., Inokuchi, T. & Ikeda, H. (2006). Enhanced susceptibility of mouse squamous cell carcinoma to photodynamic therapy combined with low-dose administration of cisplatin. Journal of Oral and Maxillofacial Surgery, vol. 64, pp. 390-396.

Vairaktaris, E., Spyridonidou, S., Papakosta, V., Vylliotis, A., Lazaris, A., Perrea, D., Yapijakis, C. & Patsouris, E. (2007). The hamster model of sequential oral oncogenesis. Oral Oncology, vol. 4(44), pp. 315-324.

Vantieghem, A., Xu, Y., Assefa, Z., Piette, J., Vandenheede, J. R., Merlevede, W., De-Witte, P. A. & Agostinis, P. (2002). Phosphorylation of Bcl-2 in G2/M phase-arrested cells following photodynamic therapy with hypericin involves a CDK1-mediated signal and delays the onset of apoptosis, Journal of Biological Chemistry, vol.277, pp. 37718–37731.

Venkitaraman, A. (2010). New approaches for the discovery and development of small molecule drugs against cancer. Abstract Book, UK-Malaysia Symposium on Cancer Drug Discovery & Development, pp. 11.

Verma,Y. K., Gangenahalli, G. U., Singh, V. K., Gupta, P., Chandra, R., Sharma, R. K. & Raj, H. G. (2006). Cell death regulation by B-cell lymphoma protein. Apoptosis, vol. 11, pp. 459-471.

Villela, L. R., Stanford, B. L. & Shah, S. R. (2006). Pemetrexed, a novel antifolate therapeutic alternative for cancer chemotherapy. Pharmacotherapy, vol. 26(5), pp. 641-654.

Volpato, J. P., Fossati, E., & Pelletier, J. N. (2007). Increasing methotrexate resistance by combination of active-site mutations in human dihydrofolate reductase. Journal of Molecular Biology, vol. 373, pp. 599-611.

Wada, T., Haradiq, M., Morita, N., Oomata, T., Koizumi, T., Kawashimu, T. & Sakamoto, T. (1995). Chemotherapy administered using two-route infusion of cisplatin and sodium thiosulfate and intravenous infusionof vinblastine and peplomycin in patients with oral cancer. Clinical Therapeutics, vol. 17(2), pp.280-289.

Wang, Q., Tsao, S. W., Ooka, T., Nicholls, J. M., Cheung, H. W., Fu, S., Wong, Y. C. & Wang, X. (2006). Anti-apoptotic role of BARF1 in gastric cancer cells. Cancer Letters, vol. 238(1), pp. 90-203.

Whitehurst, C., Byrne, K. & Moore, J. V. (1993). Development of an alternative light source to lasers for photodynamic therapy: comparative in vitro dose response characteristics. Lasers in Medical Science, vol. 8, pp. 259-267.

Wijngaarden, J., Beek, E., Rossum, G., Bent, C., Hoekman, K., Pluijm, G., Pol, M. A., Broxterman, H. J. Hinsbergh, V. W. M. & Löwik, C. W. G. M. (2007). Celecoxib enhances doxorubicin-induced cytotoxicity in MDA-MB231 cells by NF-κB-mediated increase of intracellular doxorubicin accumulation. European Journal of Cancer, vol.43(2), pp. 433-442.

Williams, G. H. & Stoeber, K. (2007). Cell cycle markers in clinical oncology. Current Opinion in Cell Biology, vol. 19, pp. 672-679.

Wu, X. M. & Pandolfi, P. P. (2001). Mouse models for multistep Tumorigenesis. Trends in Cell Biology, vol.11(11), pp. S2-S9.

World Health Organisation (WHO) (2009a). WHO > Programmes and projects > Media centre > Fact sheets N-297 http://www.who.int/mediacentre/factsheets/fs297/en/index.html (accessed on 20.12.2009).

World Health Organisation (WHO) (2009b). WHO > Features > Fact files > 10 facts about cancer. http://www.who.int/features/factfiles/cancer/01_en.html (accessed on 20.12.2009).

Wu, J., Lee, A., Lua, Y. & Lee, R. J. (2007). Vascular targeting of doxorubicin using cationic liposomes. International Journal of Pharmaceutics, vol. 337, pp. 329-335.

Wyllie, A. H., Kerr, J. F. & Currie, A. R. (1980). Cell death: the significance of apoptosis. International Review of Cytology, vol. 68, pp. 251-306.

Xu, J., Huang, H., Pan, C., Zhang, B., Liu, X. & Zhang, L. (2007). Nicotine inhibits apoptosis induced by cisplatin in human oral cancer cells. International Journal of Oral and Maxillofacial Surgery, vol. 36(8), pp. 739-744.

Yanamoto, S., Iwamoto, T., Kawasaki, G., Yoshitomi, I., Baba, N. & Izuno, A.(2004). Silencing of the p53R2 gene by RNA interference inhibits growth and enhances 5-fluorouracil sensitivity of oral cancer cells. Cancer Letters, vol. 223(1), pp. 67-76.

Yano, T., Muto, M., Minashi, K., Ohtsu, A. & Yoshida, S. (2005). Photodynamic therapy as salvage treatment for local failures after definitive chemoradiotherapy for esophageal cancer. Gastrointestinal endoscopy, vol. 62(1), pp. 31-36.

Yao, M., Epstein, J. B., Modi, B. J., Pytynia, K. B., Mundt, A. J. & Feldman, L. E. (2007). Current surgical treatment of squamous cell carcinoma of the head and neck. Oral Oncology, vol. 43, pp. 213-223.

Yoshizaki, T., Endo, K., Ren, Q., Wakisaka, N., Murono, S., Kondo, S., Sato, H. & Furukawa, M. (2007). Oncogenic role of Epstein-Barr virus-encoded small RNAs (EBERs) in nasopharyngeal carcinoma. Auris Nasus Larynx, vol. 34(1), pp. 73-78.

Yuspa, S. H. (1998). The pathogenesis of squamous cell cancer: lessons learned from studies of skin carcinogenesis. Journal of Dermatological Science, vol. 17, pp. 1–7.

Zhang, N. Z., Zhu, Y., Pan, W., Ma, W. Q. & Shao, A. L. (2007). Photodynamic therapy combined with local chemotherapy for the treatment of advanced esophagocardiac carcinoma. Photodiagnosis and Photodynamic Therapy, vol. 4, pp. 60-64.

Zhang, X., Jin, L. & Takenaka, I. (1998). MVAC chemotherapy-induced apoptosis and p53 alterations in the rat model of bladder cancer. Urology, vol. 52(5), pp. 925-931.

Zimmermann, G. R., Lehár, J. & Keith, C. T. (2007). Multi-target therapeutics: when the whole is greater than the sum of the parts. Drug Discovery Today, vol. 12(1-2), pp. 34-42.

APPENDIX (Combination Treatment Raw Data)

Appendix Table 1.1 [HYP-PDT] fixed at 0.02μg/ml,

CIS (μg/ml)	10	7	3.5	1.75	0.875	0.4375	0
Replicate 1; Viability, %	11.16544	48.42407	76.72716	85.546	87.5199	89.65298	95.0971
Replicate 2; Viability, %	12.2807	39.77955	76.01222	84.92488	92.34603	96.71141	97.58449
Replicate 3; Viability, %	11.16544	45.55515	81.11398	83.80671	86.64699	93.95057	93.69236
Average Viability, %	11.5372	44.58625	77.95112	84.7592	88.83764	93.43832	95.45799
Standard Deviation, %	0.643894	4.402953	2.762344	0.881403	3.069542	3.55699	1.970998

Appendix Table 1.2 [HYP-PDT] fixed at 0.06μg/ml,

CIS (μg/ml)	10	7	3.5	1.75	0.875	0.4375	0
Replicate 1; Viability, %	6.04727	36.35785	73.89366	81.21617	84.9411	91.11748	92.86851
Replicate 2; Viability, %	9.194282	33.34061	70.62825	82.45116	89.83593	93.69202	87.18033
Replicate 3; Viability, %	6.04727	28.43969	73.10955	75.39653	81.66728	80.96643	85.46662
Average Viability, %	7.096274	32.71272	72.54382	79.68796	85.48144	88.59198	88.50515
Standard Deviation, %	1.816928	3.996247	1.704632	3.767431	4.111046	6.728207	3.874711

Appendix Table 1.3 [HYP-PDT] fixed at 0.10μg/ml,

CIS (μg/ml)	10	7	3.5	1.75	0.875	0.4375	0
Replicate 1; Viability, %	3.178484	20.05731	50.6845	59.53518	61.1907	63.54664	72.39733
Replicate 2; Viability, %	3.411306	16.38837	52.76656	64.26207	68.33643	65.86271	58.65983
Replicate 3; Viability, %	3.178484	16.37772	37.58761	52.0841	57.21136	58.79749	60.90004
Average Viability, %	3.256091	17.6078	47.01289	58.62712	62.24616	62.73561	63.98573
Standard Deviation, %	0.13442	2.121341	8.228651	6.139556	5.637132	3.601756	7.370267

210

Appendix Table 1.4 [HYP-PDT] fixed at 0.12µg/ml,

CIS (µg/ml)	7	3.5	1.75	0.875	0.4375	0
Replicate 1; Viability, %	7.27889	26.35571	34.58683	27.42092	31.10071	35.65203
Replicate 2; Viability, %	7.622339	22.6851	21.62998	27.0875	25.63216	27.85156
Replicate 3; Viability, %	5.012015	13.04497	14.18927	13.61712	13.52558	12.15242
Average Viability, %	6.637748	20.69526	23.46869	22.70851	23.41948	25.21867
Standard Deviation, %	0.242856	2.595515	9.161877	0.23576	3.866847	5.515771

Appendix Table 1.5 [HYP-PDT] fixed at 0.14µg/ml,

CIS (µg/ml)	7	3.5	1.75	0.875	0.4375	0
Replicate 1; Viability, %	2.243383	7.827631	14.12201	19.25436	21.96578	18.15688
Replicate 2; Viability, %	2.77655	10.17823	19.31065	28.3326	37.72279	28.47989
Replicate 3; Viability, %	3.583773	5.039112	12.20666	20.82954	23.59469	18.75568
Average Viability, %	2.867902	7.681657	15.21311	22.8055	27.76109	21.79748
Standard Deviation, %	0.674848	2.572666	3.675532	4.85097	8.665445	5.794876

Appendix Table 1.6 [HYP-PDT] fixed at 0.16µg/ml,

CIS (µg/ml)	7	3.5	1.75	0.875	0.4375	0
Replicate 1; Viability, %	3.534538	9.409296	13.86378	14.41252	13.25048	15.02582
Replicate 2; Viability, %	4.093142	4.929962	6.785519	8.131708	6.676369	11.44261
Replicate 3; Viability, %	2.998055	3.387115	5.423962	4.920471	5.080673	8.788191
Average Viability, %	3.541912	5.908791	8.691088	9.154901	8.335842	11.75221
Standard Deviation, %	0.547581	3.128138	4.531119	4.828039	4.33034	3.13032

Appendix Table 1.1- Appendix Table 1.6   Combination study of HYP-PDT + CIS in HSC-2 at various concentrations. Inhibitory concentrations were found from these data by plotting graph.

Appendix Table 2.1 [HYP-PDT] fixed at 0.02μg/ml,

CIS (μg/ml)	2.5	1.8	0.9	0.45	0.225	0.1125	0
Replicate 1; Viability, %	6.231025	20.44897	54.33181	78.81445	80.00702	86.60119	98.46754
Replicate 2; Viability, %	12.78176	11.97616	40.46521	56.11303	85.29412	82.06459	96.75125
Replicate 3; Viability, %	6.231025	14.82412	65.48367	83.73116	86.80905	93.96985	96.82789
Average Viability, %	8.414604	15.74975	53.4269	72.88621	84.03673	87.54521	97.34889
Standard Deviation, %	3.78207	4.311576	12.53376	14.73255	3.571089	6.008508	0.969536

Appendix Table 2.2 [HYP-PDT] fixed at 0.06μg/ml,

CIS (μg/ml)	2.5	1.8	0.9	0.45	0.225	0.1125	0
Replicate 1; Viability, %	3.570912	15.92424	30.55068	49.52648	71.76429	75.30691	68.74781
Replicate 2; Viability, %	7.197746	9.207997	49.84621	43.42561	53.30642	69.10804	72.26067
Replicate 3; Viability, %	3.570912	16.17462	41.45729	63.97613	75.78518	84.73618	79.08291
Average Viability, %	4.779857	13.76895	40.61806	52.30941	66.95196	76.38371	73.3638
Standard Deviation, %	2.093953	3.951887	9.675101	10.55412	11.98718	7.869521	5.255119

Appendix Table 2.3 [HYP-PDT] fixed at 0.10μg/ml,

CIS (μg/ml)	2.5	1.8	0.9	0.45	0.225	0.1125	0
Replicate 1; Viability, %	2.963713	19.57208	36.30305	39.49491	48.12347	54.26166	59.41775
Replicate 2; Viability, %	5.840164	10.70742	48.7697	61.34179	65.60938	72.76048	68.3391
Replicate 3; Viability, %	2.963713	17.46231	45.25754	46.16834	48.96357	50.50251	53.76884
Average Viability, %	3.92253	15.91394	43.44343	49.00168	54.23214	59.17488	60.50856
Standard Deviation, %	1.66072	4.630728	6.428265	11.19564	9.861931	11.91466	7.346121

Appendix Table 2.4 [HYP-PDT] fixed at 0.12μg/ml,

CIS (μg/ml)	2.5	1.8	0.9	0.45	0.225	0.1125	0
Replicate 1; Viability, %	2.211942	12.13641	39.8997	41.98596	45.03511	38.29488	30.37444
Replicate 2; Viability, %	2.202869	15.18064	34.00729	34.83593	35.53199	28.90288	36.39377
Replicate 3; Viability, %	2.211942	6.227834	17.77557	14.79643	19.59143	18.85374	30.85544
Average Viability, %	2.208917	11.18163	30.56085	30.53944	33.38617	28.68384	32.54122
Standard Deviation, %	0.005238	4.552132	11.45765	14.09477	12.85685	9.722424	3.345065

Appendix Table 2.5 [HYP-PDT] fixed at 0.14μg/ml,

CIS (μg/ml)		1.8	0.9	0.45	0.225	0.1125	0
Replicate 1; Viability, %		7.041123	12.57773	28.22467	34.44333	44.99498	36.20863
Replicate 2; Viability, %		5.071263	11.70036	20.05303	25.22373	35.63142	30.06298
Replicate 3; Viability, %		3.986381	6.937154	11.95914	19.39282	30.6852	17.37835
Average Viability, %		5.366256	10.40508	20.07895	26.35329	37.10387	27.88332
Standard Deviation, %		1.548589	3.035185	8.132796	7.588569	7.267636	9.602499

Appendix Table 2.6 [HYP-PDT] fixed at 0.16μg/ml,

CIS (μg/ml)		1.8	0.9	0.45	0.225	0.1125	0
Replicate 1; Viability, %		4.540935	8.253232	8.717269	6.794829	4.706662	9.579052
Replicate 2; Viability, %		2.993332	3.333806	4.724074	3.362179	6.341325	2.993332
Replicate 3; Viability, %		0.974612	0.950547	1.143063	1.359644	3.236674	4.199254
Average Viability, %		2.836293	4.179195	4.861469	3.838884	4.761554	5.590546
Standard Deviation, %		1.78834	3.724018	3.788971	2.748772	1.553053	3.506379

Appendix Table 2.1- Appendix Table 2.6 Combination study of HYP-PDT + CIS in HSC-3 at various concentrations. Inhibitory concentrations were found from these data by plotting graph.

213

Appendix Table 3.1 [HYP-PDT] fixed at 0.02μg/ml,

CIS (μg/ml)	4	2	1	0.5	0.25	0
Replicate 1; Viability, %	5.855065	18.31745	25.31344	33.53811	60.89519	92.94132
Replicate 2; Viability, %	4.154728	17.23105	26.03543	37.18416	58.75228	88.68195
Replicate 3; Viability, %	4.710487	19.23336	28.11446	39.10109	64.25968	98.16439
Average Viability, %	4.90676	18.26062	26.48777	36.60779	61.30238	93.26256
Standard Deviation, %	0.866994	1.002367	1.454265	2.825922	2.776191	4.749378

Appendix Table 3.2 [HYP-PDT] fixed at 0.06μg/ml,

CIS (μg/ml)	4	2	1	0.5	0.25	0
Replicate 1; Viability, %	4.67653	21.40171	25.33852	33.16199	53.07172	86.89819
Replicate 2; Viability, %	5.847877	22.12816	32.86012	40.62256	58.88252	88.6559
Replicate 3; Viability, %	3.684708	23.30949	32.40653	41.77352	61.72223	97.46255
Average Viability, %	4.736371	22.27978	30.20172	38.51935	57.89216	91.00555
Standard Deviation, %	1.082826	0.962887	4.217763	4.675171	4.409475	5.660566

Appendix Table 3.3 [HYP-PDT] fixed at 0.10μg/ml,

CIS (μg/ml)	4	2	1	0.5	0.25	0
Replicate 1; Viability, %	3.321177	23.48268	30.61995	34.0323	32.49544	60.0026
Replicate 2; Viability, %	2.415981	15.91308	36.69861	45.14779	47.03739	57.6731
Replicate 3; Viability, %	3.550576	22.42386	27.97854	26.88444	24.61207	26.84235
Average Viability, %	3.095911	20.60654	31.7657	35.35484	34.71497	48.17269

	4	2	1	0.5	0.25	0
Standard Deviation, %	0.599904	4.098988	4.471517	9.203228	11.37622	18.50929

Appendix Table 3.4 [HYP-PDT] fixed at 0.12μg/ml,

CIS (μg/ml)	4	2	1	0.5	0.25	0
Replicate 1; Viability, %	1.441441	2.966043	6.680527	7.179487	13.13929	24.17186
Replicate 2; Viability, %	3.558346	7.116693	14.62585	13.99791	19.25693	26.94924
Replicate 3; Viability, %	1.488612	1.825259	4.160749	9.294619	10.00999	4.791963
Average Viability, %	2.1628	3.969332	8.489042	10.15734	14.13541	18.63769
Standard Deviation, %	1.496878	2.934953	5.618192	4.821351	4.325825	1.963902

Appendix Table 3.5 [HYP-PDT] fixed at 0.14μg/ml,

CIS (μg/ml)	4	2	1	0.5	0.25	0
Replicate 1; Viability, %	0.183538	1.736552	3.487223	10.91345	14.47127	10.09459
Replicate 2; Viability, %	0.748441	1.053361	1.607762	7.207207	10.56133	7.761608
Replicate 3; Viability, %	1.88383	2.773417	7.613815	14.88749	10.54422	13.7101
Average Viability, %	0.938603	1.854443	4.236266	11.00272	11.85894	10.5221
Standard Deviation, %	0.86595	0.866067	3.07229	3.840921	2.26236	2.9972

Appendix Table 3.6 [HYP-PDT] fixed at 0.16μg/ml,

CIS (μg/ml)	4	2	1	0.5	0.25	0
Replicate 1; Viability, %	0.776507	1.510659	2.583651	2.894254	3.910772	5.60497
Replicate 2; Viability, %	1.108801	1.801802	2.577963	2.467082	4.102564	3.575884
Replicate 3; Viability, %	1.614855	1.656935	1.783178	2.666877	3.7189	3.466414
Average Viability, %	1.166721	1.656466	2.314931	2.676071	3.910745	4.215756
Standard Deviation, %	0.234967	0.205869	0.004022	0.302056	0.135617	1.434781

Appendix Table 3.1- Appendix Table 3.6   Combination study of HYP-PDT + CIS in HSC-4 at various concentrations. Inhibitory concentrations were found from these data by plotting graph.

Appendix Table 4.1 [HYP-PDT] fixed at 0.02µg/ml,

DOX (µg/ml)	1	0.5	0.25	0.125	0.0625	0
Replicate 1; Viability, %	12.35687	58.28562	78.3874	80.90013	83.82634	96.77163
Replicate 2; Viability, %	4.094133	41.84397	69.1167	76.11219	79.755	88.68472
Replicate 3; Viability, %	3.401938	24.18831	48.72208	66.96138	78.64274	91.84647
Average Viability, %	6.617647	41.4393	65.40873	74.6579	80.74136	92.43427
Standard Deviation, %	4.982348	17.05226	15.17629	7.082256	2.728938	4.075372

Appendix Table 4.2 [HYP-PDT] fixed at 0.06µg/ml,

DOX (µg/ml)	1	0.5	0.25	0.125	0.0625	0
Replicate 1; Viability, %	4.723282		69.13168	74.88868	75.493	75.27036
Replicate 2; Viability, %	2.901354	21.17988	68.92328	77.78852	74.59703	80.56093
Replicate 3; Viability, %	4.692932	34.12514	75.60834	78.62109	80.51371	95.80919
Average Viability, %	4.105856	27.65251	71.2211	77.09943	76.86792	83.88016
Standard Deviation, %	1.04324	9.153682	3.800893	1.959302	3.188975	10.66414

Appendix Table 4.3 [HYP-PDT] fixed at 0.10µg/ml,

DOX (µg/ml)	1	0.5	0.25	0.125	0.0625	0
Replicate 1; Viability, %	1.542621	10.83015	35.25763	37.61132	47.02608	50.65204
Replicate 2; Viability, %	2.70793	2.740168	32.23727	63.79755	68.31077	70.53514
Replicate 3; Viability, %	4.770182	5.079181	16.97567	33.2754	42.15913	71.16647
Average Viability, %	3.006911	6.2165	28.15686	44.89476	52.49866	64.11788
Standard Deviation, %	1.63442	4.163182	9.80025	16.51323	13.90823	11.66604

Appendix Table 4.4 [HYP-PDT] fixed at 0.12µg/ml,

DOX (µg/ml)	1	0.5	0.25	0.125	0.0625	0
Replicate 1; Viability, %	2.798945	2.916178	3.385111	7.986518	14.31712	26.12837
Replicate 2; Viability, %	3.980194	3.637402	9.998096	22.94801	30.29899	27.70901
Replicate 3; Viability, %	1.938109	1.440408	1.147642	1.411131	3.255555	12.74117
Average Viability, %	2.905749	2.664663	4.843616	10.78189	15.95722	22.19285
Standard Deviation, %	1.025223	1.119885	4.601963	11.0372	13.59611	8.223462

Appendix Table 4.5 [HYP-PDT] fixed at 0.14µg/ml,

DOX (µg/ml)	1	0.5	0.25	0.125	0.0625	0
Replicate 1; Viability, %	3.033411	2.71102	2.593787	5.964244	13.2034	17.54103
Replicate 2; Viability, %	3.370787	3.523138	4.43725	18.18701	28.92782	29.38488
Replicate 3; Viability, %	3.021944	2.445141	2.746082	8.112853	15.03448	18.721
Average Viability, %	3.142047	2.8931	3.259039	10.7547	19.05524	21.8823
Standard Deviation, %	0.198177	0.561591	1.023198	6.525607	8.598791	6.524151

Appendix Table 4.6 [HYP-PDT] fixed at 0.16µg/ml,

DOX (µg/ml)	1	0.5	0.25	0.125	0.0625	0
Replicate 1; Viability, %	3.795428	3.560961	3.092028	3.707503	4.938453	15.19637
Replicate 2; Viability, %	3.904018	3.789754	3.561226	5.046658	11.97867	17.69187
Replicate 3; Viability, %	2.92163	2.244514	2.420063	2.344828	2.746082	7.711599
Average Viability, %	3.540359	3.19841	3.024439	3.699663	6.554402	13.53328
Standard Deviation, %	0.538579	0.833981	0.573576	1.350932	4.823758	5.193827

Appendix Table 4.1- Appendix Table 4.6   Combination study of HYP-PDT + DOX in HSC-2 at various concentrations. Inhibitory concentrations were found from these data by plotting graph.

217

Appendix Table 5.1 [HYP-PDT] fixed at 0.02µg/ml,

DOX (µg/ml)	0.7	0.35	0.175	0.0875	0.04375	0
Replicate 1;Viability, %	39.63134	67.74194		86.10422	70.08153	86.84864
Replicate 2;Viability, %	30.56266	59.15033	81.03154	81.88406	69.43734	91.57431
Replicate 3;Viability, %	28.16399	48.75223	63.8369	72.41533	67.13458	86.58645
Average Viability, %	32.786	58.54816	72.43422	80.13454	68.88448	88.33647
Standard Deviation, %	6.04834	9.509164	12.15845	7.010138	1.549312	2.807118

Appendix Table 5.2 [HYP-PDT] fixed at 0.06µg/ml,

DOX (µg/ml)	0.7	0.35	0.175	0.0875	0.04375	0
Replicate 1;Viability, %	2.48139		57.95817	62.63736	62.46012	78.76639
Replicate 2;Viability, %	0.862366	16.78165	76.68161	64.98793	68.29941	66.4712
Replicate 3;Viability, %	1.292981	29.02813	65.20318	76.14379	76.45638	77.87724
Average Viability, %	1.545579	22.90489	66.61432	67.92303	69.07197	74.37161
Standard Deviation, %	0.838548	8.659572	9.44115	7.215747	7.030039	6.856387

Appendix Table 5.3 [HYP-PDT] fixed at 0.10µg/ml,

DOX (µg/ml)	0.7	0.35	0.175	0.0875	0.04375	0
Replicate 1;Viability, %	1.276302	1.345291	16.28148	72.71473	74.8534	56.22628
Replicate 2;Viability, %	1.690821	1.861324	18.03069	49.06223	48.40864	58.09889
Replicate 3;Viability, %	1.646345	1.260483	1.260483	43.19082	25.31255	48.46427
Average Viability, %	1.537823	1.489033	11.85755	54.98926	49.52486	54.26315
Standard Deviation, %	0.227573	0.32519	9.218911	15.6289	24.78928	5.108514

Appendix Table 5.4 [HYP-PDT] fixed at 0.12μg/ml,

DOX (μg/ml)	0.7	0.35	0.175	0.0875	0.04375	0
Replicate 1;Viability, %	0.637162	0.29275	0.843809	7.835371	25.02153	35.18168
Replicate 2;Viability, %	1.256632	1.200782	3.099693	7.511868	5.989947	27.43647
Replicate 3;Viability, %	0.758032	0.902418	1.76874	1.359644	2.610997	25.73698
Average Viability, %	0.883942	0.79865	1.904081	5.568961	11.20749	29.45171
Standard Deviation, %	0.328369	0.462824	1.134015	3.648962	12.08201	5.034529

Appendix Table 5.5 [HYP-PDT] fixed at 0.14μg/ml,

DOX (μg/ml)	0.7	0.35	0.175	0.0875	0.04375	0
Replicate 1;Viability, %	-0.12054	0.086103	0.464956	4.597899	27.60462	22.95505
Replicate 2;Viability, %	0.698129	0.390952	1.200782	6.562413	20.23178	27.14326
Replicate 3;Viability, %	1.143063	0.878354	0.709903	1.094934	1.672482	24.00433
Average Viability, %	0.573549	0.451803	0.79188	4.085082	16.50296	24.70088
Standard Deviation, %	0.640949	0.399615	0.3747	2.769579	13.36215	2.179253

Appendix Table 5.6 [HYP-PDT] fixed at 0.16μg/ml,

DOX (μg/ml)	0.7	0.35	0.175	0.0875	0.04375	0
Replicate 1;Viability, %	0.499397	0.120544	0.154985	0.602721	2.01481	7.904253
Replicate 2;Viability, %	1.228707	1.396258	1.535884	2.122312	2.624965	6.11561
Average Viability, %	0.864052	0.758401	0.845435	1.362517	2.319887	7.009932
Standard Deviation, %	0.5157	0.902066	0.976443	1.074513	0.431445	1.264762

Appendix Table 5.1- Appendix Table 5.6   Combination study of HYP-PDT + DOX in HSC-3 at various concentrations. Inhibitory concentrations were found from these data by plotting graph.

Appendix Table 6.1 [HYP-PDT] fixed at 0.02μg/ml,

DOX (μg/ml)	1.2	0.9	0.3	0.1	0.033333	0.011111	0
Replicate 1; Viability, %	8.589186		47.30238		89.29318	93.42894	97.65788
Replicate 2; Viability, %	6.027987	22.19985	49.88674	52.37856	71.55802	83.01032	95.99751
Replicate 3; Viability, %	8.589186	8.401814	32.56142	56.80079	86.56401	88.11278	93.48762
Average Viability, %	7.735453	15.30083	43.25018	54.58967	82.47174	88.18401	96.8277
Standard Deviation, %	1.478709	9.756684	9.346492	3.126995	9.549557	5.209676	2.099503

Appendix Table 6.2 [HYP-PDT] fixed at 0.06μg/ml,

DOX (μg/ml)	0.9	0.3	0.1	0.033333	0.011111	0
Replicate 1; Viability, %	2.885822	46.21497	64.89614	78.19601		79.72954
Replicate 2; Viability, %	2.013592	47.44526	56.43091	72.18726	87.51573	88.62321
Replicate 3; Viability, %	2.045374	30.51605	53.62643	79.01728	93.07629	78.45304
Average Viability, %	2.314929	41.39209	58.31782	76.46685	90.29601	82.2686
Standard Deviation, %	0.494663	9.438998	5.867022	3.728911	3.931909	5.540142

Appendix Table 6.3 [HYP-PDT] fixed at 0.10μg/ml,

DOX (μg/ml)	0.9	0.3	0.1	0.033333	0.011111	0
Replicate 1; Viability, %	1.07347	6.20382	27.45016	31.57675	34.1698	34.47651
Replicate 2; Viability, %	1.334005	5.008809	36.74805	41.20312	39.79361	
Replicate 3; Viability, %	2.515575	2.891736	24.68555	28.89385	29.59915	41.30716
Average Viability, %	1.641017	4.701455	29.62792	33.89124	34.52085	37.89183
Standard Deviation, %	0.768511	1.677297	6.319251	6.472804	5.106285	4.829999

Appendix Table 6.4 [HYP-PDT] fixed at 0.12μg/ml,

DOX (μg/ml)	0.9	0.3	0.1	0.033333	0.011111	0
Replicate 1; Viability, %	0.713986	1.469971	9.645807	19.9216	18.32563	22.58155
Replicate 2; Viability, %	0.963343	3.540598	16.82722	18.6288	18.4036	
Replicate 3; Viability, %	1.15946	1.650525	10.46242	19.49257	22.76633	19.51985
Average Viability, %	0.945596	2.220365	12.31182	19.34766	19.83186	21.0507
Standard Deviation, %	0.223267	1.146914	3.931716	0.65847	2.541631	2.16495

Appendix Table 6.5 [HYP-PDT] fixed at 0.14μg/ml,

DOX (μg/ml)	0.9	0.3	0.1	0.033333	0.011111	0
Replicate 1; Viability, %	0.041999	0.153997	1.161977	4.605908	14.15372	6.00588
Replicate 2; Viability, %	1.113474	1.088452	3.390467	7.018641	11.07219	8.820218
Replicate 3; Viability, %	0.976631	0.930124	3.883269	4.48785	10.32438	3.929776
Average Viability, %	0.710701	0.724191	2.811904	5.3708	11.8501	6.251958
Standard Deviation, %	0.583141	0.500108	1.449969	1.428293	2.029731	2.45449

Appendix Table 6.6 [HYP-PDT] fixed at 0.16μg/ml,

DOX (μg/ml)	0.9	0.3	0.1	0.033333	0.011111	0
Replicate 1; Viability, %	0.293994	0.937981	1.805964	2.561949	2.533949	3.961921
Replicate 2; Viability, %	1.35043	1.377711	1.323148	7.188651	8.416314	7.734279
Replicate 3; Viability, %	1.488199	1.581211	1.464946	1.627718	1.860249	2.906639
Average Viability, %	1.044208	1.298968	1.531353	3.792772	4.270171	4.867613
Standard Deviation, %	0.653345	0.328765	0.248163	2.977783	3.606431	2.538058

Appendix Table 6.1- Appendix Table 6.6 Combination study of HYP-PDT + DOX in HSC-4 at various concentrations. Inhibitory concentrations were found from these data by plotting graph.

Appendix Table 7.1 [HYP-PDT] fixed at 0.02µg/ml,

VIN (µg/ml)	0.015	0.005	0.00125	0.000625	0.000313	0
Replicate 1;Viability, %	50.47811	51.78661	61.09713	71.76648	76.84952	91.04177
Replicate 2;Viability, %	48.50478	56.35965	68.75997	78.76794	86.90191	101.9338
Replicate 3;Viability, %	52.15875	57.60545	69.5284	83.74294	83.51046	94.40385
Average Viability, %	50.38055	55.25057	66.46183	78.09246	82.42063	95.79315
Standard Deviation, %	1.828936	3.063862	4.661827	6.016736	5.114044	5.577341

Appendix Table 7.2 [HYP-PDT] fixed at 0.06µg/ml,

VIN (µg/ml)	0.015	0.005	0.00125	0.000625	0.000313	0
Replicate 1;Viability, %	40.71465	36.63815	46.30096	50.47811	61.29844	71.0619
Replicate 2;Viability, %	43.04226	44.59729	53.64833	65.5303	72.50797	90.37081
Replicate 3;Viability, %	48.17336	44.78579	62.02258	73.91232	67.56891	87.9276
Average Viability, %	43.97676	42.00707	53.99062	63.30691	67.12511	83.1201
Standard Deviation, %	3.816161	4.650581	7.866401	11.87427	5.61793	10.51392

Appendix Table 7.3 [HYP-PDT] fixed at 0.10µg/ml,

VIN (µg/ml)	0.015	0.005	0.00125	0.000625	0.000313	0
Replicate 1;Viability, %	37.59436	32.6623	33.71917	32.05838	33.66885	39.40614
Replicate 2;Viability, %	49.46172	48.94338	54.24641	58.5925	61.82217	75.25917
Replicate 3;Viability, %	62.08901	58.40252	63.41747	65.01162	73.51378	80.85354
Average Viability, %	49.71503	46.6694	50.46102	51.8875	56.33493	65.17295
Standard Deviation, %	12.24929	13.01991	15.20671	17.46988	20.48138	22.48934

Appendix Table 7.4 [HYP-PDT] fixed at 0.12µg/ml,

VIN (µg/ml)	0.015	0.005	0.00125	0.000625	0.000313	0
Replicate 1;Viability, %	27.00766	23.10353	18.90289	17.61799	19.24883	16.97554
Replicate 2;Viability, %	43.03301	40.53524	34.04103	32.00714	29.08118	42.0339
Replicate 3;Viability, %	57.95747	49.13015	38.85309	32.50644	39.72294	46.35954
Average Viability, %	42.66605	37.58964	30.59901	27.37719	29.35098	35.12299
Standard Deviation, %	15.47817	13.26098	10.41097	8.455402	10.23972	15.86428

Appendix Table 7.5 [HYP-PDT] fixed at 0.14µg/ml,

VIN (µg/ml)	0.015	0.005	0.00125	0.000625	0.000313	0
Replicate 1;Viability, %	7.734124	8.425995	9.760316	9.760316	14.50457	8.673091
Replicate 2;Viability, %	13.84478	17.34166	17.80553	18.59054	31.40054	18.91169
Replicate 3;Viability, %	10.78945	12.88383	13.78292	14.17543	22.95255	13.79239
Average Viability, %	10.78945	12.88383	13.78292	14.17543	22.95255	13.79239
Standard Deviation, %	4.320887	6.304327	5.688826	6.243914	11.94725	7.23978

Appendix Table 7.6 [HYP-PDT] fixed at 0.16µg/ml,

VIN (µg/ml)	0.015	0.005	0.00125	0.000625	0.000313	0
Replicate 1;Viability, %	15.19644	11.53941	7.042254	4.620707	4.37361	5.016061
Replicate 2;Viability, %	14.20161	12.41748	12.13202	12.13202	7.136485	9.56289
Replicate 3;Viability, %	28.60825	22.90593	14.52964	12.14562	12.40335	17.07474
Average Viability, %	19.33543	15.62094	11.23464	9.632783	7.971149	10.55123
Standard Deviation, %	8.045885	6.324241	3.823508	4.340591	4.079422	6.089791

Appendix Table 7.1- Appendix Table 7.6 Combination study of HYP-PDT + VIN in HSC-2 at various concentrations. Inhibitory concentrations were found from these data by plotting graph.

223

Appendix Table 8.1 [HYP-PDT] fixed at 0.02µg/ml,

VIN (µg/ml)	0.005	0.0025	0.00125	0.000625	0.000313	0
Replicate 1; Viability, %	36.79383	31.45022	32.30094	69.73282	86.9334	84.40782
Replicate 2; Viability, %	31.31783	28.94057	32.45478	73.12661	81.05943	80
Replicate 3; Viability, %	35.63044	30.27893	30.78379	64.73558	82.32993	88.23678
Average Viability, %	34.5807	30.22324	31.84651	69.19834	83.44092	84.21487
Standard Deviation, %	2.884982	1.255752	0.923544	4.220974	3.09057	4.121778

Appendix Table 8.2 [HYP-PDT] fixed at 0.06µg/ml,

VIN (µg/ml)	0.005	0.0025	0.00125	0.000625	0.000313	0
Replicate 1; Viability, %	26.45221	29.11073	34.58727	44.29084	59.36462	73.74718
Replicate 2; Viability, %	20.28424	22.60982	30.2584	48.24289	45.89147	
Replicate 3; Viability, %	27.22454	26.69443	32.80323	43.70819	45.80336	52.56847
Average Viability, %	24.65366	26.13833	32.54963	45.41398	50.35315	63.15782
Standard Deviation, %	3.803686	3.285939	2.175548	2.467176	7.804283	14.97561

Appendix Table 8.3 [HYP-PDT] fixed at 0.10µg/ml,

VIN (µg/ml)	0.005	0.0025	0.00125	0.000625	0.000313	0
Replicate 1; Viability, %	33.52386	33.31118	33.60362	35.65067	32.77948	46.17839
Replicate 2; Viability, %	11.44703	12.29974	14.75452	10.10336	9.767442	11.78295
Replicate 3; Viability, %	18.99533	21.54487	9.20106	15.53704	15.63802	4.85927
Average Viability, %	21.32207	22.38526	19.1864	20.43036	19.39498	20.9402
Standard Deviation, %	11.22083	10.5309	12.79071	13.45826	11.95719	22.12937

Appendix Table 8.4 [HYP-PDT] fixed at 0.12μg/ml,

VIN (μg/ml)	0.005	0.0025	0.00125	0.000625	0.000313	0
Replicate 1; Viability, %	11.63446	13.7547	8.789587	5.434783	2.831455	2.858293
Replicate 2; Viability, %	10.92389	5.611881	4.783664	4.126803	1.813508	4.098244
Replicate 3; Viability, %	10.29692	17.76083	11.49551	9.016617	5.529828	4.60365
Average Viability, %	10.95176	12.3758	8.356252	6.192734	3.391597	3.853396
Standard Deviation, %	0.669205	6.190739	3.376838	2.531489	1.920437	0.898071

Appendix Table 8.5 [HYP-PDT] fixed at 0.14μg/ml,

VIN (μg/ml)	0.005	0.0025	0.00125	0.000625	0.000313	0
Replicate 1; Viability, %	1.140633	3.073001	0.899087	0.952764	3.019324	0.711218
Replicate 2; Viability, %	1.128088	1.04241	1.356561	1.013851	1.270884	0.671141
Replicate 3; Viability, %	1.134361	2.057705	1.127824	0.983308	2.145104	0.69118
Average Viability, %	0.008871	1.435844	0.323483	0.043195	1.236334	0.028339
Standard Deviation, %						

Appendix Table 8.6 [HYP-PDT] fixed at 0.16μg/ml,

VIN (μg/ml)	0.005	0.0025	0.00125	0.000625	0.000313	0
Replicate 1; Viability, %	6.454643	4.200215	1.086957	1.19431	0.442834	1.516371
Replicate 2; Viability, %	2.270456	1.527917	1.013851	0.842496	1.07097	0.35699
Replicate 3; Viability, %	2.642332	2.04304	1.52547	1.280305	1.116862	0.381367
Average Viability, %	3.789143	2.59039	1.208759	1.105704	0.876889	0.751576
Standard Deviation, %	2.315867	1.417741	0.276704	0.231964	0.376602	0.662444

Appendix Table 8.1- Appendix Table 8.6   Combination study of HYP-PDT + VIN in HSC-3 at various concentrations. Inhibitory concentrations were found from these data by plotting graph.

225

Appendix Table 9.1 [HYP-PDT] fixed at 0.02μg/ml,

VIN (μg/ml)	0.005	0.0025	0.00125	0.000625	0.000313	0
Replicate 1; Viability, %	73.297	61.8208	63.93653	84.13207	86.40808	96.47379
Replicate 2; Viability, %	61.66505	70.79703	64.21426	80.83253	100.2904	98.22523
Replicate 3; Viability, %	69.60268	61.75203	62.00734	76.24063	81.15526	91.23983
Average Viability, %	68.18825	64.78996	63.38604	80.40174	89.28458	95.31295
Standard Deviation, %	5.943571	5.202393	1.202041	3.963321	9.886571	3.634507

Appendix Table 9.2 [HYP-PDT] fixed at 0.06μg/ml,

VIN (μg/ml)	0.005	0.0025	0.00125	0.000625	0.000313	0
Replicate 1; Viability, %	59.35246	57.5573	60.21798	72.14297	84.70909	82.62542
Replicate 2; Viability, %	55.82446	52.17812	58.79316	71.57147	85.0597	85.60826
Replicate 3; Viability, %	51.73129	50.80581	52.36955	69.25164	86.74007	84.37849
Average Viability, %	55.63607	53.51374	57.1269	70.98869	85.50295	84.20406
Standard Deviation, %	3.814076	3.568414	4.181121	1.531235	1.085622	1.499051

Appendix Table 9.3 [HYP-PDT] fixed at 0.10μg/ml,

VIN (μg/ml)	0.005	0.0025	0.00125	0.000625	0.000313	0
Replicate 1; Viability, %	46.65812	42.87546	39.66982	42.13816	44.51034	51.78715
Replicate 2; Viability, %	36.17296	30.71959	30.36463	27.68635	27.71862	35.1081
Replicate 3; Viability, %	41.96585	30.57284	32.67911	31.94511	29.83884	23.58385
Average Viability, %	41.59898	34.72263	34.23786	33.92321	34.0226	36.82637
Standard Deviation, %	5.252199	7.06094	4.844469	7.426195	9.144307	14.17994

Appendix Table 9.4 [HYP-PDT] fixed at 0.12μg/ml,

VIN (μg/ml)	0.005	0.0025	0.00125	0.000625	0.000313	0
Replicate 1; Viability, %	37.82712	34.84536	37.12926	32.59318	36.84377	40.20619
Replicate 2; Viability, %	34.65664	39.39491	43.52489	35.2009	31.16696	29.72627
Replicate 3; Viability, %	38.60095	29.38686	32.46951	30.23374	34.56978	37.31369
Average Viability, %	37.02824	34.54238	37.70789	32.67594	34.19351	35.74871
Standard Deviation, %	2.089992	5.010901	5.550357	2.484612	2.857052	5.412395

Appendix Table 9.5 [HYP-PDT] fixed at 0.14μg/ml,

VIN (μg/ml)	0.005	0.0025	0.00125	0.000625	0.000313	0
Replicate 1; Viability, %	16.16178	14.25852	12.06979	16.00317	29.26249	12.13323
Replicate 2; Viability, %	18.87306	14.26285	12.88619	13.65455	22.87498	6.259004
Replicate 3; Viability, %	17.51742	14.26069	12.47799	14.82886	26.06874	9.196116
Average Viability, %	17.51742	14.26069	12.47799	14.82886	26.06874	9.196116
Standard Deviation, %	1.917166	0.003056	0.577282	1.660724	4.516652	4.153703

Appendix Table 9.6 [HYP-PDT] fixed at 0.16μg/ml,

VIN (μg/ml)	0.005	0.0025	0.00125	0.000625	0.000313	0
Replicate 1; Viability, %	24.47264	11.05472	7.184774	7.343378	6.264869	5.979381
Replicate 2; Viability, %	23.00304	9.81271	8.243957	7.891788	8.275972	9.748679
Replicate 3; Viability, %	32.36789	17.97087	15.39634	18.78388	19.42751	18.51287
Average Viability, %	26.61452	12.9461	10.27502	11.33968	11.32278	11.41364
Standard Deviation, %	5.036449	4.395665	4.466697	6.452691	7.09056	6.430488

Appendix Table 9.1- Appendix Table 9.6   Combination study of HYP-PDT + VIN in HSC-4 at various concentrations. Inhibitory concentrations were found from these data by plotting graph.

227